



TECHNISCHE UNIVERSITÄT MÜNCHEN

Max Planck Institute of Biochemistry



Functional Organization of the Actin System in *Dictyostelium*

Hellen Cristina Ishikawa-Ankerhold

Vollständiger Abdruck der von der Fakultät für Chemie der
Technischen Universität München zur Erlangung des akademischen
Grades eines Doktors der Naturwissenschaften genehmigten
Dissertation.

Vorsitzender: Univ.-Prof. Dr. J. Buchner

Prüfer der Dissertation:

1. Hon.-Prof. Dr. W. Baumeister
2. Univ.-Prof. Dr. S. Weinkauf

Die Dissertation wurde am 02.12.2008 bei der Technischen Universität München
eingereicht und durch die Fakultät für Chemie am 08.04.2009 angenommen.

Table of Contents

1	Introduction.....	1
1.1	<i>Dictyostelium discoideum</i> as a model to study actin dynamics.....	1
1.2	Cytokinesis.....	3
1.3	The centrosome	4
1.4	Phagocytosis in <i>D. discoideum</i>	5
1.5	Chemotaxis	8
1.6	Function of cAMP.....	10
1.7	The actin cytoskeleton	11
1.8	Actin-associated proteins in <i>Dictyostelium discoideum</i>	12
1.8.1	The Arp2/3 complex.....	14
1.8.2	WASP and neural (N)-WASP	16
1.8.3	The SCAR complex.....	17
1.8.4	Coronin.....	19
1.8.5	Actin-interacting protein 1	26
1.8.6	LimE protein	28
1.9	Oscillations in cell biology	29
1.9.1	Oscillations of cytoskeletal structures	30
1.10	Microfluidic device.....	31
1.11	Caged compounds.....	32
1.12	Aim of this study.....	33
2	Materials and Methods.....	34
2.1	Materials.....	34
2.1.1	Antibodies	34
2.1.2	Dyes and others	34
2.1.3	Antibiotics.....	34
2.1.4	Buffers and solutions.....	34
2.1.5	Agar overlay	35
2.2	Cell Biological Methods.....	37
2.2.1	Cell Culture	37
2.2.2	Preservation of <i>Dictyostelium discoideum</i>	38
2.2.3	Transformation and electroporation of <i>Dictyostelium</i> cells.....	38
2.2.4	Cell lines transformed	38
2.2.5	Other cell lines transformed	39

2.2.6	Cell isolation via Laser Microdissection and Pressure Catapulting.....	40
2.2.7	Microfluidic device.....	41
2.2.8	Fluorescence microscopy and photo-activation	42
2.2.9	Image processing.....	43
2.2.10	Total Internal Reflection Fluorescence Microscopy.....	44
2.2.11	Micropipette assay	44
2.2.12	Phagocytosis assay.....	45
2.2.13	Cell velocity assay.....	45
2.2.14	Immunofluorescence labeling.....	45
2.3	Biochemical Methods and Immunoblotting	46
2.3.1	SDS-Polyacrylamide gel electrophoresis	46
2.3.2	Coomassie blue staining	46
2.3.3	Western blots and immunostaining	47
2.3.4	Estimation of the G-/F-actin ratio	47
2.3.5	Quantitative F-actin assay.....	48

3 Results

Actin-filament turnover mediated by coronin and Aip1 is required for proper cytokinesis, phagocytosis and motility in *D. discoideum*.....49

3.1	CorA/Aip1-null mutants have high filamentous actin content.....	50
3.2	Aggregation of <i>D. discoideum</i> cells is delayed in the absence of CorA and Aip1 ..	53
3.3	CorA and Aip1 contribute to chromosome segregation and cytokinesis.....	54
3.4	The phagocytosis process is prolonged in the absence of CorA and Aip1	56
3.5	CorA/Aip1 double-mutant cells migrate slowly but still orient towards a cAMP gradient	58

4 Results

Well-defined chemoattractant stimuli modulate protein recruitment to the cell cortex of *D. discoideum*.....61

4.1	The temporal pattern of cAMP stimulation affects CorA and Aip1 translocation to the cell cortex	63
4.2	The rates of actin assembly and disassembly are affected in the absence of CorA and Aip1	66
4.3	Pulses of cAMP promote resonant actin responses with periods of 20 or 40 seconds.....	71
4.4	Resonant actin response is promoted in the presence of CorA and Aip1, but not in their absence.....	75

5 Results

Cell-autonomous oscillations of actin polymerization in the cortex of SCAR-deficient cells.....80

5.1	Autonomous and periodic fluctuations of actin polymerization in the cortex of SCAR-deficient cells	81
5.2	The developmental stage of SCAR-deficient cells has no influence on autonomous fluctuations of actin polymerization in the cell cortex	85
5.3	Development of <i>D. discoideum</i> appears not to be affected by the absence of SCAR and PIR121	87
5.4	Actin redistribution at the basal cell cortex exhibits different patterns in the absence of SCAR or PIR121	88
5.5	Localization of the Arp2/3 complex is not disturbed in the absence of SCAR	92
5.6	CorA is recruited to the leading edge in the absence of SCAR	94
5.7	External cAMP stimulation promotes a shift in the phase of actin oscillations in SCAR and PIR121-deficient cells	95
5.8	The Arp2/3 complex is poorly recruited to the leading edge in the absence of SCAR in a gradient of cAMP	99

6 Discussion 102

6.1	CorA and Aip1 contribute to an effective chromosome segregation and act cooperatively in cytokinesis	102
6.2	CorA and Aip1 participate in actin turnover during phagocytosis and cell motility.....	104
6.3	CorA and Aip1 regulate the temporal dynamics of actin polymerization and depolymerization.....	107
6.4	cAMP pulses promote an actin resonance response in wild-type but not in CorA or/and Aip1-null cells	110
6.5	SCAR and PIR121 suppress intrinsic actin oscillations	111

7 References 119

8 Movie legends 134

Acknowledgments 136

Curriculum Vitae 137

Zusammenfassung

Aktin bildet in seinen verschiedenen Formen die Basis für Zellbewegung, Zellform und die intrazelluläre Organisation in eukaryontischen Zellen. Viele andere zelluläre Prozesse wie beispielsweise Endozytose und Zytokinese werden ebenfalls mit dynamischen Veränderungen im Aktin Zytoskelett assoziiert. Eine wichtige Grundvoraussetzung für die funktionelle Diversität von Aktin ist seine intrinsische Fähigkeit schnell Filamente auf- und auch wieder abzubauen. Diese Prozesse sind räumlich und zeitlich genau kontrolliert. Eine große Anzahl von Proteinen, die mit Aktin interagieren, sind die sogenannten Aktin-Bindeproteine. Sie regulieren im Detail verschiedenste Aktin Zustände.

Der Fokus der vorliegenden Arbeit liegt auf der funktionellen Analyse von zwei Klassen von Proteinen und ihrer Bedeutung für die Aktin Dynamik: Auf der einen Seite sind das aktin-bindende Protein Coronin (CorA) und aktin-interagierendes Protein (Aip1), die beide mit der Regulierung des Aktin Abbaus in Verbindung gebracht werden. Auf der anderen Seite sind es Proteine wie SCAR und PIR121, die Bestandteile des SCAR Komplexes sind und durch die Interaktion mit anderen Proteinen in die Regulierung des Aktin Aufbau involviert sind.

Als experimentelles Model für die vorliegenden Experimente wurde die „soziale Amöbe“ *Dictyostelium discoideum* gewählt. *D. discoideum* ist sehr gut für Lebendzell-Experimente geeignet, seine Genetik gestattet eine einfache Generierung von Funktionsverlust-Mutanten, und die Zellen reagieren auf Stimulation mit dem Chemoattraktor cAMP mit einer chemotaktischen Antwort und reorganisieren ihr Aktin Netzwerk. Hier wurden Einzel- und Doppelmutanten, denen entsprechend ein oder zwei Zielproteine fehlen, in Lebendzell-Experimenten mit konfokaler Mikroskopie untersucht. Dabei wurde eine neue Methode für Chemotaxis Experimente angewendet. Diese Methode basiert auf einem Mikrofluidik-Chip in Kombination mit photoinduzierter cAMP Freisetzung und gestattet eine hochpräzise örtliche und zeitliche Kontrolle des Experiments, so dass in einem Versuchsansatz viele verschiedene Einzelzelexperimente durchgeführt werden können.

Zellen, denen CorA und Aip1 fehlen, weisen einen erhöhten F-Aktin Anteil auf. Die Zellen zeigen Defekte in der Chromosomen Segregation, Zytokinese, ein

verzögertes Aggregationsverhalten, langsamere Phagozytose und migrieren langsamer als Wild-Typ Zellen, aber die Zellen zeigen weiterhin ein chomotaktisches Verhalten. Nach kurzen cAMP Pulsen oder in Reaktion auf eine kontinuierliche cAMP Stimulation, werden CorA und Aip1 in den Zellkortex verlagert. In Zellen, denen diese Proteine fehlen, ist besonders die Geschwindigkeit des Aktin Abbaus im Vergleich zu Wild-Typ Zellen reduziert.

Wiederholte kurze cAMP Pulse mit einer Periodizität von 20 oder 40 Sekunden, führen dazu, dass Wild-Typ Zellen in eine Resonanz-Reaktion mit zusätzlichen Zyklen kortikalen Aktin Ab- und Aufbaus verfallen. In der Abwesenheit von CorA und/oder Aip1 können keine Resonanzen im Aktin-System beobachtet werden.

Bei Zellen, denen SCAR und/oder PIR121 fehlen, konnte in dieser Arbeit ein besonderes Phänomen entdeckt werden. Diese Mutanten zeigen eine zellautonome Oszillation der kortikalen Aktin Polymerisation/Depolymerisation mit einer Periode von 20 Sekunden. cAMP Stimulation kann die Phase der Oszillation verschieben oder zurücksetzen, was dafür spricht, dass das oszillierende System mit dem chemosensorischen Signalweg in Verbindung steht. cAMP Stimulation hat aber keinen Einfluss auf die Amplitude der Oszillationen. In dieser Arbeit konnte SCAR Protein als ein Hauptregulator für die Unterdrückung von Aktin Oszillationen in Wild-Typ Zellen identifiziert werden. Ein Schema des Protein Netzwerkes, das in die Generierung dieser Oszillationen involviert ist, wird vorgeschlagen und diskutiert.

Es lässt sich zusammenfassen, dass die hier untersuchten Proteine eine entscheidende Rolle in der Regulierung der zellulären Aktin Dynamik spielen und SCAR Protein in einem Proteinnetzwerk Oszillationen im Aktin System von Wild-Typ Zellen unterdrückt.

Summary

Actin provides through its various forms of assembly the basic framework for cell motility, cell shape and intracellular organization in eukaryotic cells. Many other cellular processes, for example endocytosis and cytokinesis, are also associated with dynamic changes of the actin cytoskeleton. Important prerequisites for the functional diversity of actin are its intrinsic ability to rapidly assemble and disassemble filaments and its spatially and temporally well-controlled organization. A large number of proteins that interact with actin, collectively referred to as actin-binding proteins, carefully orchestrate different scenarios.

This study focuses on a functional analysis of two classes of protein and their involvement in actin dynamics: First, the actin-binding proteins coronin (CorA) and actin-interacting protein (Aip1) that are suggested to be involved in the regulation of actin disassembly and second, the proteins SCAR and PIR121, members of the SCAR complex that seem to be involved in the regulation of actin assembly through the interaction with other proteins.

As an experimental model the 'social amoeba' *Dictyostelium discoideum* was chosen. *D. discoideum* is well suited for live-cell imaging experiments, its genetics allows to easily generate loss-of-function mutants, and the cells respond to cAMP stimulation with a distinct chemotactic response by rearranging their actin network. Here, single- and double-mutants lacking one or two proteins of interest were analyzed in confocal live-cell experiments, employing a new approach for chemotaxis experiments. Very precise spatial and temporal control allows performing several single cell experiments in one setup. This technique uses a microfluidic device in combination with photo-induced uncaging of the chemoattractant.

Cells lacking CorA and Aip1 have highly elevated filamentous actin content. The cells show defects in chromosome segregation, cytokinesis, delayed aggregation, have a prolonged phagocytosis and migrate slowly in comparison to wild-type but they still display chemotactic responses. Upon short pulse or continuous cAMP stimulation, CorA and Aip1 are translocated to the cell cortex. In cells lacking these proteins in particular the rate of actin disassembly is decreased relative to wild-type cells.

Repetitive short pulses of cAMP at a periodicity of 20 or 40 seconds, lead the wild-type cells to fall into a resonance response with additional cycles of cortical actin assembly and disassembly. However, in the absence of CorA and/or Aip1 such resonance in the actin system has not been observed. These data indicate that the system is capable of oscillating in the presence, but not in the absence of CorA and Aip1.

In cells lacking SCAR and/or PIR121, an intriguing phenomenon is observed: These mutant cells exhibit autonomous oscillations of cortical actin polymerization with a period of 20 seconds. cAMP stimulation can shift and reset the phase of the oscillations indicating that the oscillatory system is linked to the chemosensory pathway. However, cAMP has no influence on the amplitude of the oscillations. Thus, this work provides evidence that SCAR protein is a major regulator that suppresses actin oscillations in wild-type cells.

In conclusion, the proteins investigated in this work play a major role in the regulation of cellular actin dynamics and within a protein network SCAR suppresses oscillations in the actin system of wild-type cells.

List of Publications

Parts of this thesis have been contributed to the following publications:

- Bretschneider, T.; Anderson, K.; Mary Ecke, M.; Müller-Taubenberger, A.; Schroth-Diez, B.; **Ishikawa-Ankerhold, H.C.**; Gerisch, G. (2009). The Three-Dimensional Dynamics of Actin Waves, a Model of Cytoskeletal Self-organization. *Biophys J.* **96**. 2888-2900.
- Etzrodt, M.; **Ishikawa, H.C.**; Dalous, J.; Müller-Taubenberger, A.; Bretschneider, T.; Gerisch, G. (2006). Time-resolved responses to chemoattractant, characteristic of the front and tail of *Dictyostelium* cells. *Febs Letters.* **580**, 6707-6713.
- **Ishikawa-Ankerhold, H.C.**; Bretschneider, T.; Gerisch, G.; Müller-Taubenberger, A.; Insall, R.H.; Bodenschatz, E.; Beta, C. Cell-autonomous oscillations of actin polymerization in the cortex of SCAR-deficient cells. (*in preparation for resubmission*)
- **Ishikawa-Ankerhold, H.C.**; Gerisch, G.; Müller-Taubenberger, A. Dynamic actin turnover mediated by coronin and Aip1 is required for proper, cytokinesis, phagocytosis and motility in *D. discoideum*. (*in preparation*)

Oral presentations:

- **Ishikawa-Ankerhold, H.C.** (2006). Coronin and Actin-interacting protein 1 (Aip1) double mutants are defective in cytokinesis and phagocytosis in *Dictyostelium*. International Titisee Conference on Phagocytosis. Titisee, Germany.
- **Ishikawa-Ankerhold, H.C.** (2007). Temporally programmed chemoattractant signals: Responses in mutant cells deficient in regulators of the actin system. Department Meeting. Seon, Germany.

Poster presentation:

- **Ishikawa-Ankerhold, H.C.**; Bretschneider, T.; Gerisch, G.; Bodenschatz, E.; Beta, C. (2007). Actin response to spatiotemporally programmed chemoattractant signals in mutant cells deficient in regulators of the actin system. European Life Scientist Organization (ELSO) meeting. Dresden, Germany.
- **Ishikawa-Ankerhold, H.C.**; Bretschneider, T.; Gerisch, G.; Müller-Taubenberger, A.; Insall, R.H.; Bodenschatz, E.; Beta, C. (2007). Actin response to programmed chemoattractant signals in mutant cells deficient in regulators of the actin system. 1st Life-Science PhD Symposium. Martinsried/Munich, Germany.
- **Ishikawa-Ankerhold, H.C.**; Bretschneider, T.; Gerisch, G.; Müller-Taubenberger, A.; Insall, R.H.; Bodenschatz, E.; Beta, C. (2007). Actin dynamics in SCAR-deficient cells. International *Dictyostelium* Conference 2007. Rotenburg an der Fulda, Germany.
- Beta, C.; **Ishikawa-Ankerhold, H.C.**; Bretschneider, T.; Gerisch, G.; Müller-Taubenberger, A.; Insall, R.H.; Bodenschatz, E. (2008). Actin dynamics in SCAR-deficient cells. Meeting of the American Physical Society (Division of Polymer Physics). New Orleans, LA.
- Beta C; **Ishikawa-Ankerhold, H.C.**; Bretschneider T; Gerisch G, Müller-Taubenberger A; Insall R, Bodenschatz E (2008). Actin dynamics in SCAR-deficient cells. Deutsche Physikalische Gesellschaft e.V. Berlin, Germany.
- Westendorf, C.; **Ishikawa-Ankerhold, H.C.**; Gerisch, G.; Bodenschatz, E.; Beta, C. (2008). Dynamics of the actin cytoskeleton in response to periodic stimuli. Symposium on Laserscanning Microscopy. Kirchhoff-Institute of Physics. Heidelberg, Germany.

Abbreviations

Abi	Abelson murine leukemia oncogene 1 (Abl)-interactor
ACA	Adenylyl cyclase A
ADF	Actin-depolymerizing factor
ADP	Adenosine diphosphate
Aip1	Actin-interacting protein 1
Arp 2/3	Actin-related protein 2/3
ATP	Adenosine-5'-triphosphate
BCIP	5'-Bromo-4'-chloro-3'-indolyl phosphate
BSA	Bovine serum albumin
cAMP	Cyclic adenosine 3'-5'-monophosphate
cAR	cAMP receptor
CG	Guanylyl cyclase
cGMP	Cyclic guanosine monophosphate
CorA	<i>Dictyostelium</i> coronin A
csA	Contact site A
DAG	Diacylglycerol
DAPI	4',6'-diamidino-2-phenylindole
Dd	<i>Dictyostelium discoideum</i>
DMNB	4',5'-dimethoxy-2-nitrobenzyl
DNA	Desoxyribonucleic acid
EGTA	Ethyleneglycol-bis-(2-aminoethylether)-N,N'-tetra-acetic acid
F-actin	Filamentous actin
G-actin	Globular monomeric actin
GBD	GTPase-binding domain
GFP	Green fluorescent protein
GTP	Guanosine-5'-triphosphate
HSPC300	Hematopoietic stem-cell progenitor
kDa	Kilo Daltons
LEGI	Local excitation global inhibition
LSM	Laser scanning microscopy
mRFP	Monomeric red fluorescent protein
MT	Microtubule
MTOC	Microtubule organizing center

NAP125	Non-catalytic region of tyrosine kinase adaptor protein (Nck) 125-associated protein
NBT	Nitro blue-tetrazolium chloride
NPF	Nucleation promoting factor
N-WASP	Neural-Wiskott-Aldrich syndrome protein
PAGE	Polyacrylamide gel electrophoresis
PB	Phosphate buffer
pH	Negative decadic logarithm of proton concentration
PI3K	Phosphoinositide 3-kinase
PIR121	p53-inducible mRNA protein
PLC	Phospholipase C
PP	Poly-proline
PtdIns(4,5)P2	Phosphatidylinositol-(4',5')-2-bisphosphate
PTEN	Phosphoinositide 3-phosphatase
rpm	Revolutions per minute
SCAR	Suppressor of cyclic AMP receptor protein
SDS	Sodium dodecyl sulfate
SH3	Rous sarcoma oncogene (Src)-homology 3-domain
TBS	Tris buffered saline
TEMED	N,N,N,N'-tetramethylenediamine
TIRF	Total internal reflection fluorescence
Tris	Tris-hydroxymethyl-ammoniummethane
TRITC	TetramethylrhodaminyI
Triton-X-100	T-Octylphenoxy polyethoxethanol
Tween 20	Polyoxyethylene-sorbianemonolaureate
WASP	Wiskott-Aldrich syndrome protein
WAVE	WASP-family verprolin-homologous
WD	tryptophan-aspartic amino acids
WH1	WASP-homology 1-domain
WIP	WASP-interacting protein
Wt	Wild-type

1 Introduction

1.1 *Dictyostelium discoideum* as a model to study actin dynamics

Dictyostelium discoideum is a haploid eukaryotic microorganism that grows as free-living amoeba in the soil, feeding on bacteria and multiplies by equal mitotic division. Upon exhaustion of the food supply *D. discoideum* undergoes a complex multicellular morphogenesis (Figure 1.1).

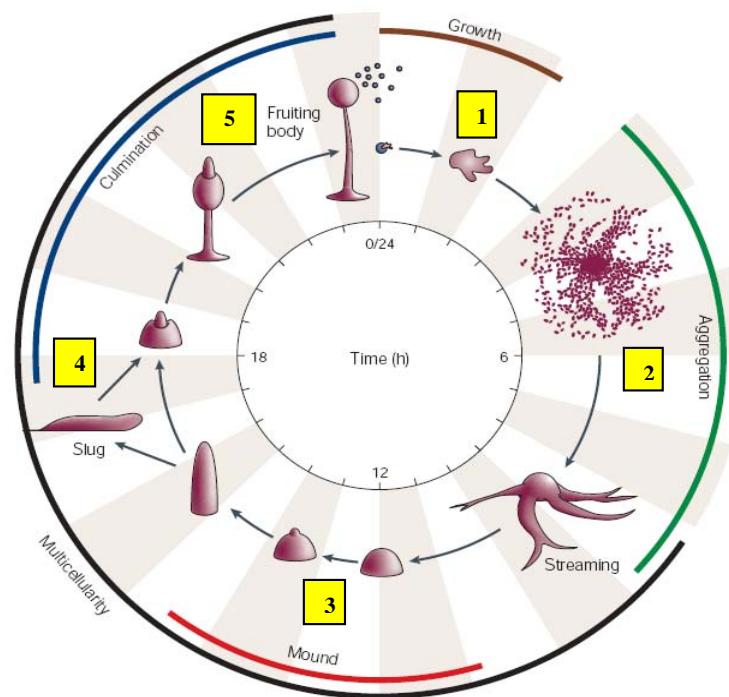


Figure 1.1. Life cycle of *D. discoideum*. The life cycle of *D. discoideum* starts from single, vegetative amoebae (1) and ends with the formation of the mature fruiting body with a spore head on the top of a stalk (5). One important transition occurs between growth and aggregation, which is mediated by the chemotaxis of cells towards cyclic AMP to form a multicellular aggregate (2). During this process cells stream towards a central domain or aggregation center. Aggregation results in the formation of a multicellular organism known as a mound, in which the precursors of the mature spore and stalk cells differentiate and sort out, forming a tipped mound (3). As development proceeds, the tip extends and an anterior-posterior axis forms, which is maintained through the slug and early culmination stages (4). Culmination, the formation of the fruiting body, completes morphogenesis. During this stage, the precursor populations differentiate, producing a spore head on top of a stalk (5). The entire process from starvation of vegetative cells to the formation of a mature fruiting body takes about 24 hours (Chisholm *et al.*, 2004).

Introduction

The cells can be cultivated easily in the laboratory at 23 °C. As long as nutrients are available, the free-living amoeboid cells grow and multiply by binary fission (growth or vegetative stage). Upon starvation *D. discoideum* cells enter the developmental stage and exhibit an impressive multicellular cooperativity. The solitary cells aggregate by chemotaxis in response to relayed cAMP signals. The aggregate of approximately 100.000 cells undergoes a series of morphogenetic changes (Eichinger and Noegel, 2003). After the formation of a motile slug the differentiation culminates in the production of a fruiting body consisting of 80% spore cells and 20% dead stalk cells.

D. discoideum is amenable to diverse biochemical, cell biological and molecular genetic approaches. It can be transformed with DNA, and the availability of multiple selection markers allows for the isolation of triple and even quadruple mutants. In particular the haploid nature of the genome of *D. discoideum* is a major advantage compared with other model systems as it allows the generation of a rich variety of mutants (Noegel and Schleicher, 2000; Martens *et al.*, 2002). The genetic treatments include conventional mutagenesis, targeted gene disruption, gene silencing utilizing RNA interference (RNAi), antisense technique, gene replacement, green fluorescence protein (GFP)-fusions and restriction enzyme mediated integration (REMI).

Although the evolutionary position of *D. discoideum* is located before the branching of metazoa and fungi (Baldauf *et al.*, 2000), almost all of the cytoskeletal proteins are also found in mammalian cells. Moreover, *D. discoideum* shares its chemotactic capacity with leukocytes, and the process of particle uptake in *D. discoideum* looks remarkably similar to macrophage phagocytosis (Noegel and Schleicher, 2000; Rupper and Cardelli, 2001). The similarities between *D. discoideum* and mammalian cells also extend to membrane trafficking, endocytic transit and sorting events (Solomon and Isberg, 2000; Cardelli, 2001). All in all, *D. discoideum* offers the advantages of a simple organism that is easy to cultivate while possessing a set of genes much closer related to higher eukaryotes than those of other model organisms such as *S. cerevisiae*.

Therefore, in this work *D. discoideum* has been chosen as model to study the functional organization of the actin system in particular during actin-dependent physiological processes like cytokinesis, phagocytosis and cell migration. In the following these processes and the proteins involved will be introduced.

1.2 Cytokinesis

During mitosis in *D. discoideum* a number of events lead to cytokinesis. First an intranuclear spindle forms and the chromosomes become aligned at the metaphase plate (Figure 1.2A). During early anaphase, the chromosomes begin to move towards the poles as the spindle elongates. In late anaphase, the spindle has elongated and the cell begins to become more cylindrical (Figure 1.2B). The astral microtubules begin to grow out to the cortex and some of the microtubules are re-organized to extend across the equatorial plane of the cell into the opposite hemisphere once the chromosomes have migrated towards the poles. Several contractile ring proteins, including myosin II and cortexillin I begin to assemble at the equatorial zone (Weber *et al.*, 2000), and other proteins like coronin A (CorA) and actin-interacting protein 1 (Aip1) are found at the poles of a dividing cell (de

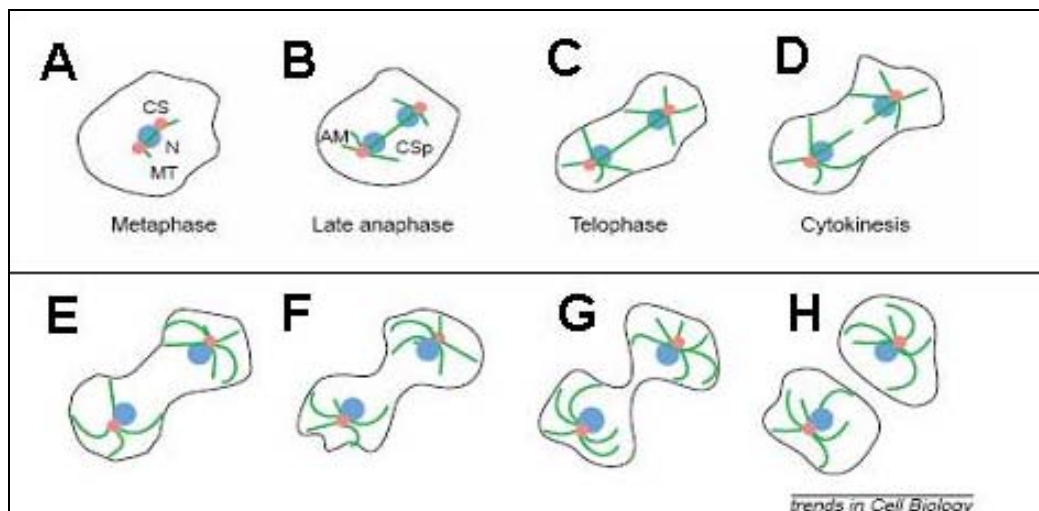


Figure 1.2. Time course for *D. discoideum* cytokinesis. (A) Cell in metaphase showing a spherical and quiescent shape. The green lines represent microtubule (MT) bundles; the blue dot represents the nucleus (N). In *D. discoideum*, the nuclear envelope does not completely break down during mitosis. The red dots represent the centrosomes (CS). (B) The cell has entered late anaphase and the nuclei are separating, indicating the elongation of the spindle. The MTs extending between the nuclei are bundled to antiparallel microtubules that make up the central spindle (CSp). The astral microtubules (AM) are beginning to grow out towards the cell cortex. (C) The cell has reached telophase and becomes more elongated and cylindrical. (D) The cleavage furrow begins to constrict. *D. discoideum* is somewhat different from other organisms in that the central spindle has already begun to disassemble by this time and the interphase MT networks begin to reform. From (D-G) the cell contracts until a residual connection is left. (H) Disruption of this connection completely separates the two daughter cells (adapted from Robinson and Spudich, 2000).

Hostos, 1999; Konzok *et al.*, 1999). At the end of telophase the contractile ring constricts down to the midbody until only a thin intercellular bridge connects the two daughter cells (Figure 1.2D-G) (Robinson and Spudich, 2000). Additional proteins are used in this late phase to set up the complete separation of the two daughter cells, like dynamin A (Wienke *et al.*, 1999) and Lim (Schneider *et al.*, 2003).

1.3 The centrosome

The centrosome or microtubule organizing center (MTOC) plays an important role during many cellular processes. First of all, most eukaryotic cells, apart from higher plant cells and female meiotic cells, possess such a structure. The centrosome is the site of microtubule nucleation and is therefore involved in regulation of the interphase microtubule cytoskeleton. Second, after its duplication it is crucial for the building of the mitotic spindle and for proper cytokinesis and passage from G1/S-phase (Hinchcliffe and Sluder, 2001; Khodjakov and Rieder, 2001; Piel *et al.*, 2001). The presence of supernumerary centrosomes is a hallmark of tumor cells (Lingle *et al.*, 2002; Nigg, 2002).

In *D. discoideum*, centrosome duplication occurs during mitosis at G2/M-phase and not at G1/S-phase, which is absent in its lifecycle (Weeks and Weijer, 1994). The *D. discoideum* centrosome cycle is unusual (Ueda *et al.*, 1999) and its structure is different from the mammalian and the yeast MTOCs (Gräf *et al.*, 2000). Like the yeast spindle pole body it also lacks centrioles but exhibits a compact layered structure. Similar to mammalian centrosomes this structure is surrounded by an electron-dense, amorphous matrix that is functionally equivalent to the pericentriolar material (PCM) of higher cells.

During interphase the centrosome resides in the cytoplasm and is tightly connected to the nucleus by a fibrous linkage. During mitosis it inserts itself into an opening in the nuclear envelope. The centrosome-nucleus attachment is a prerequisite for faithful chromosome segregation during mitosis (Omura and Fukui, 1985). In *D. discoideum* the protein Sun-1 has been addressed to function in the centrosome-nucleus connection and to maintain genome stability (Xiong *et al.*, 2008).

1.4 Phagocytosis in *D. discoideum*

Phagocytosis is the process of engulfing a foreign particle. It is of fundamental importance for a wide diversity of organisms. Since *D. discoideum* feeds on bacteria and yeast and can internalize a remarkable number of particles, phagocytosis plays an important role for this organism.

Phagocytosis is an important first line of defense against invading pathogens, and is normally performed by leukocytes that migrate to the site of infection. The internalized pathogen is contained in a membrane-limited vacuole termed the phagosome that interacts via fission and fusion reactions with the endo-lysosomal system, leading to the death of the microbe (Cardelli, 2001).

Phagocytosis consists of at least four different stages that include: (1) particle binding to the cell surface via interaction with a receptor, (2) activation of a signaling pathway that leads to recruitment of proteins regulating F-actin formation, (3) engulfment of the particle by pseudopod extension dependent on actin polymerization, and most likely vesicle tracking, and (4) removal of the actin coat from the newly formed phagosome, followed by fission and fusion reactions to generate a mature phagolysosome (Rupper and Cardelli, 2001).

D. discoideum has proven to be a useful model system to determine the role of the actin cytoskeleton in a variety of cell processes including phagocytosis and macropinocytosis (Eichinger *et al.*, 1999). Macropinocytosis is the invagination of the cell membrane to form a pocket which then pinches off into the cell to form a vesicle filled with extracellular fluid (and molecules within it). The filling of the pocket occurs in a non-specific manner. The vesicle then travels into the cytosol and fuses with other vesicles such as endosomes and lysosomes (Cardelli, 2001).

A number of recent studies have shown that macropinocytosis and phagocytosis are actin-dependent processes. This conclusion rests on two experimental outcomes: First, F-actin accumulates below the forming phagocytic cup as demonstrated using fluorescent phalloidin (Maniak *et al.*, 1995), a fungal toxin that binds F-actin, and as shown using green fluorescent protein (GFP)-tagged domains that bind to F-actin (Pang *et al.*, 1998). Second, F-actin polymerization is required for building a protrusion of the plasma membrane and for engulfment of particles or fluid as demonstrated using cytochalasin or latrunculin that interfere with F-actin formation (Maniak *et al.*, 1995; Hacker *et al.*,

1997). What has not been determined yet is how the formation of F-actin is regulated spatially and temporally.

Given the important function of the actin cytoskeleton, a number of studies have been performed to examine the role of a large group of proteins that regulate formation and organization of the actin cytoskeleton. These proteins belong to a number of subgroups that play different functions in actin dynamics (reviewed in Eichinger *et al.*, 1999).

In this study the roles of two *D. discoideum* actin-binding proteins, CorA and Aip1 have been studied during the phagocytosis process. CorA is found enriched in phagocytic cups within 1 minute after attachment of particles and is released within 1 minute after internalization. The rate of phagocytosis is reduced by 65% in CorA-null cells (Maniak *et al.*, 1995). Clarke and Maddera, 2006 have shown that CorA is involved in actin filament dynamics during phagocytic cup formation and phagosome internalization in *D. discoideum*. *D. discoideum* Aip1, a homologue of the yeast actin-binding protein 1 (Aip1p), localizes to phagocytic and macropinocytic cups. Aip1-null mutant cells are significantly impaired in phagocytosis (Konzok *et al.*, 1999).

In many ways, phagocytosis in *D. discoideum* appears mechanistically similar to phagocytosis in mammalian cells. A model of phagocytosis in *D. discoideum* is shown in Figure 1.3. The model proposes that particle binding to the cell surface via receptors yet to be defined initiates a signaling cascade that activates phospholipase C (PLC), possibly through interaction with the β -subunit of the heterotrimeric G protein. The products generated, diacylglycerol (DAG) and phosphoinositide-3 (IP3), both contribute to the signaling pathway, the former perhaps by activating Rap1 and/or RasS and the latter by increasing cytosolic calcium levels.

In the next step, members of the Rho family, like RacC, are activated and may play a direct role in actin polymerization, perhaps through recruitment of members of the WASP family such as SCAR. Other actin-associated proteins like *D. discoideum* CorA, Aip1 and actin cross-linking protein (ABP-120) could contribute to the formation and stability of the dynamic actin cytoskeleton associated with the growing phagocytic cup. In addition, Rab GTPases such as RabB and Rab7 could function directly or indirectly to deliver internal membrane to the growing phagocytic cup.

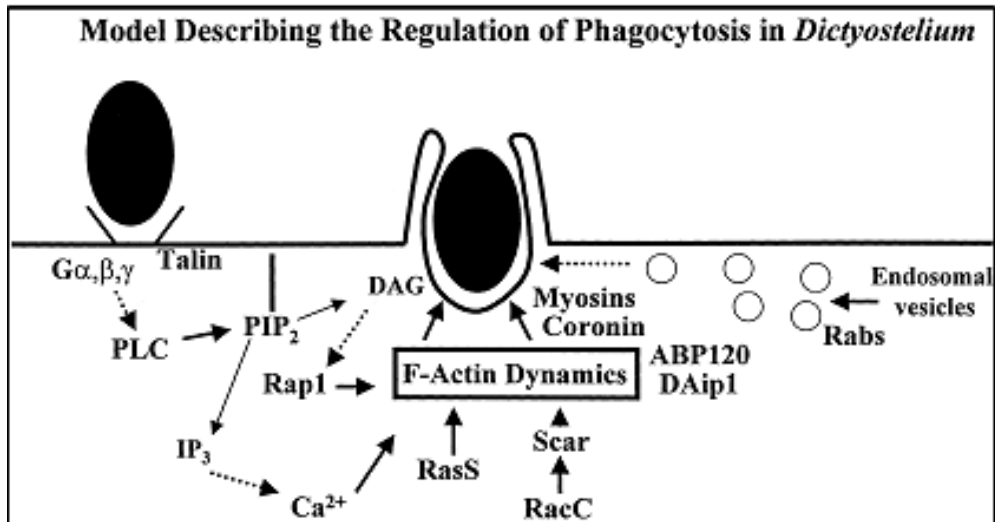


Figure 1.3. Model describing the signal transduction pathway regulating phagocytosis in *Dictyostelium*. The model emphasizes the importance of recruiting proteins in spatial and temporal patterns, which regulate the formation and structure of F-actin. The model also predicts that internal membranes are necessary for 'building' the phagocytic cup. (taken from Rupper and Cardelli, 2001).

The involvement of molecular motors to generate force during extension of phagocytic cup formation to engulf the particle was reported. Seven class I myosins, were described in *Dictyostelium* (Soldati *et al.*, 1999; Titus, 2000), and some of these myosins play a minor role in regulating phagocytosis. For instance, the class I myosin MyoK was reported to regulate the morphology of the cortical actin, and in null-mutants the rate of phagocytosis is reduced by 30% (Schwarz *et al.*, 2000). Consistent with this, MyoB and MyoC were reported to play a minor role in phagocytosis (Jung *et al.*, 1996).

Mutations in the human gene encoding myosin VII result in blindness and deafness (Steel *et al.*, 1997), and little is known concerning the function of this protein. *Dictyostelium* myosin VII null-mutants demonstrate an 80% decrease in the uptake of particles (Titus, 1999) that is not the result of an inability of cells to bind particles or initiate formation of the cup. Instead, the phagocytic defect appears to be due to an inability of these mutants to engulf particles, suggesting an active and direct role for this myosin in this process (Rupper and Cardelli, 2001).

1.5 Chemotaxis

Chemotaxis, or the directed migration of cells in response to external chemical cues, is essential for development and homeostasis. For example, without proper directional migration, tissues do not form properly and embryonic development is severely impaired (Böttcher and Niehrs, 2005). In adult mammals, chemokine-guided migration is critical for wound healing and for the migration of lymphocytes during immune responses (Eccles, 2004; Martin and Parkhurst, 2004). Chemotaxis also plays an important role in the development and progression of many diseases including asthma, arthritis, atherosclerosis, and cancers (Trusolino and Comoglio, 2002; Charo and Taubman, 2004; Eccles, 2004). Further insight into the molecular mechanism of directional sensing and cell migration is crucial for the development of treatments of these disorders, as well as for understanding normal biological processes.

Chemotaxis is necessary for *D. discoideum* cells to find bacteria in the vegetative stage and to aggregate when faced with starvation. Aggregation of starving *D. discoideum* cells occurs in response to a concentration gradient of cyclic adenosine 3', 5' monophosphate (cAMP). Thus, cAMP acts as a chemoattractant to bring the cells together, and it also acts as a morphogen to induce genes required for this process. Chemotaxing cells of *D. discoideum* are highly motile and respond by rapid mobilization of their cytoskeleton (Schleicher and Noegel, 1992; Diez *et al.*, 2005). Mechanisms of chemotaxis in *D. discoideum* are outlined in Figure 1.4.

Chemotaxis consists of three distinct and separable cellular processes: polarization, directional sensing and migration. Under starvation conditions, cells become polarized, a process characterized not only by elongation, but also by localization of specific proteins to either pole. Polarity only enhances the ability of a cell to move, since both polar and non-polar cells are able to migrate randomly (Franca-Koh and Devreotes, 2004).

Studies on signals required for directional sensing and the role of actin polymerization in chemotaxis have resulted in a model termed local excitation, global inhibition (LEGI). The LEGI model describes the ability of a cell to sense direction and adapt to stimuli, and depends on a balance between excitation and inhibition. In a gradient of chemoattractant the cells must translate cAMP levels

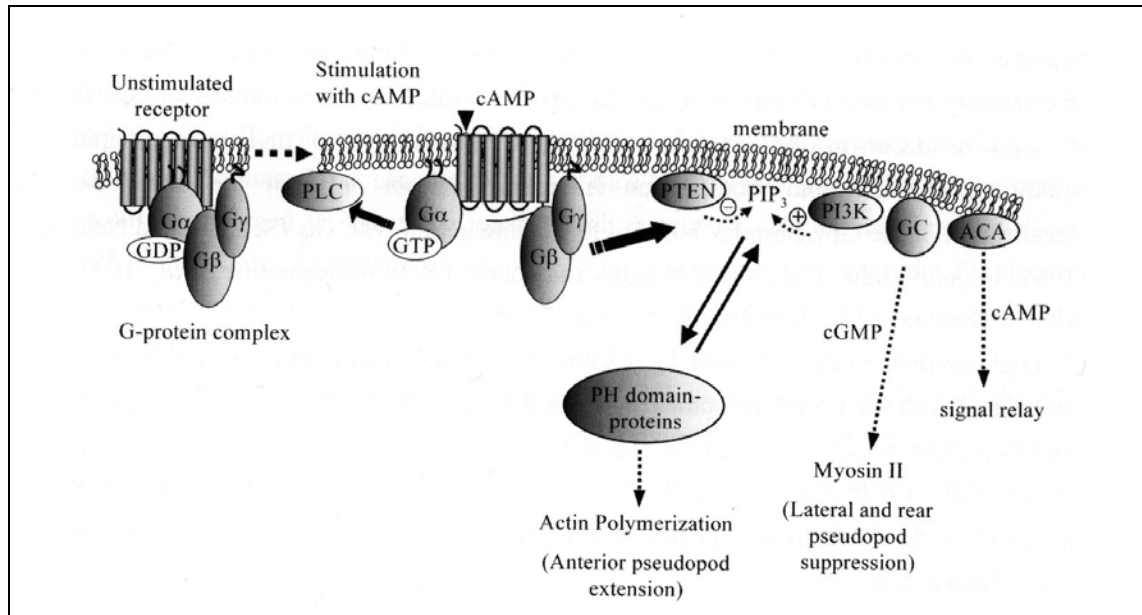


Figure 1.4. Transduction of chemotactic signals. A simplified scheme of the events leading to chemotaxis via transmembrane receptors coupled to heterotrimeric G-proteins. Binding of cAMP molecules stimulates the receptors and results in dissociation of the G-protein complex into G $\beta\gamma$ and G α , which can then activate downstream effectors PLC (phospholipase C), PI3K (phosphoinositide 3-kinase), PTEN (PI3 phosphatase), GC (guanylyl cyclase A). PI3K increases PIP₃ (phosphatidylinositol triphosphate) levels at the membrane leading to translocation of PH (Pleckstrin homology)-domain containing proteins from the cytoplasm to the membrane (Parent, 2003 and Manahan *et al.*, 2004). This step is thought to be responsible for the induction of actin polymerization. PIP₃ is degraded by the phosphatase PTEN. The second messengers cGMP and cAMP produced by GC and ACA (adenylyl cyclase A) are responsible for suppression of lateral and rear pseudopods and for signal relay, respectively (taken from Ruchira, 2005).

outside the cell into directional information inside the cell. A number of proteins are spatially restricted to either the high (the side of the cell experiencing the highest concentration of chemoattractant) or low side of the cell in a gradient (Willard and Devreotes, 2006).

Myosin II and acto-myosin bundles are found at the low side of the cell or back region (Laevsky and Knecht, 2003; Etzrodt *et al.*, 2006) and are thought to participate in contraction, while the actin-binding proteins like CorA and Aip1 are examples of many proteins targeted to the high side of the cell or front region (Fukui *et al.*, 1997; Chen *et al.*, 2003; Etzrodt *et al.*, 2006).

In this work *D. discoideum* cells expressing GFP-LimE Δ or mRFP-LimE Δ , constructs lacking the coiled-coil domain of the LimE Δ of *D. discoideum*, were used to visualize cortical F-actin in live-cell experiments upon cAMP

chemoattractant (Bretschneider *et al.*, 2004; Fischer *et al.*, 2004; Etzrodt *et al.*, 2006).

1.6 Function of cAMP

The evolution of signaling in *D. discoideum* has particularly favored cAMP as a central player. The manifold usages of cAMP are summarized in Figure 1.5 and can be broadly subdivided into its role as first messenger outside the cell and second messenger inside the cell.

Outside, cAMP acts as chemoattractant, which coerces amoebae to convert from solitary predators into gregarious community members (Konijn *et al.*, 1967). cAMP also acts on gene regulation to induce the alterations in phenotype that are required for chemotactic aggregation and for initiation of prespore differentiation (Gerisch *et al.*, 1975b; Kay, 1982; Schaap and Van Driel, 1985). As inhibitor of terminal stalk cell differentiation, cAMP plays a critical role in cell-type choice (Berks and Kay, 1988; Hopper *et al.*, 1993a).

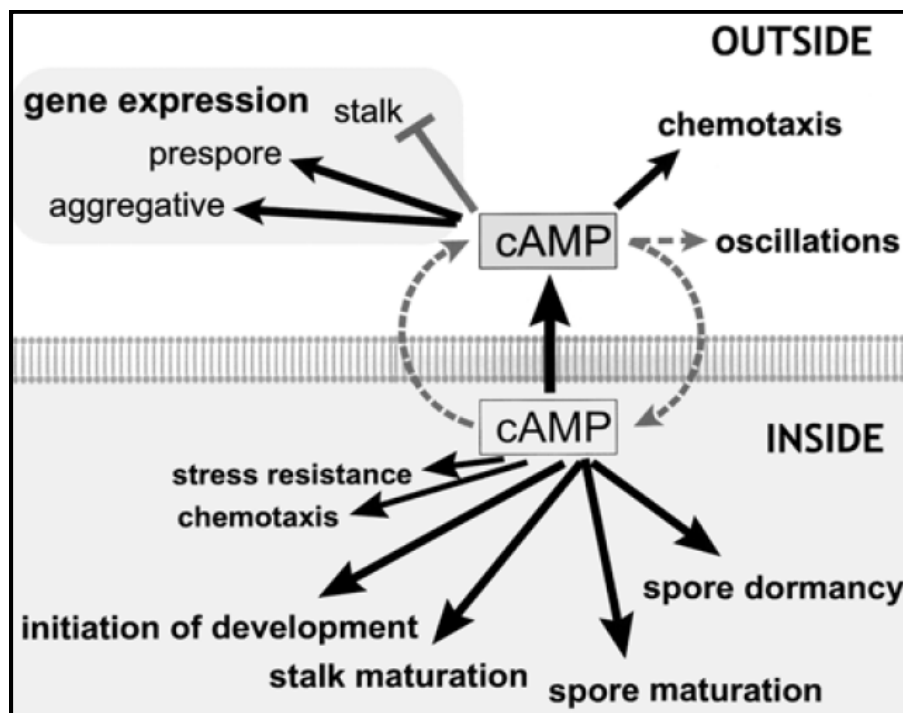


Figure 1.5. Functions of extracellular and intracellular cAMP in *D. discoideum* (taken from Saran *et al.*, 2002).

Within the cell, cAMP triggers initiation of development (Schulkes and Schaap, 1995; Mann *et al.*, 1997), maturation of spores and stalk cells (Harwood *et al.*, 1992; Hopper *et al.*, 1993b; Mann and Firtel, 1993) and maintenance of spore dormancy (Van Es *et al.*, 1996). cAMP also mediates resistance to osmotic stress (Schuster *et al.*, 1996) and contributes to the process of orientation in chemotactic gradients (Wessels *et al.*, 2000). cAMP is transiently synthesized upon stimulation of aggregation competent cells with cAMP. The accumulation of cAMP peaks at 2 min of stimulation (Devreotes and Steck, 1979) and requires the heterotrimeric G-protein G2 (Kesbeke *et al.*, 1988; Kumagai *et al.*, 1989).

1.7 The actin cytoskeleton

The actin cytoskeleton underpins almost every aspect of cellular life, from pinching off the contractile ring during cell division to triggering membrane blebbing during apoptosis. Actin can switch between a filamentous polymer (F-actin) and a monomeric, globular (G-actin) form, a conversion that is central to the dynamic nature of the cytoskeleton.

Each actin monomer binds a molecule of ATP that is rapidly hydrolyzed following polymerization. This creates polarity in an actin filament, such that the 'newest' (barbed) end contains ATP-bound monomers, the neighboring portion of the filament is composed of monomers containing ADP and unreleased-phosphate (ADP-Pi) and the 'oldest' (pointed) end contains ADP-bound monomers from which phosphate has been released (Figure 1.6).

The association and dissociation constants are such that ATP-bound monomers preferentially add to the barbed end, whereas at the pointed end monomers are primarily lost from the filament. Thus, filament growth is driven in the direction of the barbed end (Pollard *et al.*, 2000; Pollard and Borisy, 2003).

Actin polymerization can proceed spontaneously, but elongation (the addition of monomers onto the end of a preexisting filament) is energetically more favorable than nucleation (the polymerization of monomers to form a filament *de novo*). To overcome this kinetic barrier to nucleation, evolution has produced various nucleators like the Arp2/3 complex, spires and formins (Machesky *et al.*, 1999; Yarar *et al.*, 1999).

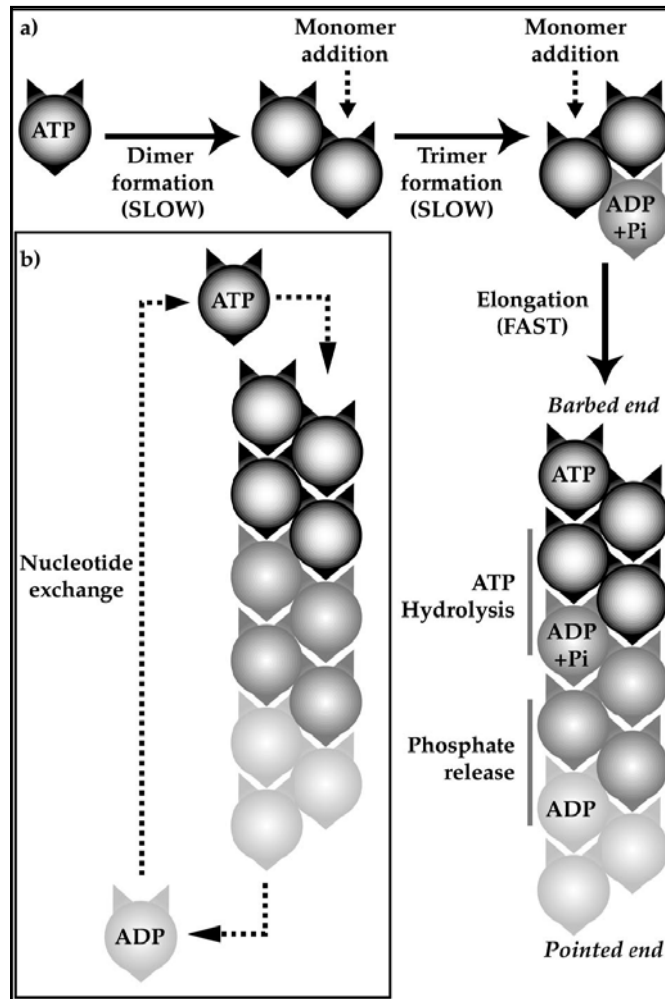


Figure 1.6. The polymerization of actin filaments. (a) The association of individual actin monomers is slow, but assembly onto the end of a preexisting filament (elongation) is rapid. Shortly after polymerization, ATP is hydrolyzed, increasing the likelihood of filament disassembly. (b) The actin filament is polar; monomer addition occurs primarily at the barbed end, and monomer loss occurs mainly from the pointed end (taken from May, 2001).

The dynamics of actin-based structures depends on the rates of polymerization and depolymerization, whereas the diversity of F-actin structures and its associated cellular function relies on a variety of actin-associated proteins.

1.8 Actin-associated proteins in *Dictyostelium discoideum*

The actin cytoskeleton of a cell is required for cell-shape changes, cell motility and chemotaxis, as well as for cytokinesis, intracellular transport

Introduction

processes, development and signal transduction. It is composed of actin, actin-associated proteins and myosin motors. Their interactions are highly dynamic, and constant reorganization of the actin network is required to perform its functions. *D. discoideum* is a valuable and convenient experimental model system to study the role of actin-binding proteins in several actin-dependent physiological processes.

In *Dictyostelium* there are 138 currently known proteins that interact with actin filaments. They are divided into seven different categories (Table I)

Table I. Currently known actin-interacting proteins in *Dictyostelium* (Eichinger *et al.*, 2005).

Class	Proteins
<i>G- actin binding</i>	Profilin (3), Cap (1), Actobinding-like (3), WH2-containing (5), Twinfilin-like (1)
<i>Capping and/or severing</i>	Cap32/34 Aginactin (2), Cofilin (6), Severin (1), GRP125 (1), Gelsolin-related (2)
<i>Actin capping and nucleation</i>	Arp2/3 complex (7), SCAR (1) , WASP (1), WASP-related (2), Vasp (1), Formin (10)
<i>Actin cross-linking</i>	ABP34 (1), eEF1- α ABP50 (2), eEF1- β (3), Dynacortin (1), Fimbrin (1), Fimbrin type ABD-containing (5), Filamin (gelation factor) (1), α -actinin (1), Cortexillin (2), α -actinin type ABD-containing (3), Protovillin (Cap100) (1), Villin-related (1), Flightless/Villin-related (1), Villidin (1), Kelch-related (1)
<i>Lateral actin-binding</i>	Smoothelin-related (1), GAS2-related (1), CH-containing (19), VHP-containing (3), Coronin (1) (CorA) , Coronin-like (1), Aip1 (1) , Coactosin (1), Coactosin-related (3), Abp1 (1), Glia maturation factor-related (1), Lim domain-containing (3)
<i>Membrane-associated</i>	Interaptin (1), Ponticulin (2), Ponticulin-related (2), Comitín (1), Comitín-related (1), Hisactophilin (3), TalinA (filopodin) (1), TalinB (1), SLA-2-like (1), Annexin (2), Vinculin/ α -catenin-related (2)
<i>Motors</i>	Conventional myosins (1) and Unconventional myosins (12)

Proteins printed in bold have been studied in this work. The numbers of proteins found in *Dictyostelium* are indicated between brackets.

(Eichinger *et al.*, 2005). Many of these proteins are also found in metazoa, fungi and plants.

In the following an outline will be given on the actin-associated proteins and complexes that have been investigated in this work. The general information will be set in relation to the specific roles of these proteins in *D. discoideum*.

1.8.1 The Arp2/3 complex

The polymerization and depolymerization of actin filaments is a highly regulated process, and the molecules and mechanisms involved in the regulation of the actin cytoskeleton have been an area of intense study for decades. One crucial component in the regulation of actin polymerization is the Arp2/3 complex.

Arp2/3 associates with the side of a growing actin filament, where it nucleates the formation of a daughter filament at a characteristic 70° angle to the mother filament (Welch and Mullins, 2002). This activity causes the formation of a branched actin network and is required for the formation of a number of actin-based structures (Bretschneider *et al.*, 2004). The actin-nucleating and actin-branching activities of the Arp2/3 complex are activated by nucleation promoting factors (NPFs). These include the 'suppressor of cAMP receptor and Wiskott-Aldrich syndrome protein (WASP) family verprolin homology protein' (SCAR/WAVE) and WASP families of proteins, but might also be modulated by other nucleating factors.

The structure of the Arp2/3 complex

The Arp2/3 complex consists of seven subunits: two actin-related proteins, Arp2 and Arp3, stabilized in an inactive state by five other subunits (Figure 1.7). The accepted nomenclature for these subunits is ARPC1 (for the 40-kDa subunit), ARPC2 (35-kDa subunit), ARPC3 (21-kDa subunit), ARPC4 (20-kDa subunit), and ARPC5 (16-kDa subunit) (Goley and Welch, 2006). Metazoans, fungi, amoebae, and plants express all of these subunits. Upon activation the Arp2 and Arp3 subunits are proposed to form a pseudo-dimer that nucleates actin polymerization. In the crystal structure of the inactive complex, these subunits have been shown to be too far apart to form such a nucleus (Kelleher *et al.*, 1995).

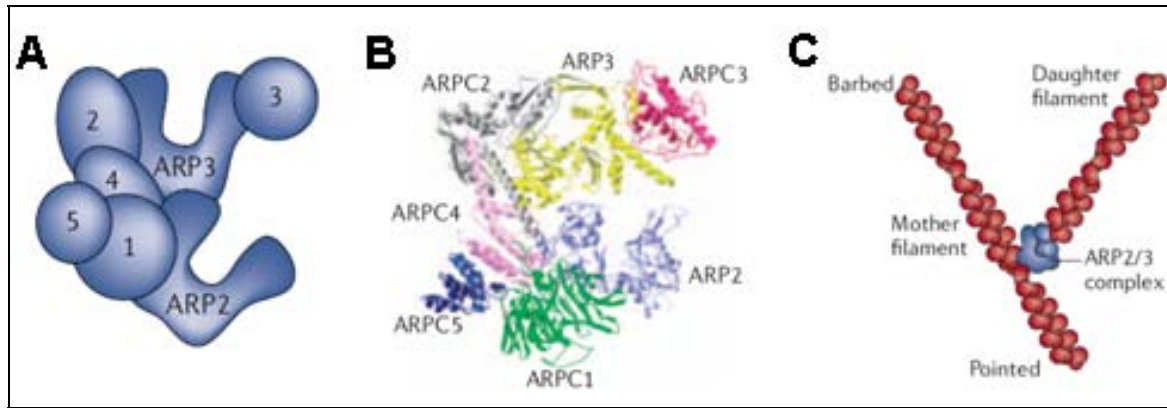


Figure 1.7. Structure and function of the actin-related protein-2/3 (Arp2/3) complex. (A) Cartoon representation of the subunit organization in the inactive Arp2/3 complex. Subunits ARP2, ARP3 and ARP complex-1 (ARPC1) through ARPC5 are labelled as 1-5. (B) Ribbon diagram of the crystal structure of bovine ARP2/3 complex (Protein Data Bank (PDB) accession code 1A8K) with subunits labeled and displayed in different colors. (C) Cartoon diagram of Arp2/3 complex binding to the side of the mother filament and the pointed end of the daughter filament in a y-branch. The two filaments are oriented in a $\sim 70^\circ$ angle (taken from Goley and Welch, 2006).

Regulation of the Arp2/3 complex

The Arp2/3 complex possesses little biochemical activity on its own. However, when engaged by NPF proteins, it is activated to initiate the formation of a new (daughter) filament that emerges from an existing (mother) filament in a y-branch configuration (Goley and Welch, 2006). Recent studies demonstrated the regulation of the Arp2/3 complex via phosphorylation on threonine or tyrosine residues of the Arp2 subunit for actin-nucleating activity. This phosphorylation is necessary but not sufficient for nucleating activity of the complex, which must be stimulated by NPFs. However, NPFs are not sufficient in the absence of Arp2/3 complex phosphorylation (LeClaire *et al.*, 2008).

The mechanism of three Arp2/3-complex NPFs, WASP, neural (N)-WASP and SCAR complex will be discussed below.

1.8.2 WASP and neural (N)-WASP

Under resting conditions, WASP and N-WASP exist in an autoinhibited conformation in which intramolecular interactions between the GTPase-binding domain (GBD) and the central (C) region mask the regions that are required for Arp2/3 activation (Figure 1.8a). WASP-interacting protein (WIP) or related proteins interact with WASP and N-WASP through the WASP-homology-1 (WH1) domains and modulate their activities. The autoinhibition is regulated by binding of the second messenger lipid phosphatidylinositol-(4,5)-bisphosphate (PtdIns(4,5)P₂) to the basic (B) region, the binding of GTP-loaded CDC42 to the GBD region, and the binding of Src-homology-3 (SH3)-domain-containing proteins such as Nck, Grb2 and Toca1 to the poly-proline (PP) region. These factors function both individually and in combination to relieve autoinhibition and to promote Arp2/3 activation. WASP has emerged as a central player in controlling actin nucleation.

In *D. discoideum* cells GFP-WASP preferentially localizes to the leading

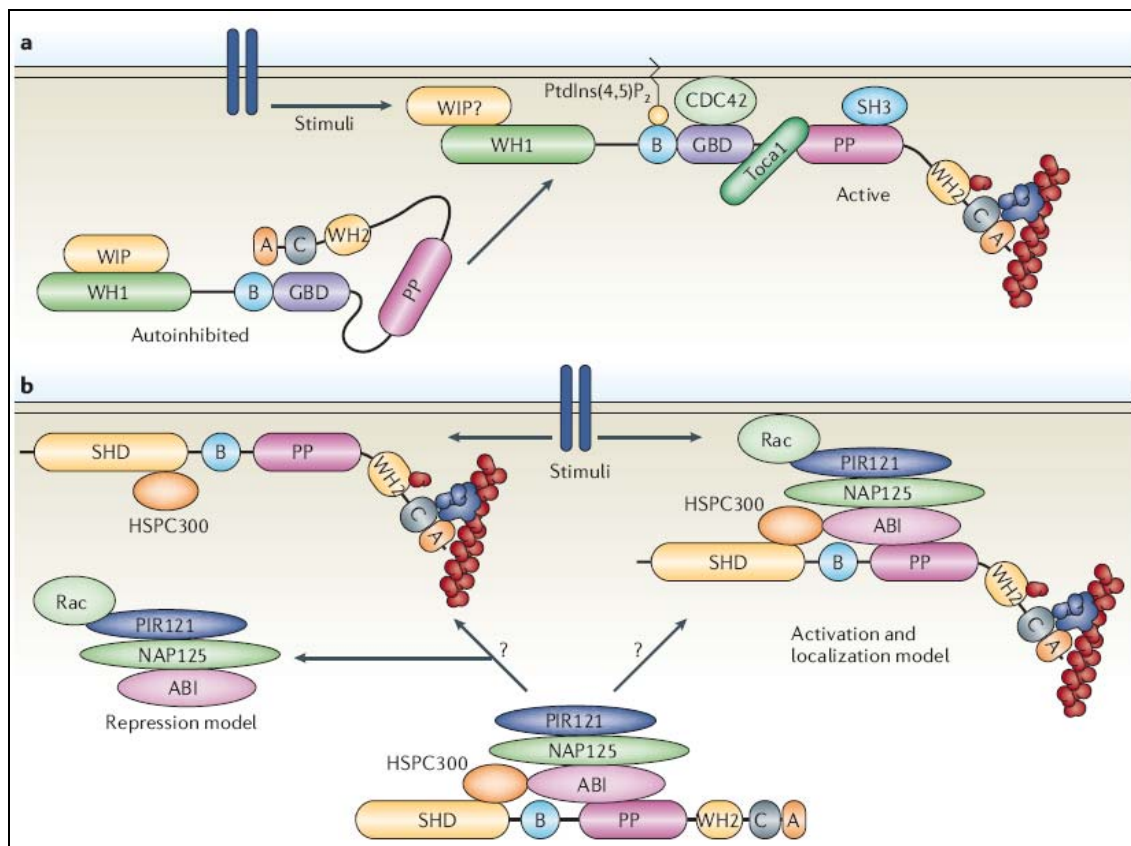


Figure 1.8. Arp 2/3 regulation by signaling pathway involving WASP and SCAR complex (taken from Goley and Welch, 2006).

edge and uropod of chemotaxing cells. *D. discoideum* WASP participates in organizing polarized F-actin assembly during chemotaxis. Cells expressing very low levels of WASP have reduced F-actin levels and significant defects in polarized F-actin assembly, resulting in an inability to establish axial polarity during chemotaxis (Myers *et al.*, 2005 and 2006).

1.8.3 The SCAR complex

During *Dictyostelium* development, the extracellular cAMP functions as a chemoattractant and morphogenetic signal that is transduced via a family of G protein-coupled receptors, the cARs. In a strain where the cAR2 receptor gene is disrupted by homologous recombination, the *D. discoideum* developmental program arrests before tip formation. In a genetic screen for suppressors of this phenotype, a gene encoding a protein related to the Wiskott-Aldrich Syndrome protein was discovered. This protein called SCAR (suppressor of cAR), restores tip formation and most later development to cAR2 strains, and causes a multiple-tip phenotype in a cAR2 strain as well as leading to the production of extremely small cells in suspension culture. The authors conclude the SCAR may be a conserved negative regulator of G protein-coupled signaling, and that it plays an important role in regulating the actin cytoskeleton (Bear *et al.*, 1998).

SCAR was subsequently identified as a WASP-related protein capable of activating the Arp2/3 complex (Machesky *et al.*, 1998 and 1999). SCAR protein forms a complex with four other proteins: PIR121 (p53-inducible mRNA), NAP125 (Non-catalytic region of tyrosine kinase adaptor protein (Nck)-associated protein), Abi1 (Abelson murine leukemia oncogene 1 (Abl)-interactor), and HSPC300 (hematopoietic stem-cell progenitor). Abi and HSPC300 directly bind to SCAR and Abi1 links PIR121 and NAP125 to the SCAR. Upon stimulation, GTP-bound Rac binds directly to PIR121 and leads to SCAR activation. Two models have been proposed to explain the activation of actin nucleation. In the repression model, association of PIR121, NAP125 and Abi with SCAR inhibits the activity of SCAR protein and Rac binding dissociates these factors to activate actin nucleation. In the activation and localization model, binding of activated Rac to PIR121 causes the recruitment of the entire SCAR complex to the membrane, where it can

function in promoting the nucleating activity of the Arp2/3 complex (Goley and Welch, 2006 and Figure 1.8b).

To dissect the roles of the members of the SCAR complex, genetic disruption of these members has been done using *D. discoideum*. Disruption of the SCAR gene, in *D. discoideum* gives rise to small cells with reduced F-actin levels and deficiencies in movement (Bear *et al.*, 1998).

Disruption of the gene encoding PIR121 in *D. discoideum* results in extremely large mutant cells, containing an exceptionally high proportion of F-actin, extending protrusions at an uncontrolled rate all over their surface, and displaying severe defects in movement and chemotaxis. PIR121-nulls cells have very low amounts of full-length SCAR protein but the levels of mRNA remain unchanged. Therefore, a posttranscriptional process, most likely proteolysis, is responsible for the lack of SCAR protein in PIR121-null cells (Blagg *et al.*, 2003). Thus, PIR121 must be essential to protect SCAR against degradation. The double-mutant cells lacking SCAR and PIR121 have reduced F-actin levels, a reduced number of cell protrusions and deficiencies in movement, phenotypes that are similar as in SCAR-null cells (Blagg *et al.*, 2003 and 2004).

The *Dictyostelium* homologue of NAP125 (NAP1) protein forms part of the SCAR complex. NAP1 mutant cells are smaller and less motile than the parent, with smaller actin structures and reduced levels of F-actin. In the absence of NAP1 only a small amount of PIR121 is found, suggesting NAP1 to protect PIR121 from degradation. NAP1-null cells adhered to the substrate less efficiently than either SCAR-null or PIR121-null cells. Therefore, NAP1 might use a mechanism for substrate adhesion that works independently of SCAR and PIR121 function. Therefore, NAP1 seems to have additional functions independent of PIR121 or SCAR protein (Ibarra *et al.*, 2006).

The *Dictyostelium* Abi1 protein forms part of the SCAR complex, as predicted from other organisms. In *D. discoideum* Caracino *et al.* (2007) have shown that SCAR binds to Abi1 *in vitro*. Abi1-null cells move more slowly, are more rounded and extend smaller protrusions than wild-type. These mutants show less severe defects in motility than SCAR-null cells, indicating that SCAR retains partial activity in the absence of Abi1. Furthermore, Abi1-null cells have defective cytokinesis, which is not seen in other SCAR complex mutants and is seen only when SCAR itself is present. The disruption of Abi1 does not result in a SCAR-null

phenotype, but it causes a partial loss of SCAR function during cell migration and incorrect activation of SCAR during cytokinesis (Pollitt and Insall, 2008).

SCAR interacts with Abi1 and HSPC300 via its N-terminal 96 amino acids. Removing Abi1 and HSPC300-binding sites of the SCAR protein leads in *Dictyostelium* to disruption of the SCAR containing complex, loss of SCAR localization, abnormal actin dynamics, aberrant cell adhesion and motility, and failure of normal cytokinesis (Caracino *et al.*, 2007). Therefore, the unregulated SCAR protein has significant deleterious effects on cells. This finding may explain the need to keep SCAR protein activity tightly controlled *in vivo* either by assembly in a complex or by rapid degradation.

In this study, an intriguing phenomenon in SCAR-deficient cells of *D. discoideum* has been discovered and analyzed. Mutants lacking the SCAR protein display an autonomous actin oscillation at the cell cortex (see Results).

In addition to localized activation by SCAR complex, WASP and phosphorylation, Arp2/3 complex is regulated through direct association with coronin.

1.8.4 Coronin

Coronin was first identified in actin-myosin preparations isolated from *D. discoideum* and was shown to bind directly to F-actin *in vitro* and colocalize with F-actin structures *in vivo* (de Hostos *et al.*, 1991). Since then, a wide variety of coronins have been characterized. Some model organisms (e.g., *Saccharomyces cerevisiae* and *Schizosaccharomyces pombe*) have a single coronin gene, while others (e.g., *D. discoideum*, *Drosophila melanogaster* and *Caenorhabditis elegans*) have 2-3 coronin genes and mammals have up to seven different coronin-related genes (Utrecht and Bear, 2006). Most coronins have a characteristic three-part domain layout, consisting of the β -propeller domain, followed by a highly variable 'unique' segment and a C-terminal coiled-coil domain (Figure 1.9).

The β -Propeller Domain

The signature domain of coronin family proteins is the WD-repeat region (de Hostos, 1999). Crystallization of murine Coronin 1A (lacking its coiled-coil domain) revealed that it forms a seven-bladed β -propeller structure assembled from five canonical WD repeats and two noncanonical repeats (Figure 1.9) (Appleton *et al.*, 2006). In addition, two tandem stretches of conserved residues located in the C-terminal extension of the WD-repeat region closely associate with the underside of the propeller, possibly providing additional structural integrity. Although in principle β -propeller structures can support multiple protein-protein interactions, only one binding partner of its propeller domain has been identified, F-actin. Binding to F-actin was first demonstrated for *Dictyostelium* coronin CorA (de Hostos, 1991) and

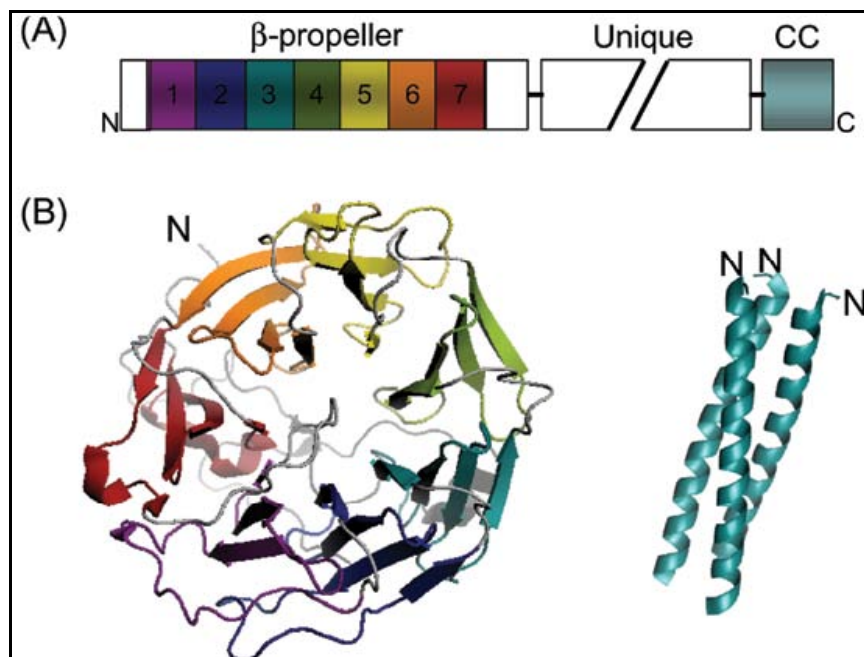


Figure 1.9. Coronin domain organization and protein structure. A) Scheme of coronin domain organization. The β -propeller domain is approximately 400 residues in length and is comprised of seven repeats (5 WD repeats and 2 unconventional repeats; numbered and colored) flanked by short N- and C-terminal extensions (open). This is followed by the unique region (highly variable in sequence and length) and coiled-coil domain (approximately 35-50 residues in length). B) Crystal structures of mouse Coronin 1A β -propeller domain (Appleton *et al.* 2006, 5 PDB accession number 2AQ5) and coiled-coil domain (Kammerer *et al.* 2005, 53 PDB accession number 2AKF). The blades of the β -propeller are color-coded to match the scheme in A. The C-terminal extension (dark grey) associates with the underside of the blades. The coiled-coil domain of Coronin 1A (shown) forms parallel trimers, whereas the coiled-coil domains of some other coronins form dimers. N, amino terminus (taken from Gandhi and Goode, 2008).

later this activity was dissected for yeast coronin, where it was shown that an intact propeller domain is sufficient to bind actin filaments (Goode *et al.*, 1999).

Unique Region

The unique region of coronin is highly variable in length and sequence and its function(s) are poorly understood. Interestingly, the unique regions of *S. cerevisiae* Crn1 and *D. melanogaster* Dpod1 share sequence homology with the microtubule-binding region of mammalian MAP1B and the corresponding purified coronin proteins bind to microtubules and crosslink microtubules and actin filaments *in vitro* (Goode *et al.*, 1999; Rothenberg *et al.*, 2003).

Coiled-Coil Domain

Remarkably, the smallest functional region of coronin, its C-terminal coiled-coil domain (~35-50 residues, 4-7 heptad repeats), mediates at least three different functional interactions (with itself, F-actin and Arp2/3 complex). The first interaction defined for the coiled-coil domain was homo-oligomerization (forming dimers or trimers), which is required for actin filament bundling by coronin (Goode *et al.*, 1999; Spoerl *et al.*, 2002; Oku *et al.*, 2005).

This observation has led to the widely accepted model that coronin bundles actin filaments through multimerization of its β -propeller actin binding site domain (Figure 1.10A). However, oligomerization has only been demonstrated in solution in the absence of F-actin and thus alternative models for bundling remain possible. For instance, bundling may result from individual (non-oligomerized) coronin molecules utilizing two separate actin-binding sites to crosslink filaments (Figure 1.10B). In support of this alternative model, deletion of the coiled-coil domain dramatically weakens the actin binding affinity of coronin (Cai *et al.*, 2007; Gandhi and Goode, 2008). The presence of a second actin binding site in the coiled-coil domain would allow coronin to bundle F-actin by a mechanism using two distinct actin-binding domains (one in the β -propeller, one in the coiled-coil domain). (Gandhi and Goode, 2008 and Figure 1.10B).

The coiled-coil domain of coronin also mediates direct interactions with the Arp2/3 complex both *in vivo* and *in vitro*. (Humphries *et al.*, 2002; Cai *et al.*, 2005; Foger *et al.*, 2006). The specific effects of coronin on Arp2/3 complex activity and

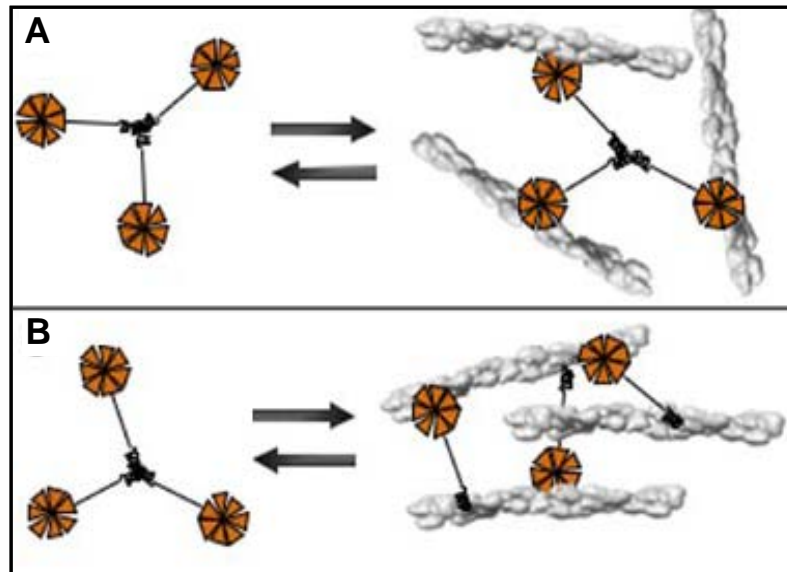


Figure 1.10. Actin filament bundling by coronin. Two possible mechanisms for bundling of filaments by coronin. In the first model (A), coiled-coil mediated self-interaction of coronin multimerizes the F-actin binding β -propeller domain, thereby cross-linking filaments. In the second model (B), a single coronin polypeptide (non-oligomerized) cross-links actin filaments using two distinct actin-binding sites (in the β -propeller domain and coiled-coil domain) and coronin oligomerizes specifically when free in solution (taken from Gandhi and Goode, 2008).

how this interaction contributes to the regulation of cellular actin dynamics are addressed in section on Coronin-Arp2/3 Complex.

All coronins examined to date (with the exception of mammalian coronin 7) bind to F-actin *in vitro* and localize to actin-rich cellular structures, underscoring the conservation and importance of the coronin-F-actin interaction. Genetic disruptions of coronin in *S. cerevisiae*, *D. discoideum*, *C. elegans*, *D. melanogaster*, and mammals have further demonstrated the important roles coronins play in a wide variety of actin-based cellular processes (e.g., phagocytosis, endocytosis, cytokinesis, cell motility) and physiological functions (e.g., early embryonic development and lymphocyte function) (Mishima and Nishida, 1999; Yan *et al.*, 2005; Foger *et al.*, 2006; Cai *et al.*, 2007).

For example, in *Dictyostelium*, coronin localizes to crown-like cortical projections of cells and deletion of the coronin gene causes approximately 3-fold decreases in endocytosis and cell motility, defects in cytokinesis (which in *Dictyostelium* depends on efficient cell migration) and defects in phagocytosis (de Hostos *et al.*, 1993; Maniak *et al.*, 1995).

The mechanisms of coronin underlying these actin-based cellular functions will be described below.

Coronin-Arp2/3 complex

The Arp2/3 complex alone has inherently weak nucleation activity, but can be activated and transformed into a strong nucleator. Activation requires direct binding of Arp2/3 complex to a NPF, such as a WASp/SCAR/WAVE family protein and possibly interaction with the side of a pre-existing mother filament (Goley and Welch, 2006).

The potent nucleation and branching activities of Arp2/3 complex must be tightly regulated in cells. This is achieved by multiple cell signaling pathways, which converge on WASp/SCAR/WAVE proteins and other NPFs to direct spatial and temporal activation of Arp2/3 complex. In addition to localized activation by NPFs, Arp2/3 complex is regulated through direct association with coronin. The first clue to coronin-Arp2/3 functional interactions was the observation that Coronin 1A cofractionates with Arp2/3 complex isolated from neutrophil cell lysates through multiple chromatography steps (Machesky *et al.*, 1997).

Subsequently, a direct interaction between yeast Crn1 and Arp2/3 complex was reported, which was shown to depend on the Crn1 coiled-coil domain (Humphries *et al.*, 2002). Purified Crn1 directly inhibited the nucleation activity of WASp-stimulated Arp2/3 complex *in vitro*. However, inhibition occurred specifically in the absence of pre-existing actin filaments and was relieved fully by the addition of preformed filaments. In the presence of filaments, full-length Crn1, which has a high-affinity interaction with F-actin, recruited Arp2/3 complex to the sides of mother filaments (Goode *et al.*, 1999). These observations led to a model suggesting that coronin has two distinct effects on Arp2/3 complex. It inhibits Arp2/3 complex nucleation activity in regions of the cell where pre-existing filaments are sparse, suppressing spontaneous and/or unbranched nucleation events. On the other hand, in regions where filaments are abundant (e.g., leading edge networks), coronin recruits Arp2/3 complex to the sides of existing filaments, thereby promoting rather than inhibiting nucleation and branching (i.e., coronin reinforces the expansion of existing filament networks) (Humphries *et al.*, 2002). By acting as a spatial regulator of Arp2/3 complex activity, coronin has a net positive effect on the assembly of Arp2/3-dependent filament networks.

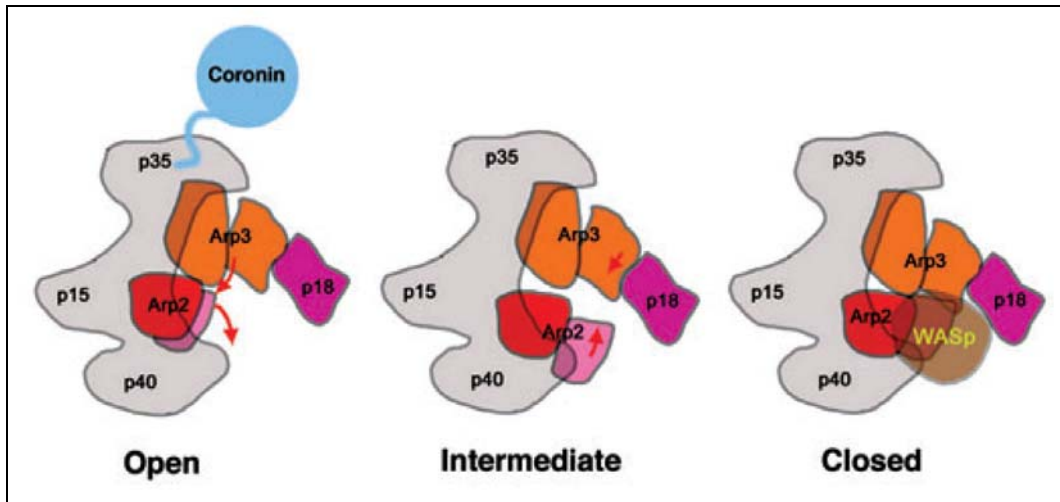


Figure 1.11. Model for structural rearrangements during activation of the Arp2/3 complex. Arrows indicate conformational changes leading to the next structure in the activation sequence. In the transition from the open to the intermediate conformation, Arp2 and Arp3 subunits move toward the center of the gap separating the two subunits. Next there is a further closure of the gap between Arp2 and Arp3 by a movement of Arp2 and Arp3, and possibly a small movement of Arc 18 toward the center of the gap, creating the closed conformation. WASP has been shown to bind to Arp2 and Arp3, and possibly also to p40 stabilizing the closed conformation. Coronin has been shown to bind to p35 stabilizing the open conformation (taken from Rodal *et al.*, 2005).

The molecular mechanism for coronin inhibition of Arp2/3 complex addressed using electron microscopy and single particle analysis to solve the structures of free and Crn1-bound yeast Arp2/3 complexes (Rodal *et al.*, 2005). Free Arp2/3 complex was evenly distributed among three separate conformations- 'open', 'intermediate' and 'closed' (Figure 1.11).

Mutational analysis and docking of the crystal structure of inactive Arp2/3 complex showed that the open conformation of the complex is inactive, whereas the closed conformation is active (primed for nucleation). Crn1 inhibits Arp2/3 complex by stabilizing the open (inactive) conformation. These effects appear to be mediated by a direct interaction between the coronin coiled-coil domain and the p35/ARPC2 subunit of Arp2/3 complex (Figure 1.11).

In summary, the coronin-Arp2/3 complex interaction is highly conserved across distantly related species and depends on a direct physical interaction between the coronin coiled-coil domain and a conserved surface on the p35/ARPC2 subunit of Arp2/3 complex. This interaction is regulated by coronin phosphorylation at Serine 2 in mammalian cells. Binding of coronin stabilizes the open (inactive) conformation of Arp2/3 complex, suppressing actin nucleation until

these inhibitory effects are overridden by association of coronin and Arp2/3 with pre-existing filaments. Coronin actually assists in recruiting Arp2/3 complex to the sides of pre-existing filaments, thereby promoting actin nucleation and branching. Thus, coronin has the unique ability to spatially control Arp2/3 complex activity, selectively promoting the growth and expansion of existing networks. How coronin may affect actin filament branch turnover and Arp2/3 complex recycling remains to be determined.

Here some insights are presented how coronin in *D. discoideum* (CorA) regulates the rate of actin assembly and disassembly (see Results). Coronin seems to participate not only in actin assembly as described above but also in its disassembly. This involvement of coronin in actin disassembly is outline bellow.

Coronin-cofilin activity

While actin nucleation represents one key control point in determining the dynamic behavior of cellular actin networks, an equally important point of control is filament disassembly. Only by maintaining actin polymers in a state of rapid turnover can cells maintain a pool of assembly-competent actin subunits for new growth and reorganize their networks rapidly in response to signals. Replenishment of subunits is accelerated by cellular factors that selectively destabilize and depolymerize the older (ADP-bound) filaments in networks. Cofilin (also called ADF) plays a central role in this process and it has emerged that coronin assists cofilin in driving these events (Aizawa *et al.*, 1995).

Cofilins are a widely conserved family of proteins that accelerate actin network disassembly and are required for dynamic actin-based processes, including cell motility, endocytosis and cytokinesis (Bamburg, 1999). Cofilin binds to the sides of actin filaments in a cooperative manner and increases the twist of filaments, leading to filament severing and disassembly. Cofilin promotes filament disassembly in concert with several other conserved actin-binding proteins, each of which makes a mechanistically distinct contribution to turnover. These include actin-interacting protein 1 (Aip1) (Aizawa *et al.*, 1999; Okada *et al.*, 1999; Rodal *et al.*, 1999), cyclase-associated protein (CAP) (Moriyama and Yahara, 2002; Balcer *et al.*, 2003), twinfilin (Moseley *et al.*, 2006) and coronin (Gandhi and Goode, 2008).

The first clue to the coronin-cofilin functional connection came from genetic interaction studies in yeast, where combining a *crn1Δ* mutation with a hypomorphic cofilin allele (*cof1-22*) caused synthetic defects in cell growth and actin organization (Goode *et al.*, 1999). Similar genetic interactions were observed between *crn1Δ* and *act1-159*, an allele of actin with decreased rates of actin turnover. More recently, it was found that *crn1Δ* causes a 4-fold reduction in rate of actin filament turnover in cells and that purified Crn1 synergizes biochemically with cofilin in severing and disassembling actin filaments (Gandhi and Goode, 2008). This functional interaction between coronin and cofilin appears to be conserved in mammals. Mammalian Coronin 1A and Aip1 are cellular factors required (together with cofilin) to promote the rapid disassembly of *Listeria* actin tails and sustain *Listeria* motility. Together, Coronin 1A and Aip1 accelerated cofilin-mediated disassembly of tails by ~10-fold, with Coronin 1A contributing about ~3-fold to this effect (Brieher *et al.*, 2006).

Here, the simultaneous involvement of CorA and Aip1 during process that involves actin turnover has been investigated in *D. discoideum*. The rate of actin assembly and disassembly has been analyzed and some actin-based process (like phagocytosis, cytokinesis and cell motility) have been monitored in absence of both proteins (see Results).

1.8.5 Actin-interacting protein 1

Actin-interacting protein 1 (Aip1) was originally identified in yeast as one of the actin-interacting proteins using a two-hybrid screen (Amberg *et al.*, 1995). Aip1 is characterized by the presence of WD40 repeats folded into typical β -propellers like CorA. In Aip1 the overall fold is formed by two connected seven-bladed β -propellers (Voegtli *et al.*, 2003), whereas coronin-1 forms one seven-bladed propeller composed of five predicted WD-repeats and two additional blades that lack any homology to the canonical WD40 motif (Appleton *et al.*, 2006).

Aip1 was discovered as a protein that binds to ADF/cofilin by affinity chromatography (Okada *et al.*, 1999). Biochemical studies revealed that Aip1 collaborates with ADF/cofilin to disassemble actin filaments (Okada *et al.*, 1999 and 2002; Rodal *et al.*, 1999; Aizawa *et al.*, 1997 and 1999; Ono *et al.*, 2004).

Actin-depolymerizing factor (ADF)/cofilin is one of the major class of actin-regulatory proteins that accelerate filament disassembly (Southwick, 2000). ADF/cofilin weakly severs filaments without capping ends and also enhances monomer dissociation from the pointed ends (Bamburg, 1999; Bamburg *et al.*, 1999; Carlier *et al.*, 1999; Maciver and Hussey, 2002). However, whether ADF/cofilin contributes to actin dynamics in cells by disassembling "old" actin filaments or by promoting actin filament assembly through their severing activity is a matter of controversy (Hotulainen *et al.*, 2005). Ichetovkin *et al.* (2000) showed that cofilin in *D. discoideum* depolymerizes F-actin by severing filaments, resulting in an increased number of depolymerizing ends.

Aip1 alone has negligible effects on the dynamics of actin filaments. However, in the presence of ADF/cofilin, it induces extensive disassembly of actin filaments. Electron microscopy showed that Aip1 and ADF/cofilin increase a population of short filaments (Okada *et al.*, 1999; Aizawa *et al.*, 1999) suggesting that filament disassembly is due to enhanced filament fragmentation (Figure 1.12).

Intracellular localization of *D. discoideum* Aip1 (here referred to as Aip1) is very similar to that of cofilin (Aizawa *et al.*, 1995 and 1997). It is enriched in dynamic actin-rich structures such as leading edges of motile cells, phagocytic cups, and macropinosomes, but not in a cleavage furrow (Konzok *et al.*, 1999). A null mutation of Aip1 causes reduced rates of growth, cytokinesis, fluid-phase uptake, phagocytosis, and cell motility (Konzok *et al.*, 1999). Overexpression of Aip1 enhances fluid-phase uptake (Konzok *et al.*, 1999) and partially impairs cytokinesis (Aizawa *et al.*, 1999). These cellular events require dynamic regulation of actin filaments, suggesting that Aip1 is important in enhancing the filament dynamics by disassembling filaments. Nonetheless, the phenotypes of Aip1-null cells are not severe, suggesting that Aip1 has a supporting role in actin dynamics mediated by cofilin and/or other actin regulatory proteins. The involvement of Aip1 together with CorA in actin disassembly during actin-related process is the goal of this study (see Results).

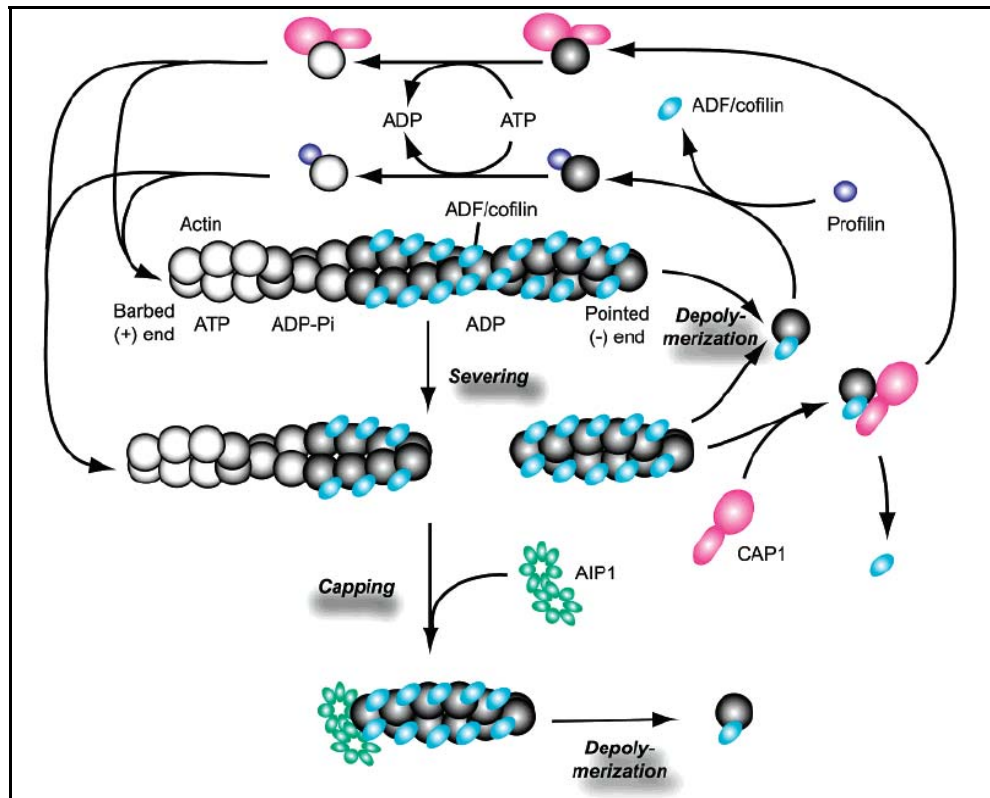


Figure 1.12. Model of the regulation of actin dynamics by ADF/cofilin, CAP1, profilin and Aip1. Actin-depolymerizing factor (ADF)/cofilin preferentially binds to ADP-actin, enhances depolymerization from the pointed ends and severs filaments. Although ADF/cofilin inhibits exchange of actin-bound nucleotides, profilin and CAP1 enhance exchange of actin-bound ADP with ATP and promote barbed-end elongation. Aip1 specifically caps ends of ADF/cofilin-bound filaments and enhances fragmentation (taken from Ono, 2003).

1.8.6 LimE protein

D. discoideum LimE (DdLimE) consists of three domains: an N-terminal Lim domain, a glycine-rich region, and a C-terminal coiled-coil domain. The latter domain comprises seven heptad repeats and is probably responsible for dimerization of the molecule. DdLimE tagged at its C- or N-terminus with GFP (green fluorescent protein) distributes similarly to cortical actin structures as shown by antibody labeling for untagged DdLimE (Prassler *et al.*, 1998).

In growth-phase cells, the GFP-DdLimE fusion accumulates at the leading edge and is recruited to macropinocytic and phagocytic cups. During cytokinesis, the protein is recruited to the polar region of the cell but is, to a lesser extent, also present within the cleavage furrow. In aggregating cells, GFP-DdLimE strongly

labels the actin-rich leading edge that protrudes toward the source of chemoattractant. To study F-actin dynamics in living cells, cells transfected with vectors encoding truncated DdLimE tagged with GFP or mRFP (monomeric red fluorescent protein) lacking the coiled-coil domain have been used. Constructs lacking the coiled-coil domain (here referred to as LimE Δ) localize in a regulated manner to the same actin-rich structures in the cell cortex as full-length DdLimE but with a lower cytoplasmatic background (Schneider *et al.*, 2003).

1.9 Oscillations in cell biology

Oscillations play an important role in many cellular processes. They can emerge as the collective dynamic behavior of an ensemble of interacting components in the cell. Examples include oscillations in cytoskeletal structures such as the axonemes of cilia. Spontaneous oscillations of mechanosensitive hair bundles have been shown to provide frequency selectivity and amplification to mechano-sensation. In some bacteria, oscillations of Min proteins are important for division site selection (Loose *et al.*, 2008). Genetic oscillators form the basis of circadian clocks. All these oscillations share general features. Models and theoretical approaches are essential for an understanding of the principles underlying these dynamic cellular processes (Kruse and Jülicher, 2005).

Active oscillators can generate spontaneous oscillations that continue indefinitely (Murray, 2002). This is in contrast to passive oscillators such as the strings of a piano, where oscillations are damped and die down. Spontaneous oscillations occur only in nonlinear dynamic systems that are open (i.e. there is a continuous flow of energy through the system from its environment) (Strogatz *et al.*, 1994). In the case of spontaneous oscillations, variables of the system change periodically in time. The shape of oscillations can be sinusoidal or follow another periodic function. Oscillations are characterized by their amplitude and their phase. The amplitude is the maximal value a variable attains during a period; the phase indicates the state of the oscillator relative to the beginning of a period.

1.9.1 Oscillations of cytoskeletal structures

During unequal cell division the mitotic spindle is positioned away from the center of the cell before cleavage. In many biological systems this repositioning is accompanied by oscillatory movements of the spindle. One theoretical description for mitotic spindle oscillations has been given by Grill *et al.*, 2001. These authors reported that the cooperative attachment and detachment of cortical force generators to astral microtubules leads beyond a critical number of force generators to spontaneous oscillations.

The generation of forces in cells is mediated by active processes in the cytoskeleton. Cytoskeletal activities can undergo oscillating instabilities, where a non-oscillating state becomes unstable and is replaced by an oscillating one upon changes in parameters. A prototype system is the generation of oscillations by molecular motors (Jülicher and Prost, 1997). A single motor, which generates a force along a filament, will attain a stable displaced state when acting on an elastic spring. If a large number of motors act together, this state can become unstable, resulting in oscillatory motion. A collection of motors can suddenly lose their grip on the filaments when the initial detachment of a few motors induces detachment of the remaining ones. If this collective detachment is followed by a renewed build-up of force, oscillatory motion is generated.

Mechanical oscillations can be of direct importance for the biological function of a cytoskeletal system. An example is the dynamics of axonemes. These are elastic bundles of microtubule doublets that form the motile elements of eucaryotic cilia. Force generation by dynein motors leads to the sliding of microtubule doublets relative to each other, resulting in bending deformations of the bundle. The finding that force-generating systems tend to undergo oscillating instabilities if they act on elastic elements, suggests that motors and microtubules can generate oscillations in the axoneme without any other element being necessary. In this case the bending elasticity of the microtubules provides an elastic element to which motors are coupled (Brokaw, 1975; Camalet and Jülicher, 2000). Wave-like patterns thus result from the non-linear interactions between dynein motors and microtubules (Camalet and Jülicher, 2000; Brokaw, 2002).

Oscillations in force-generating systems can be further illustrated by the motion of some bacteria, such as *Listeria monocytogenes*. This bacterium propels

itself in an infected cell by polymerizing an actin gel on its surface (Theriot *et al.*, 1992). The gel material grows in the form of a comet, which trails the cell. While the velocity of the generated motion is typically constant, some mutants advance in a salutatory manner (Lasa *et al.*, 1997). Theoretical analysis suggests that these oscillations emerge by a dynamic instability of the force-generating system based on the sudden rupture of the gel from the bacterium's surface and rapid subsequent relaxation of the gel (Gerbal *et al.*, 2000; Prost, 2001).

Here, the actin cytoskeleton has been found to generate self-sustained oscillations of actin polymerization and depolymerization in the absence of SCAR and PIR121; two proteins which are involved in actin nucleation (see Results).

1.10 Microfluidic device

Chemotaxis in *D. discoideum* has been studied with classical methods by employing a micropipette (Gerisch *et al.*, 1981) or using a flow chamber (Etzrodt *et al.*, 2006). This work took advantage of a technique using a microfluidic device combined with caged compounds. Microfluidic techniques have been successfully established to generate well-controlled stimuli for single-cell experiments (Breslauer *et al.*, 2006). Stable concentration profiles can be generated ranging from linear (Chiu *et al.*, 2000) to complex periodic gradients (Jiang *et al.*, 2005) as well as exponential and parabolic profiles (Irimia *et al.*, 2006). The combination of a microfluidic device, confocal fluorescence microscopy and a caged compound (see below) allows precise spatial and temporal control of chemoattractant release (Beta *et al.*, 2007). Therefore, this novel combination has been employed to study the temporal responses of actin and actin-associated proteins during chemotaxis.

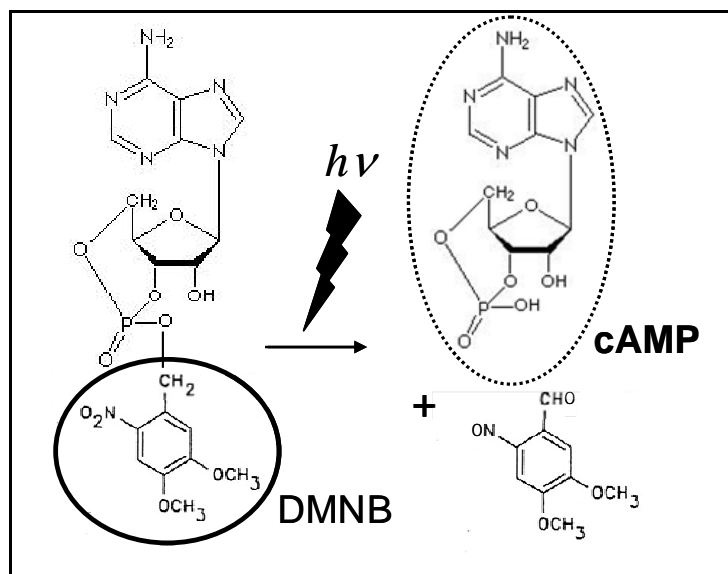


Figure 1.13. The uncaging of cAMP. Caged cAMP with the DMNB group is inactive (left side). A laser flash with a wavelength of 405 nm promotes cleavage of the caging group and release of the active cAMP (right side) (Koizumi *et al.*, 1999).

1.11 Caged compounds

Flash photolysis of ‘caged’ compounds using near-UV light has been used as a means to release biological effector molecules within a living cell on a millisecond and microsecond time scale (Lester and Nerbonne, 1982; Gurney and Lester, 1987; Kaplan and Somlyo, 1999; Marriott *et al.*, 2003).

A variety of caged compounds are available, including caged nucleotides, neurotransmitters and drugs. Caged cyclic nucleotides which rapidly release cAMP or cGMP have been used for *in situ* studies of signaling pathways inside cells (Hagen *et al.*, 1998). These nucleotides can be caged with the 4', 5'-dimethoxy-2-nitrobenzyl (DMNB) group that functionally encapsulates the cyclic nucleotide in an inactive form and affords a rapid photolysis rate (Nerbonne *et al.*, 1984). The DMNB-group is light-sensitive and upon a flash of short wavelength 405 nm ($h\nu$) the caging group is cleaved off, unmasking the biologically active cAMP (Figure 1.13). In this study cAMP caged with a DMNB-group was applied to study the temporal responses of proteins involved in chemotaxis, using *D. discoideum* cells expressing fluorescent proteins in combination with microfluidic technology.

1.12 Aim of this study

The aim of this work was to study the functional organization of the actin system in *D. discoideum* cells. Of particular interest was the role of different actin-associated proteins in regulating the dynamics of the system.

Actin dynamics is characterized by the rapid assembly and disassembly of filaments and its spatial and temporal control. Thus, proteins that are supposed to be involved in these processes were analyzed. In a first step of experiments, the role of the actin-binding proteins coronin (CorA) and Aip1, that are suggested to be involved in the regulation of actin disassembly, was analyzed. In a second set of experiments, the proteins SCAR and PIR121, members of the SCAR complex that interacts with several other proteins and seems to be involved in the regulation of actin assembly, was studied.

The question was what functional impairments in particular with respect to the actin system can be described and analyzed in cells lacking these proteins, and which functional implications for the regulation of the actin system can be deduced from these findings.

2 Materials and Methods

2.1 Materials

2.1.1 Antibodies

Goat-anti-Rabbit Alexa 488 or 594 (Molecular probes)

Goat-anti-Mouse Alexa 488 or 594 (Molecular probes)

Goat-anti-Rabbit IgG Antibody, coupled to alkaline phosphatase (Sigma)

Goat-anti-Mouse IgG Antibody, coupled to alkaline phosphatase (Sigma)

Anti- γ -tubulin anti-Rabbit (Molecular probes)

Monoclonal anti-coronin 176-3-6 (de Hostos *et al.*, 1991)

Monoclonal contact site A - csA- 33-294-17 (Bertholdt *et al.*, 1985)

Monoclonal anti-actin 224-236-1 (Westphal *et al.*, 1997)

2.1.2 Dyes and others

TRITC-conjugated phalloidin (Sigma Chemical Co)

DAPI (4',6'-diamidino-2-phenylindol) (Sigma)

4,5-dimethoxy-2-nitrobenzyl (DMNB)-caged cAMP (Invitrogen Corp., CA)

PALM DuplexDish 35 (dishes for live-cell cultivation, optimized for microdissection)

2.1.3 Antibiotics

Blasticidin S MP (ICN Biomedicals Inc)

Geneticin (G418) (Sigma Chemical Co.)

Hygromycin B (Calbiochem)

Penicillin/Streptomycin (Sigma)

2.1.4 Buffers and solutions

Buffers and solutions not listed below are described together with the method they have been used for.

Soerensen buffer (PB) (Malchow *et al.*, 1972)

14.6 mM KH_2PO_4 , 2 mM Na_2HPO_4 , pH 6.0

10 x PBS

70 mM Na₂HPO₄, 30 mM KH₂PO₄, 150 mM NaCl, pH 7.4

PBS/Glycin

100 mM Glycin in PBS, pH 7.4

5 x Laemmli sample buffer

625 mM Tris/HCl, pH 6.8, 25 % sucrose, 10 % SDS, 0.025 % bromphenol blue, 10 % 2-mercaptoethanol

10 x SDS running buffer

1 M Tris/HCl, pH 8.3, 1 % SDS (w/v), 1 M Glycin

10 x NCP

12,1 g TrisCl, 87,0 g NaCl, 5.0 ml Tween 20, 20g Sodium-azide for 1 l with H₂O, pH 8.0

AX2 Medium (Ashworth and Watts, 1970)

14.3 g/l peptone (Oxoid), 7.15 g/l yeast extract (Oxoid), 18 g/l maltose, 0.5 g/l Na₂HPO₄ · 2 H₂O, 0.45 g/l KH₂PO₄, pH 6.7

Phosphate solid medium

15 g/l bacto agar in PB

SM solid medium

10 g/l peptone (Oxoid), 1 g/l yeast extract (Oxoid), 10 g/l glucose, 20 g/l bacto agar, 1 g/l K₂HPO₄, 2.2 g/l KH₂PO₄, 1 g/l MgSO₄, pH 6.5

2.1.5 Agar overlay (Fukui *et al.*, 1986)

Solutions

- PB (pH=6.0)
- 2% Agarose in PB

Materials

- Slides
- Coverslips (24 x 24 x 0.17 mm)
- Coverslips (50 x 50 x 1.17 mm)
- Scalpel
- Razor blade
-

Procedure

1. Heat the agarose in PB until it is dissolved. Keep the agarose in a warm water bath
2. Put a clean slide onto the bench
3. Put a coverslip (24 x 24 mm, 0.17 mm thick) on each side of the slide and pipette 500 μ l hot agarose onto the slide between the coverslips (as showed in Figure 2.1)
4. Press the agarose with a 5x5 cm coverslip by putting it onto the agarose and pressing it onto the spacer
5. Remove the agarose squeezed out between the coverslips
6. Put everything with the coverslip (5x5 cm) on the bottom of a Petri dish filled with PB and remove the small coverslips (24x24 mm) and the slide with a pair of tweezers
7. Cut the agarose with a scalpel and a razor blade in pieces of about 0.5 x 0.5 cm in size

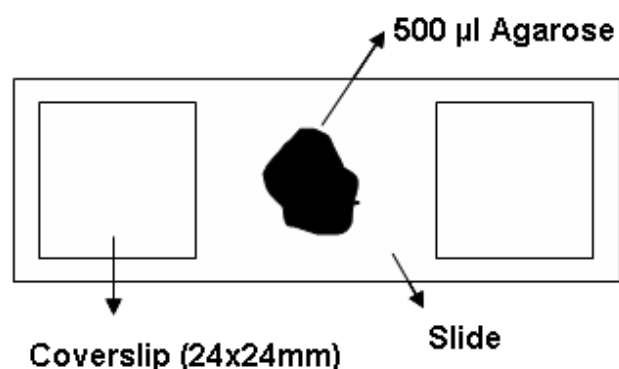


Figure 2.1. Scheme of the slide describing the preparation of agar overlay

2.2 Cell Biological Methods

2.2.1 Cell Culture

Cells of *D. discoideum* were cultivated at 23°C in nutrient AX2 medium, either in shaking culture at 150 rpm or in Petri dishes. To establish chemotactic responsiveness, cells were washed twice with PB and starved in a Petri dish. Alternatively, cells were shaken in suspension at a density of 1×10^7 /ml, and pulsed with 20 nM cAMP at 6-min intervals for 6 to 12 hours, dependent on the cell line analyzed, to stimulate development (Gerisch *et al.*, 1975a). The cell lines used in this work are listed in Table II.

Table II. *D. discoideum* cell lines used in this work

Cell Line	Clone	Strain (#clone)	# Construct	Selection marker
Coronin/ LimE in AX2	99-1-5	Coronin-GFP (# 21-1-2 ,C-terminal)	#395-6 with mRFPM Lim Δ cc	B10/G10
Aip1/ LimE in AX2	2-4-1	Aip1-GFP (# 21-1-2 GFP,C-terminal)	#395-6 with mRFPM Lim Δ cc	B10/G10
Arp3/LimE in AX3	129-4-1	GFP-Arp3 (# 252-12) In AX3	# 492-15 with mRFP-LimE Δ cc	B10/G10
Arp3/ LimE in SCAR-null	4-15	GFP-Arp2/3 (# 252-12) in SCAR-null	# 492-15 with mRFP -LimE Δ cc	G10/H33
Coronin/LimE in SCAR-null	4-7	Coronin-GFP (# 21-1-2 ,C-terminal)	#B12 with mRFP-LimE (Δ cc, C-terminal)	B10/H33
Aip1/LimE in SCAR-null	2-4-18	Aip1-GFP (# 21-1-2 GFP,C-terminal)	#B12 with mRFP-LimE (Δ cc, C-terminal)	G10/H33
LimE in AX2	27-3-5	AX2 (# 214)	#B12 with LimE-GFP(Δ cc, C-terminal)	G20
LimE in AX3	105-4-20	AX3 (provided by R. Insall)	#B12 with LimE-GFP(Δ cc, C-terminal)	G20
LimE in SCAR-null	68-3-2-6	SCAR-null in AX3 (provided by R. Insall)	#B12 with LimE-GFP (Δ cc, C-terminal)	G20
LimE in PIR121-null	66-4-1-14	PIR121-null in AX3 (provided by R. Insall)	#B12 with LimE-GFP (Δ cc, C-terminal)	G20 B10
LimE in SCAR/PIR121-null	67-4-1-15	SCAR/PIR121-null in AX3 (provided by R. Insall)	#B12 with LimE-GFP(Δ cc, C-terminal)	G20 /B10
LimE in Coronin-null	127-2-3	Coronin-null (HG 1569#2)	#411-8 with GFP-LimE (Δ cc, C-terminal)	G20/B10
LimE in Coronin/Aip1-null	11-3-25	Coronin-null (HG 1569) and Aip1-null	#B12 with LimE-GFP(Δ cc, C-terminal)	B7.5/ G10 H33
LimE in Aip1-null	28-1-21	Aip1-null	#B12 with LimE-GFP(Δ cc, C-terminal)	B7.5/G20

G=G418 (geneticin) - stock 20mg/ml
B=Blasticidin - stock 10mg/ml
H=Hygromycin B - stock 33mg/ml

2.2.2 Preservation of *Dictyostelium discoideum*

For long term storage *D. discoideum* cells were subjected to starving conditions, inducing the formation of spores, which can easily be frozen and stored. For the storage, axenically growing cells were washed twice with PB, resuspended at a density of $2-3 \times 10^8$ cells/ml. 500 μ l of the suspension were plated on freshly prepared PB agar plates. Cells formed fruiting bodies containing spores within 2-3 days. The spores were washed off with sterile PB (about 5 ml per plate), shock-frozen in 1 ml aliquots (Nunc 2.2 ml tubes) in liquid nitrogen and stored at -80°C .

2.2.3 Transformation and electroporation of *Dictyostelium* cells

D. discoideum SCAR-null mutant derived from strain AX3 was kindly provided by Robert Insall (Beatson Institute for Cancer Research, UK) and transformed with vectors encoding GFP-CorA (Maniak *et al.*, 1995), GFP-Aip1 (Konzok *et al.*, 1999), GFP-Arp3 (Insall *et al.*, 2001), mRFP-LimE Δ lacking the coil-coiled domain (Fischer *et al.*, 2004) by electroporation.

D. discoideum CorA/Aip1 double-mutant cells derived from *D. discoideum* strain AX2 were kindly provided by Annette Müller-Taubenberger (Ludwig-Maximilians-University of Munich, Germany) and transformed with a vector encoding GFP-LimE Δ .

2.2.4 Cell lines transformed

- a) GFP-Arp2/3 + mRFP-LimE Δ in AX3 cells; selection markers (geneticin G418- 5 μ g/ml and blasticidin 10 μ g/ml)
- b) GFP-Arp2/3 + mRFP-LimE Δ in SCAR-null cells; selection markers (geneticin G418- 5 μ g/ml and hygromycin 10 μ g/ml)
- c) GFP-CorA + mRFP- LimE Δ in SCAR-null cells; selection markers (blasticidin 10 μ g/ml and hygromycin 10 μ g/ml)
- d) GFP-Aip1 + mRFP-LimE Δ in SCAR-null cells; selection markers (geneticin G418- 5 μ g/ml and hygromycin 10 μ g/ml)

For electroporation, the cells were cultivated axenically in suspension culture to a density of 3×10^6 cells/ml, then chilled on ice and washed in ice-cold

17 mM Na/K-phosphate buffer, pH 6.0 (PB). The cells were washed once more and resuspended in cold PB at a concentration of 1×10^8 cells/ml.

35 μ g DNA was mixed with 800 μ l of AX3 or SCAR-null cell suspension. The mixture was transferred to a chilled cuvette (4-mm) and the cells were electroporated with the Bio-Rad Gene Pulser set at 1 kV and 3 μ F. After poration the cells were transferred to a well of a Costar dish and incubated at room temperature for 15 min. Subsequently, 100 mM CaCl_2 and MgCl_2 were added to a final concentration of 1 mM each and the cells were shaken gently for 15 min at 23°C. From this well the cells were transferred to a Petri dish with 10 ml of nutrient medium. The plate was incubated for 24 h before changing the medium and adding the appropriate selection marker.

To get an individual clone, the cells were resuspended from the Petri dish and 150 μ l of cell suspension were spread to *E.coli* plates. After 5 days the individual colonies were picked up with a sterile wood stick and transferred to a well with 1 ml of nutrient medium. After 3 days fluorescent clones were selected by microscopic inspection.

2.2.5 Other cell line transformed

e) GFP-LimE Δ in CorA/Aip1-null cells (blastocidin, 7.5 μ g/ml; geneticin G418 5 μ g/ml; and hygromycin, 10 μ g/ml).

For electroporation the cells were cultivated axenically in suspension culture and adjusted to 1×10^8 cells/ml as described above.

35 μ g DNA was mixed with 800 μ l of CorA/Aip1-null cell suspension and the mixture electroporated as described above. After poration the cells were transferred to a well of a Costar dish and incubated at room temperature for 15 min. Subsequently, 100 mM CaCl_2 and MgCl_2 were added to a final concentration of 1 mM each and the cells were shaken gently for 15 min at 23°C. The cells were transferred to a Petri dish with 10 ml of nutrient medium. The selection markers were added 5 days after the transformation. The plates with the transformants fluorescent cells were checked. Only few transformed cells showed fluorescence. To optimize the selection of these transformants, the few fluorescent cells were isolated using laser microdissection (see below) and subsequently recultivated.

2.2.6 Cell isolation via Laser Microdissection and Pressure Catapulting

To generate enriched cell cultures of GFP-LimEΔ expressing cells, fluorescent cells were isolated for subsequent re-cultivation using the PALM MicroBeam system (Carl Zeiss). This system employs the technique of laser microdissection followed by pressure catapulting (Figure 2.2).

A pulsed UV-A laser (ultra-violet, 355 nm) is coupled into an inverted research microscope (AxioObserver, Carl Zeiss) and focused via the objective lens to a micron-sized spot diameter. Using a laser in the UV-A-range offers the

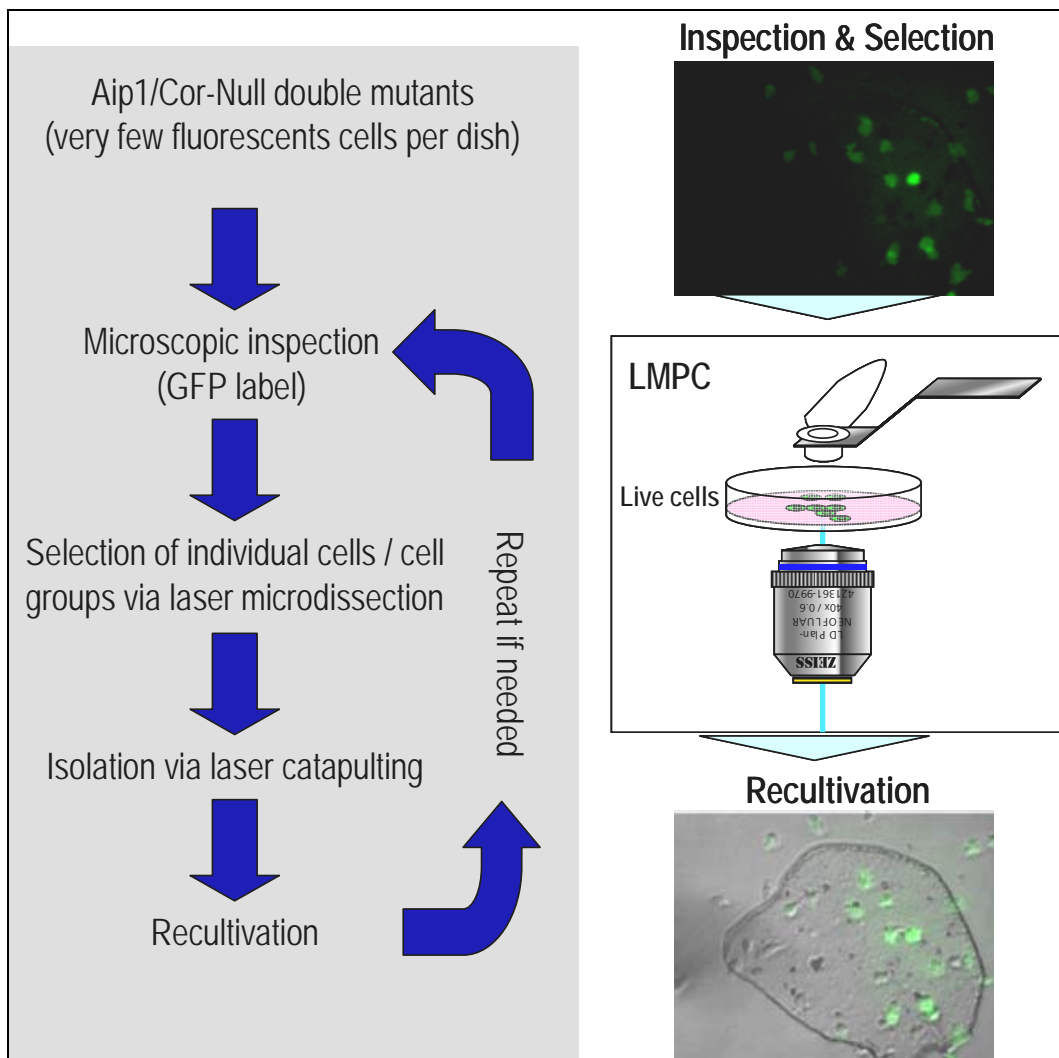


Figure 2.2. The fluorescent cells were visualized with a fluorescence microscope using a 488 nm laser, and selected with a software-controlled laser beam and catapulted by a laser pulse into an Eppendorf cap. Subsequently the cell was transferred to a new Petri dish with fresh medium for recultivation.

advantages that a higher spatial resolution can be achieved than with IR-lasers (infrared, 1064 nm). In addition, radiation in the UV-A-range (between 320 nm and 400 nm) lies well outside of the local absorption maxima of DNA (260 nm) and proteins (280 nm). Therefore no harm to biomolecules occurs, neither to tissue nor to living cells is expected. Only in the narrow laser focus the energy is sufficient to ablate material and to cut around the cells of interest (laser microdissection), whereas the surrounding tissue remains unaffected. This process relies on plasma formation supported by linear absorption. The formation and breakdown (collapse) of this locally restricted plasma take place during nanoseconds. There is no time for heat transfer into the neighbouring cells or tissue. Using the high energy which is created by the laser pulse selected material is lifted up into a capture device (pressure catapulting) (Vogel and Venugupalan, 2003).

This is a non-contact process, as only focused light is used for the transport of the selected area, thus avoiding the risk of contamination of the isolated samples. Only the fluorescent cells expressing GFP-LimE Δ have been selected, catapulted and collected in an Eppendorf cap. They were transferred to Petri dishes with new medium to be re-cultivated.

2.2.7 Microfluidic device

Microfluidic channels of width $x = (500 \pm 0.5) \mu\text{m}$, length $y = (3000 \pm 0.5) \mu\text{m}$, and height $z = (25 \pm 0.5) \mu\text{m}$ were produced by standard soft lithography techniques. Channels were produced by molding premixed polydimethylsiloxane (PDMS, Sylgard 184, Dow Corning, MI) against the “master” wafer. Inlets and outlets were punched through the PDMS using a sharpened syringe tip (19 GA x 1”, McMaster, NJ), and the channels were sealed with a glass coverslip (24 x 60 mm, #1, Gerhard Menzel Glasbearbeitungswerk GmbH & Co. KG, Germany) for 2 min treatment in air plasma (PDC-002, Harrick Plasma, NY). The microfluidic device is shown in Figure 2.3 (See Beta *et al.*, 2007 for details about the device). The microfluidic device and all the uncaging experiments have been performed in collaboration with Eberhard Bodenschatz’s group from the Max Planck Institute for Dynamics and Self-Organization in Göttingen.



Figure 2.3. Image of microfluidic device with three microchannels in parallel. At the middle microchannel there are the inlet and outlet connected with the tubing in both extremities.

Solution delivery

Teflon tubing (#39241, Novodirect GmbH, Germany) was used to connect the microfluidic device to a non-peristaltic syringe pump (PHD 2000, Harvard Apparatus Inc., US), operated with a 500 μ l gas-tight glass syringe (1750 TTLX, Hamilton Bonaduz AG, Switzerland) to maintain a constant flow of phosphate buffer through the channel. The flow velocity was 111 ± 2 μ m/second unless stated otherwise. In preparation for stimulation of *D. discoideum* cells 10 μ M of 4,5-dimethoxy-2-nitrobenzyl (DMNB)-caged cAMP (Invitrogen Corp., US) was added to the flow.

2.2.8 Fluorescence microscopy and photo-activation

Imaging was performed with an inverted confocal laser scanning microscope (Fluoview FV1000, Olympus Corp., Japan). It was equipped with an additional scanning unit to move a 405-nm laser (25 mW, FV5-LD405, Olympus Corp., Japan). Separately from the imaging lasers inside the field of view. Before the experiment, a microfluidic channel with starved, chemotactically responsive cells was mounted on the microscope with the coverslip toward the objective. Photo-activation was initiated by rapidly scanning the 405-nm laser over a defined region in the flow upstream of a cell (Figure 2.4).

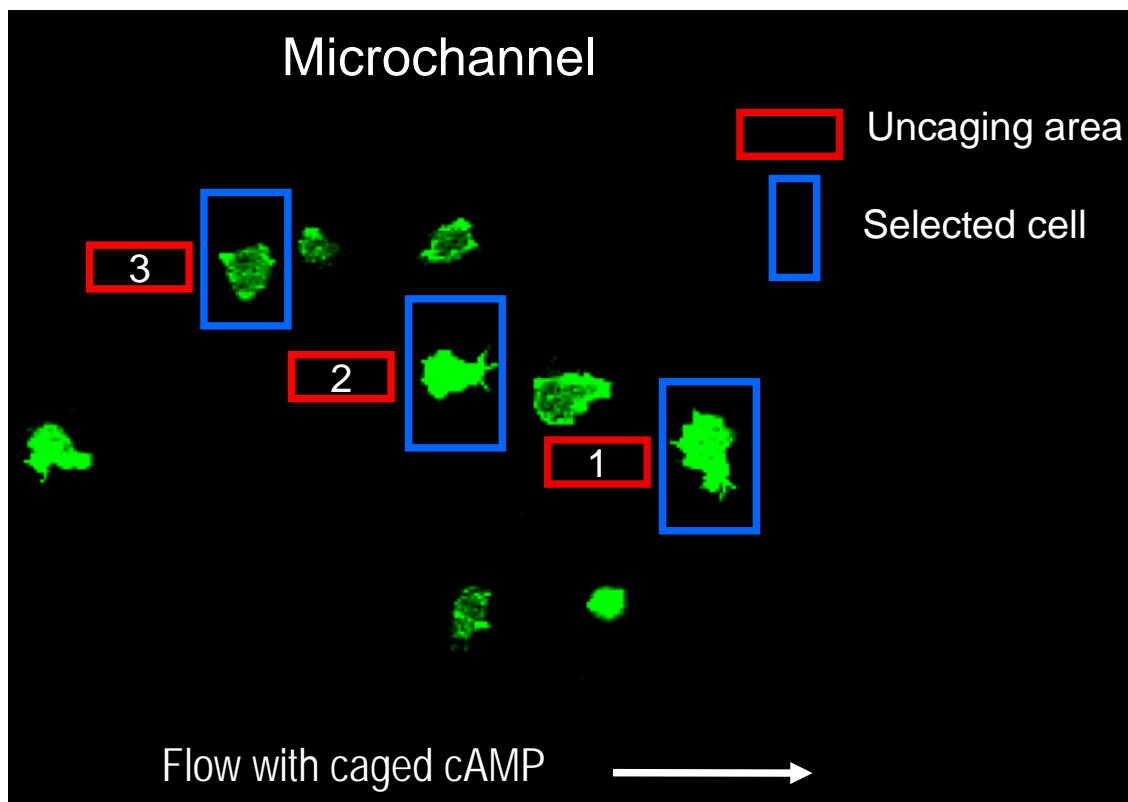


Figure 2.4. Image of a microfluidic channel showing *D. discoideum* cells (green) attached on the bottom glass plate of the channel. The blue rectangles are drawn to select the cell to be stimulated with cAMP. The red rectangles are drawn to select the area illuminated by the uncaging laser. The flow with the caged cAMP is running from the left to the right side. The numbers inside the red rectangles indicate the upstream sequence of uncaging and recording, to stimulate non-exposed cells by the flow of uncaged cAMP.

2.2.9 Image processing

Single cells were tracked and fluorescence intensities in the cortex and interior of these cells were calculated using the QuimP package (Dormann *et al.*, 2002) for the ImageJ software (<http://rsb.info.nih.gov/ij>). QuimP uses an iterative active contour algorithm to automatically outline the cell perimeter, which is characterized by a local high contrast between the bright cell border and the dark background. The cell outline, the “outer chain”, is shrunk by a certain number of pixels and yields the “inner chain” as a closed contour, which separates the cell cortex from the interior. 100 equidistant lines are created which connect the inner and outer chain. The maximum intensity along each line is determined and the average of all 100 maxima defined as the “cortical intensity”. All of the proteins studied are enriched close to the plasma membrane. Therefore, the maxima

determined along the segmented cortical layer provide a measure that does not depend on the distance between outer and inner chain. The averaged grey values enclosed by the inner chain define the fluorescence intensity of the cell interior. As a measure for cAMP-induced responses, the ratio of fluorescence intensities in the cortex and interior of the cells was calculated. Using this measure, variations in expression levels or in illumination, and also changes caused by bleaching are canceled out. After cAMP-stimulation, the GFP- or mRFP-tagged proteins served as an internal reference for timing the cortical accumulation in the cell cortex. Only cells that showed a clear peak in the red and green signal were included into the analysis.

2.2.10 Total Internal Reflection Fluorescence (TIRF) Microscopy

To analyze the details of actin dynamics close to the substrate total internal reflection fluorescence (TIRF) microscopy was applied to the highly motile cells of *D. discoideum*. TIRF microscopy selectively illuminates structures within an evanescent field extending only about 150 nm from the substrate surface into the cell. In *Dictyostelium* cells the membrane-anchored actin filament network has a thickness of 100-200 nm (Hanakam *et al.*, 1996), meaning its entire structure is amenable to visualization by TIRF microscopy.

The TIRF experiments were done in collaboration with Stefan Diez's group at MPI-CBG in Dresden, using a Zeiss Axiovert 200M microscope setup. For details about the setup see Diez *et al.* (2005). For Figure 5.10 (G-I) red/green colored consecutive frames were superimposed with Image J software (<http://rsb.info.nih.gov/ij/>) with customized macros and plugins.

2.2.11 Micropipette assay

To record chemotactic responses, cells were washed twice in PB, and shaken at a density of 1×10^7 cells/ml in PB and pulsed with 20 nM cAMP at 6 min intervals for 7 to 8 hours. The cells were transferred into an open chamber and were stimulated with a micropipette filled with 10^{-4} M cAMP. Confocal images were taken at intervals of 20 seconds using an inverted Carl Zeiss LSM 410 microscope with a 100 x Neofluar 1.3 oil-immersion objective or a Carl Zeiss LSM 510 Meta

microscope with a 63 x Neofluar 1.3 oil-immersion objective. For excitation, the 488 nm argon-ion laser line was used, and emission was collected using a 510-525 nm band-pass filter.

2.2.12 Phagocytosis assay

A *D. discoideum* culture was diluted to 1×10^6 cells/ml with nutrient medium and the cells were allowed to settle on a coverslip to which a plastic ring of 2 cm diameter was sealed with silicone. After about 15 min the medium was removed and the cells washed 1x with PB. 500 μ l of a suspension of heat-killed cells of the yeast *Saccharomyces cerevisiae* diluted in PB (Maniak *et al.*, 1995) were added to the cells. One piece of agar overlay (0.5 x 0.5 cm) was put onto the cells. The medium was gently removed by a piece of tissue paper. One coverslip (24 x 24 x 0.17 mm) was put on the top of the ring to minimize the evaporation of the solution. Phagocytosis was recorded at 10 second intervals using a Carl Zeiss LSM 510 Meta microscope.

2.2.13 Cell velocity assay

To measure cell movement GFP-LimE Δ -expressing cell lines of the wild-type AX2 (Diez *et al.*, 2005) and CorA-null, Aip1-null (Etzrodt *et al.*, 2006), and CorA/Aip1-null mutants (this study) derived from this strain were recorded. Time series were recorded at intervals of 30 seconds for 30 min in the growth phase or aggregation-competent stage using a Carl Zeiss LSM 510 Meta confocal microscope equipped with a 40 x Neofluar 1.3 oil immersion objective. Images were analyzed using the Image J software package and a custom-made plug-in for cell motility analysis that was kindly provided by Till Bretschneider (University of Warwick, UK). The velocity is based on computing the translocation of the cell's centroid (cell's center of mass). Results from six to seven experiments for each strain in growth and developmental stage were pooled.

2.2.14 Immunofluorescence labeling

Cells of an exponentially growing *D. discoideum* culture were diluted to 1×10^6 cells/ml with nutrient medium and allowed to settle on a round coverslip. After

about 20 min the medium was removed and the cells were fixed with 15% picric acid/2% formaldehyde in 1% PIPES, pH= 6.0 for 20 min and post-fixed with 70% ethanol for 10 min (Humbel and Biegelmann, 1992). After post-fixation, cells were washed once with 10 mM PIPES and twice with 1% PBS/Glycin. The cells were incubated with 2% BSA/PBS for 1 hour. Immunolabelling to identify chromosomes, nucleus and actin was carried out by incubating the fixed samples with primary antibodies anti α -tubulin diluted in 1 % BSA/PBS or with antiserum at room temperature for 1 h. Unbound antibodies were removed by 3 x 5 min washes with 1% PBS/Glycin and the samples were incubated for 1 h with the respective secondary antibodies anti-mouse (10 μ g/ml Alexa 488 or Alexa 594 conjugates), including DAPI (1 μ g/ml) to visualize nuclear DNA or TRITC-conjugated phalloidin (1:100 from stock solution 0.1 mg/ml) to visualize F-actin. Coverslips were mounted in Gevatol (Langanger *et al.*, 1983) and kept overnight at 4° C.

2.3 Biochemical Methods and Immunoblotting

2.3.1 SDS-Polyacrylamide gel electrophoresis (PAGE)

Proteins were separated on discontinuous SDS-polyacrylamide gels (Laemmli, 1970). 12.5 % polyacrylamide gels were prepared and run in Biorad minigel System chambers at 30 mA per gel for 45 min. Samples and high-molecular weight standard (Sigma) were mixed with 1/4 volume 5 x Laemmli sample buffer (Laemmli, 1970).

2.3.2 Coomassie blue staining

Gels were stained for 30-60 min in Coomassie blue staining solution, rinsed with H₂O and destained with 10 % acetic acid. Gels were scanned (Epson 1200 Photo) and dried between two sheets of cellophane stretched by a plexiglas frame.

Staining solution

7.5 % acetic acid, 50 % methanol, 0.25 % Coomassie Brilliant Blue R250 (Sigma).

2.3.3 Western blots and immunostaining

Polyacrylamide gels were blotted by the semidry procedure using the buffer system of Kyhse-Anderson (Kyhse-Anderson, 1984). Blotting was carried out for 1 h at 1 mA/cm² and blots were reversibly stained with 0.1% Ponceau S (Sigma) in 5 % acetic acid prior to immunostaining. Marker bands were labeled on the blot before blocking in 4% BSA in 1x NCP at room temperature for 1 hour. Incubation with the primary antibody diluted in 1% BSA in 1x NCP was carried out for 1 h at room temperature, followed by washes in 1x NCP (3 x 5 min) and incubation with the secondary of anti-rabbit or anti-mouse antibodies coupled to alkaline phosphatase diluted in 1x NCP for 40 min at room temperature. Blots were washed 4 x 5 min with 1x NCP and color was developed by 5-30 min incubation in alkaline phosphatase reaction buffer (100 mM Tris/HCl pH 9.5, 100 mM NaCl, 50 mM MgCl₂) supplemented with 4.5 µl/ml NBT (75 mg/ml stock in 70 % dimethylformamide) and 3.5 µl/ml BCIP (50 mg/ml in demethylformamide). Alternatively, antibody bound were detected using ECL kit detection system (GE Healthcare Amersham RPN 2106), according to the instructions of the manufacturer. Luminescence was detected by exposure to x-ray films.

2.3.4 Estimation of the G-/F-actin ratio

Following the procedure of Gräf *et al.*, (1998) cells were cultivated in Petri dishes to approximately 50% confluence yielding about 3 x 10⁶ cells per ml. Subsequently, the nutrient medium was exchanged by PB with or without 0.2 mM latrunculin A (Sigma, Deisenhofen, Germany) and cells were incubated for 1 h at room temperature. Cells were lysed on ice by the addition of 2 ml of ice cold lysis buffer (80 mM Na-PIPES, pH 6.8, 5 mM EGTA, 5 mM MgCl₂, 1 mM dithiothreitol, 1% Triton X-100, 25% glycerol, and protease inhibitors. 250 µl of the lysate were centrifuged at 80,000 rpm for 40 min at 4°C using a Beckman TLA100 rotor. The pellet containing the F-actin fraction was resuspended in 250 µl of lysis buffer. Both the pellet fraction and the supernatant containing G-actin were supplemented with SDS-gel loading buffer and separated by SDS-gel electrophoresis followed by *Western blot* analysis. Blots were stained using monoclonal antibody 224-236-1 against *D. discoideum* actin (Westphal *et al.*, 1997). Actin bands were visualized

using an enhanced chemiluminescence kit (GE Healthcare Amersham ELC *Western blotting* Detection Reagents RPN 2106).

2.3.5 Quantitative F-actin assay

To determine the F-actin content of whole cells the specific binding of tetramethylrhodaminyl (TRITC)-phalloidin to F-actin was used, followed by the extraction of the fluorescent conjugate in methanol (Howard *et al.*, 1985; Defacque *et al.*, 2000). For each experiment, samples were prepared in triplicates to minimize errors in the number of cells, and each experiment was repeated at least twice. The number of each cell line was standardized according the same amount of total protein and seeded into a well of a Costar dish for 20 min at 23 °C. Then the medium was removed and 200 μ l of cold 6% paraformaldehyde was added. After fixation for 15 min, cells were washed twice with phosphate buffer, pH 7.2. For permeabilization 0.1% Triton-X 100 was added for 3 minutes, and cells were washed twice in phosphate buffer. To minimize unspecific binding of TRITC-phalloidin to other proteins, permeabilized cells were treated with 1% BSA/phosphate buffer for about 30 minutes and washed once in the same buffer. Then 200 μ l of the staining reagent containing TRITC-phalloidin 0.2 μ g/ml diluted in phosphate buffer was added in the dark for 30 minutes. Cells were washed three times with phosphate buffer before the addition of 500 μ l of absolute methanol per well and extracted in the dark for 1 h at room temperature. After extraction, 300 μ l of the methanol solution were removed and transferred to rectangular cuvette QS-1000, 10 mm optical path (Hellma Optik, Jena, Germany). The fluorescence intensity of the extracted TRITC-phalloidin was determined in a spectrophotometer (Bio-Rad-SmartSpec Plus) at 550 nm excitation and 570 nm emission. The total protein content of each cell line was measured by a Lowry protein assay using Bio-Rad DC Protein Assay Kit (Lowry *et al.*, 1951). The F-actin content for each cell line is plotted in Figure 3.2.B as the fluorescence intensity of TRITC-phalloidin corresponding to the F-actin content relative to the total amount of protein.

3 Results

Actin-filament turnover mediated by coronin and Aip1 is required for proper cytokinesis, phagocytosis and motility in D. discoideum

Dynamic rearrangement of the actin network is necessary for a number of basic cellular processes like cytokinesis, phagocytosis and motility. In *D. discoideum* coronin (CorA) and actin-interacting protein 1 (Aip1) are regulating actin dynamics during these processes (de Hostos, 1999; Konzok *et al.*, 1999). Here, the consequences of the elimination of these proteins in *D. discoideum* cells deficient of either CorA or Aip1 (single-mutants) or deficient of both proteins (double-mutants) have been investigated.

In summary, double-mutant cells are characterized by an increase of filamentous actin compared to wild-type and single-mutant cells. This predominance of F-actin causes severe consequences for actin-dependent cellular functions: during cell division some CorA/Aip1-null mutant cells show defects in centrosome attachment and chromosome segregation. The cytokinesis is impaired resulting in multinucleate cells. The early phase of double-mutant development is retarded by about 4 hours in comparison to wild-type development. In the absence of CorA and Aip1 the formation of a phagocytic cup, from inception until the complete engulfment of a particle, is prolonged in comparison to wild-type cells, and cell motility is slowed down.

In conclusion, cells lacking both CorA and Aip1 are unable to rapidly rebuild their filamentous actin and this inability may lead to the observed impairment of actin-dependent processes like cytokinesis, phagocytosis and cell motility.

3.1 CorA/Aip1-null mutants have high filamentous actin content

The phenotypes of *D. discoideum* wild-type and CorA/Aip1-null cells expressing a marker for F-actin (GFP-LimE Δ) were compared using confocal microscopy. The double-mutant cells showed a stronger GFP-LimE Δ fluorescence label at the cell cortex, where F-actin is localized (Figures 3.1A and 3.1B). In additional experiments, a mixture of wild-type and CorA/Aip1 double-mutant cells was labeled with TRITC-phalloidin to visualize F-actin in fixed cells under exactly the same conditions (Figure 3.1C-E). Wild-type cells were distinguished from double-mutant cells by immunolabeling using anti-coronin antibodies (Figure 3.1C). The double-mutant cells showed a highly increased phalloidin labeling at the cortex, indicating a higher F-actin content (Figure 3.1D). This is consistent with

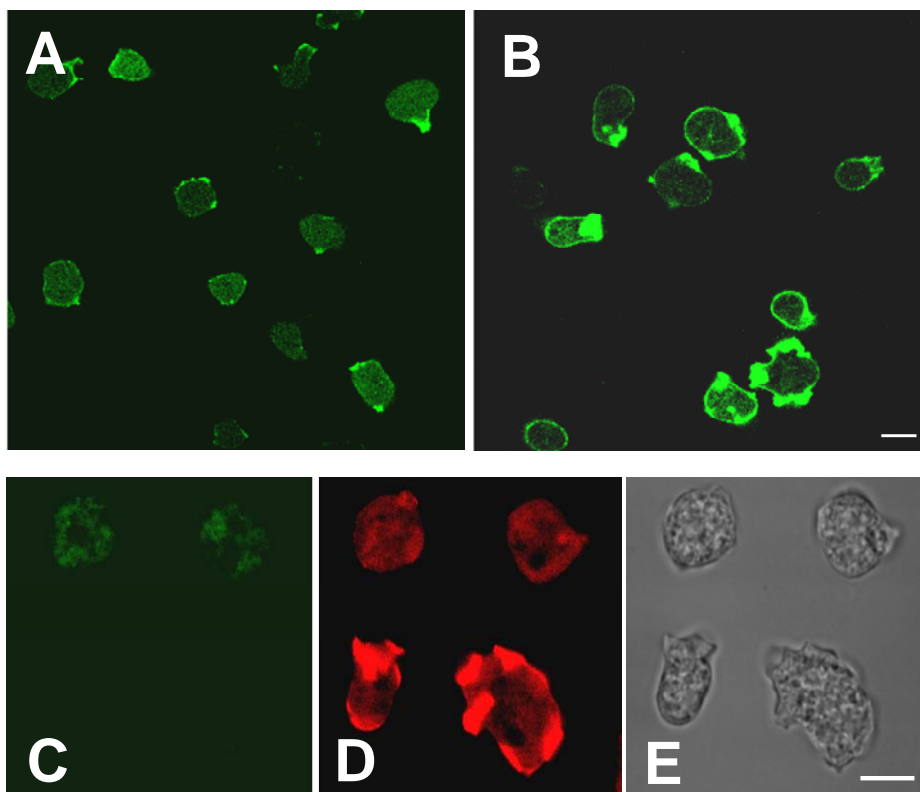


Figure 3.1. CorA/Aip1-null cells have high levels of actin polymerized at the cell cortex. (A) Wild-type and (B) CorA/Aip1-null cells expressing GFP-LimE Δ . (C-E) A mixture of wild-type and double-mutant cells was immunolabeled using anti-coronin antibodies (green) to identify wild-type cells (C), and stained with TRITC-phalloidin to label actin filaments (red) (D). The corresponding phase-contrast image is shown in (E). Scale bar, 10 μ m.

Results

the high level of F-actin at the cell cortex demonstrated by live-cell fluorescence microscopy using the GFP-LimE Δ label as shown in Figure 3.1B.

Because of this cortical actin accumulation in mutant cells, biochemical experiments were conducted to determine the degree of actin polymerization within cells deficient of CorA, Aip1 or both proteins in comparison to wild-type cells. First, the compared G- and F-actin content in the different cell lines was semi-quantitatively by *Western blot* analysis. As a reference the F-actin in wild-type cells was depolymerized to G-actin monomers with latrunculin A (Gräf *et al.*, 1998). Wild-type cells displayed the typical ratio of about equal amounts of G- and F-actin, whereas single- and double-mutant cells showed a slight increase in the F-actin fraction (Figure 3.2A).

To quantify the F-actin content in these double-mutants, a quantitative actin assay was applied. In short, the F-actin content was determined by binding tetramethylrhodaminyl (TRITC)-phalloidin specifically to F-actin and measuring the fluorescence intensity after methanol extraction (Howard *et al.*, 1985; Defacque *et al.*, 2000). The amount of F-actin was expressed as the ratio of fluorescence intensity versus total amount of cellular protein. The actin assay demonstrated that CorA/Aip1-null cells contain more F-actin relative to the total cellular protein when compared to wild-type or single-mutant cells (Figure 3.2B). The F-actin content is increased to ~35% in CorA-null cells, to ~42% in Aip1-null cells and to ~49% in CorA/Aip1-null cells over the wild-type values. Note that double-mutant cells have almost twice the F-actin content of wild-type cells and a very small proportion of G-actin. It suggests that this small amount of G-actin content might be polymerized into F-actin.

These results indicate that in the absence of CorA and Aip1 the dynamic equilibrium between G-actin monomers and F-actin is impaired and shifted towards polymerization, i.e. higher F-actin concentration.

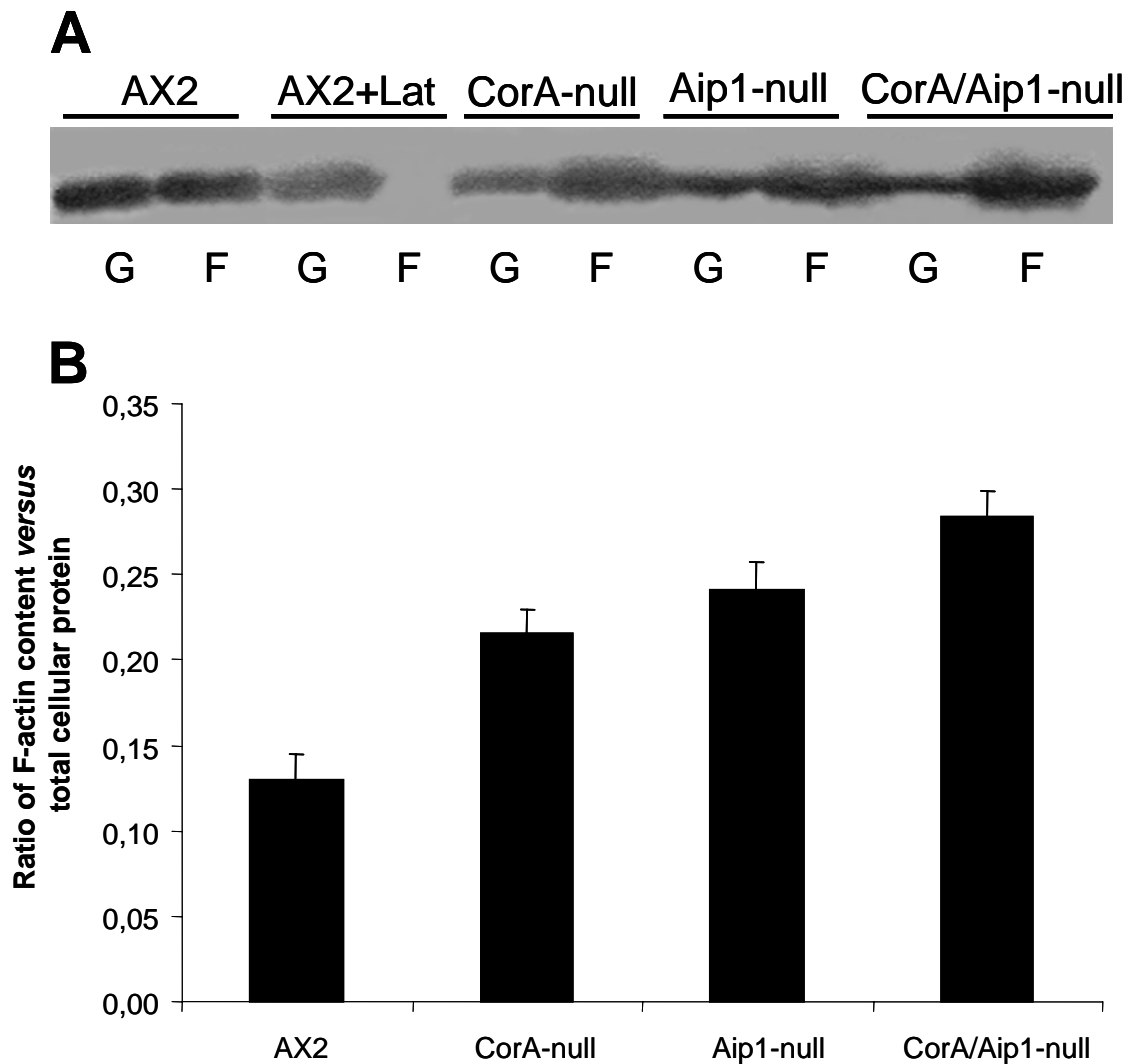


Figure 3.2. CorA/Aip1-null cells are characterized by an increased F-actin content. (A) *Western blot* analysis of cell lysates with the pellet fractions containing F-actin (F) and the supernatants G-actin (G). AX2, wild-type; AX2+Lat, wild-type cells treated with 0.2 mM latrunculin A; CorA-null and Aip1-null, single-mutants; CorA/Aip1-null, double-mutant. The blot was stained using primary anti-actin antibody 224-236-1 and secondary antibody goat-anti-mouse IgG, coupled to alkaline phosphatase (Westphal *et al.*, 1997). (B) Quantification of F-actin measured by the ratio of fluorescence intensity of bound TRITC-phalloidin versus total cellular protein of the respective cell lines. The single and double-mutant cells showed high F-actin content relative to wild-type cells. The amount of F-actin is increased to ~35% in CorA-null cells, to ~42% in Aip1-null cells and to ~49% in CorA/Aip1-null cells over wild-type cells. Error bars represent the standard errors. Number of measurements (n=3).

3.2 Aggregation of *D. discoideum* cells is delayed in the absence of CorA and Aip1

Under starvation conditions *D. discoideum* cells initiate a developmental program resulting in the aggregation of single cells into a multicellular organism. At the beginning of the aggregation stage, the cells acquire an elongated shape and become highly sensitive to cAMP (Kessin, 2001). Time lapse recordings of cells expressing GFP-LimE Δ have been carried out to identify developmental defects in the presence or the absence of CorA and Aip1.

Wild-type cells began to show the typical elongated shape after 6 hours of starvation, but CorA/Aip1-null cells needed 4 hours longer. Clumps of aggregated wild-type cells were observed after 10 hours and clumps of CorA/Aip1-null cells after 12 hours of starvation (Figure 3.3A). Hence, in the mutant cells the development seems to be retarded.

To analyze this developmental impairment a molecular marker for the transition from the growth phase to the aggregation stage was monitored. At the early period of starvation a number of genes necessary for aggregation are activated. One of the induced promoters is the contact site A (csA) gene (Faix *et al.*, 1992). The product of this gene is the csA protein (Müller and Gerisch, 1978). This cell-adhesion protein is not detected in growth-phase cells. It shows a maximal accumulation at the aggregation stage and rapidly declines during later stages of development (Noegel *et al.*, 1986). This protein can serve as an indicator for development toward the aggregation stage. To monitor the expression of csA glycoprotein, wild-type and CorA/Aip1-null cells were starved for 12 hours in shaking culture under cAMP pulses to induce aggregation. Every 2 hours aliquots of both wild-type and double-mutant cells were collected and prepared for *Western blot* analysis (Figure 3.3B). The data show that the expression of csA starts in wild-type cells after 6 hours of starvation, but in CorA/Aip1-mutant cells not before 10 hours of starvation. The 4 hours delay in csA expression observed in double-mutant cells indicates a retarded development in the absence of both proteins.

In addition, these double-mutant cells grew extremely slow both in shaking culture and on bacterial lawns (personal communication by Annette Müller-Taubenberger). Because of this impairment of growth in the mutant cells, the next

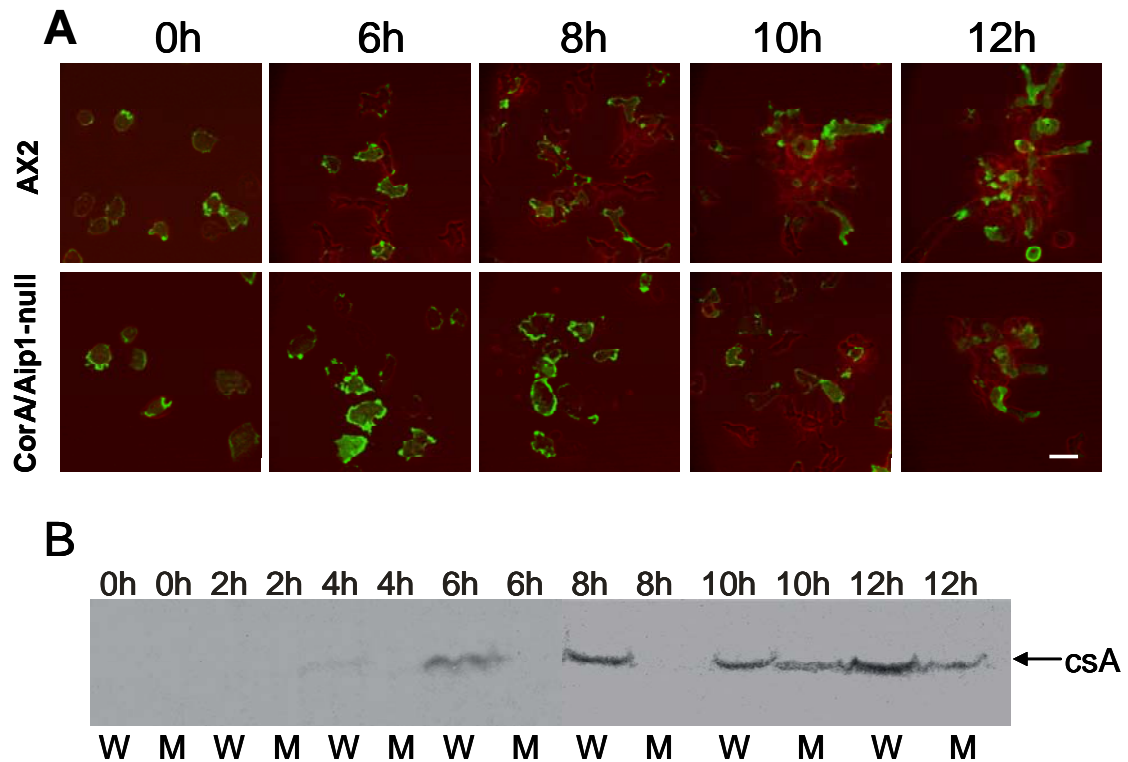


Figure 3.3. Development to the aggregation competent stage is delayed in the absence of CorA and Aip1. (A) Wild-type or CorA/Aip1-null cells expressing GFP-LimE Δ (green) were induced to develop and recorded for 12 hours. The cell shape is shown at 0, 6, 8, 10 and 12 hours (colored in red). (B) *Western blot* showing contact site A (csA) expression as a marker for development towards aggregation. Wild-type (W) and CorA/Aip1-null cells (M) were allowed to develop in shaken culture at a density of 1×10^7 cells/ml under stimulation by pulses of cAMP applied every 6 min for the stimulation of development. Every 2 hours aliquots of both cell lines were collected and subjected to SDS-PAGE and immunoblotting using anti-csA antibody (33-294-17). Scale bar in A, 10 μ m.

step was to analyze the effect of missing CorA and Aip1 on the process of cell division.

3.3 CorA and Aip1 contribute to chromosome segregation and cytokinesis

To investigate the contribution of CorA and Aip1 in mitosis and cytokinesis, the nuclei, microtubules and the actin system were visualized during cell division by fluorescent labeling in fixed CorA/Aip1-null cells using confocal microscopy.

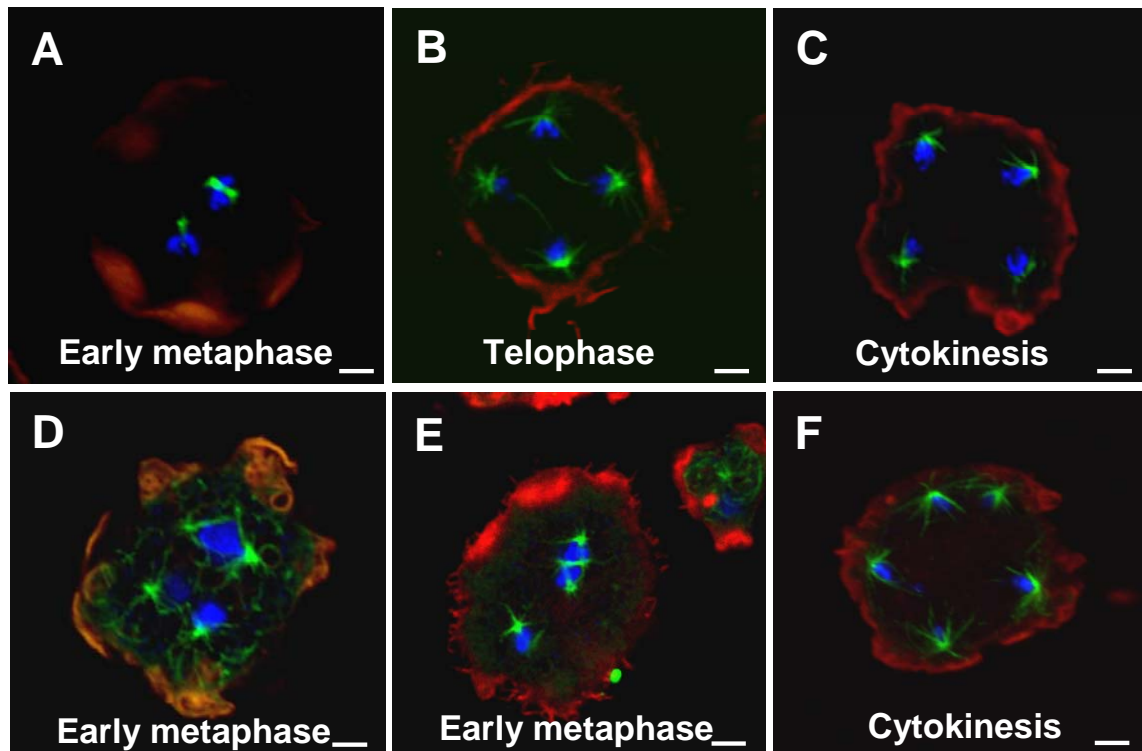


Figure 3.4. Centrosome attachment is defective in the absence of CorA and Aip1. Immunofluorescence images illustrating the relation of centrosomes to nuclei in wild-type (A-C) and in *CorA/Aip1*-null cells (D-F). Note defective centrosome attachment with three centrosomes attached to one nucleus in (D) and a cruciform configuration in (E). (F) Double-mutant cell showing unpaired poles caused by impairment of chromosome segregation. Actin (red) was visualized using TRITC-conjugated phalloidin, α -tubulin (green) was immunolabeled using polyclonal antibodies in combination with Alexa-488-labeled secondary antibodies, and DNA (blue) was labeled with DAPI. Scale bars, 10 μ m.

In contrast to wild-type cells that showed two centrosomes attached to one nucleus in early metaphase (Figure 3.4A), the double-mutant cell showed unpaired centrosome attachment e.g. three centrosomes attached to one nucleus (Figures 3.4D and E). In wild-type cells one nucleus divides in two nuclei, during chromosome segregation (Figure 3.4C). In the absence of *CorA* and *Aip1* the chromosome segregation was defective with one nucleus dividing in three nuclei (Figure 3.4F).

Figure 3.5A-C shows examples of double-mutant cells impaired in forming a cleavage furrow and in carrying out appropriate cytokinesis. The consequence of this is the generation of multinucleate cells as shown in Figure 3.5D-E. The impairment in cytokinesis is much more pronounced in the double-mutant than in the single-mutant cells (personal communication by Annette Müller-

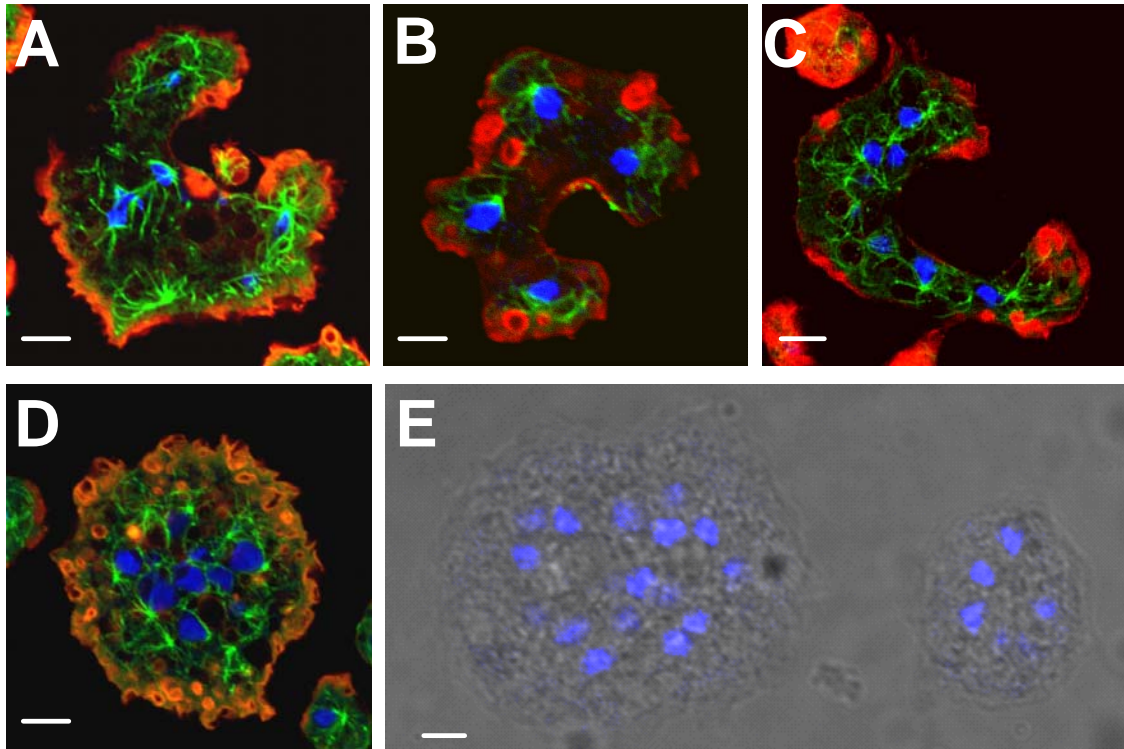


Figure 3.5. Cytokinesis is defective in mutant cells lacking CorA and Aip1. (A-C) Immunofluorescence images illustrating defective cytokinesis resulting in multinucleate cells (D-E) in the CorA/Aip1-null mutant. Actin (red) was visualized using TRITC-conjugated phalloidin, α -tubulin (green) was immunolabeled using polyclonal antibodies in combination with Alexa-488-labeled secondary antibodies, and nucleic acids were labeled with DAPI (blue). (E) Fluorescence image of a CorA/Aip1-null cell stained with DAPI superimposed on the phase-contrast image. Scale bars, 10 μ m.

Taubenberger). This suggests a cooperative function of both proteins during cell division and cytokinesis (see discussion).

3.4 The phagocytosis process is prolonged in the absence of CorA and Aip1

Phagocytosis is induced by the adhesion of a particle to the cell surface in *D. discoideum* cells as in others (Maniak *et al.*, 1995). To analyze the effects of CorA and Aip1 on the uptake mechanism, large heat-killed yeast particles of 3 μ m in diameter were fed to wild-type and CorA/Aip1-null cells expressing GFP-LimE Δ . The duration of particle uptake in wild-type and CorA/aip1-null cells was monitored in live-cell confocal imaging experiments (Figure 3.6A-B and Movies 1 and 2). In

Results

wild-type cells the formation of a phagocytic cup, from inception until the complete engulfment of a yeast particle, took between 20 and 40 seconds. In *CorA/Aip1*-null cells the duration of this process was prolonged from 20 up to 120 seconds as shown in the histogram in Figure 3.6C.

The rate of phagocytosis in the double-mutant cells was reduced in

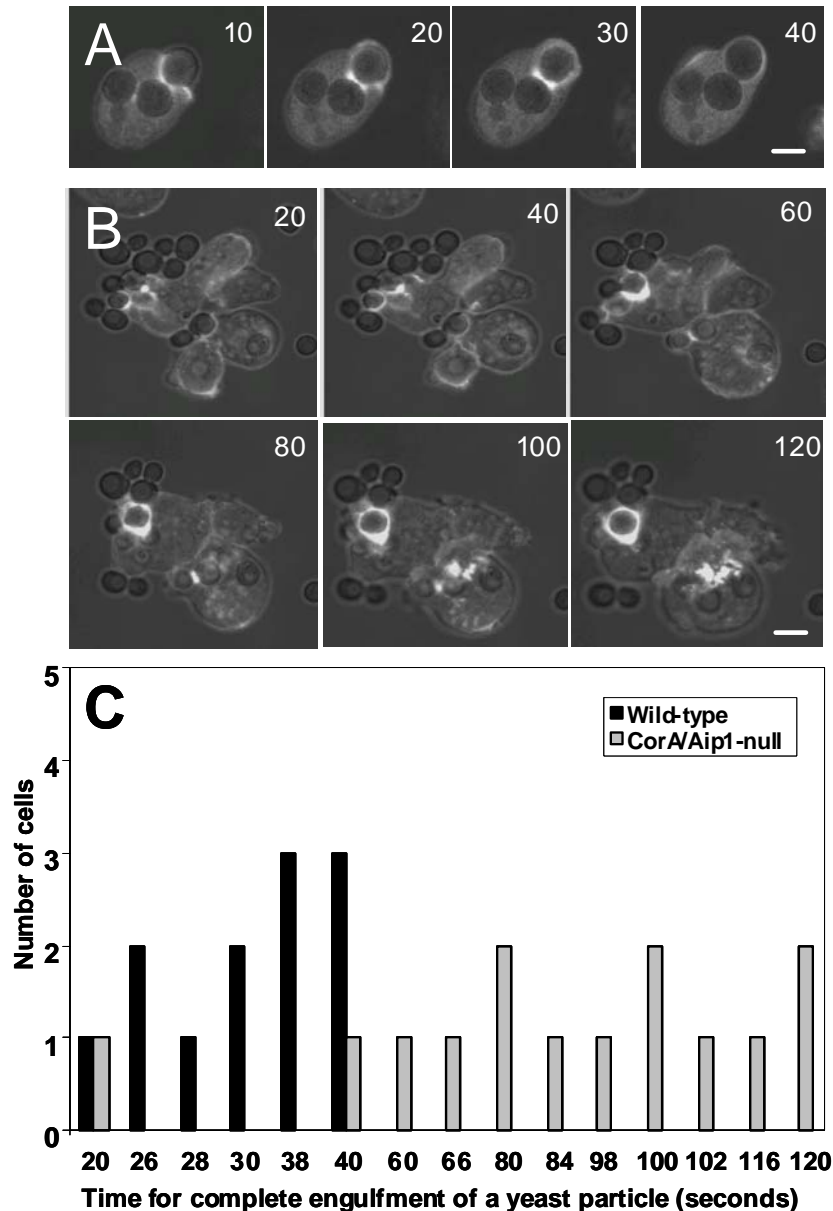


Figure 3.6. The time of phagocytic cup formation is prolonged in the absence of *CorA* and *Aip1*. Phagocytic cup formation from attachment until the complete engulfment of a yeast particle was monitored in wild-type cells ($n=12$) with one example given in (A), and in *CorA/Aip1*-null cells ($n=14$) with one example given in (B). Both cell types expressed GFP-LimE Δ . The numbers indicate time in seconds. (C) Histogram showing the duration of particle uptake. In wild-type cells (black) the complete engulfment took between 20 and 40 seconds. In *CorA/Aip1*-null cells (grey) this process needed up to 120 seconds. Scale bars, 10 μ m.

comparison to wild-type cells. However, the rate in the double-mutant is similar to that of single-mutant cells missing either Aip1 or CorA (personal communication by Annette Müller-Taubenberger). Thus, the lack of both CorA and Aip1 retards the phagocytosis process, but the effect seems to be comparable to the situation when only one of the proteins is missing, indicating a non-synergistic effect.

3.5 CorA/Aip1 double-mutant cells migrate slowly but still orient towards a cAMP gradient

Upon starvation *D. discoideum* cells become sensitive to chemotactic cues and move in direction of the attractant cAMP by rearrangement of their cytoskeleton. To study the alteration of this process when both CorA and Aip1 are missing, the double-mutant cells were subjected to chemotaxis experiments using a micropipette (Gerisch *et al.*, 1975a). Interestingly, after 8 hours of starvation CorA/Aip1-null cells displayed poor ability to move, but still had the ability to re-organize their cytoskeleton in response to a chemotactic signal (Figure 3.7 and

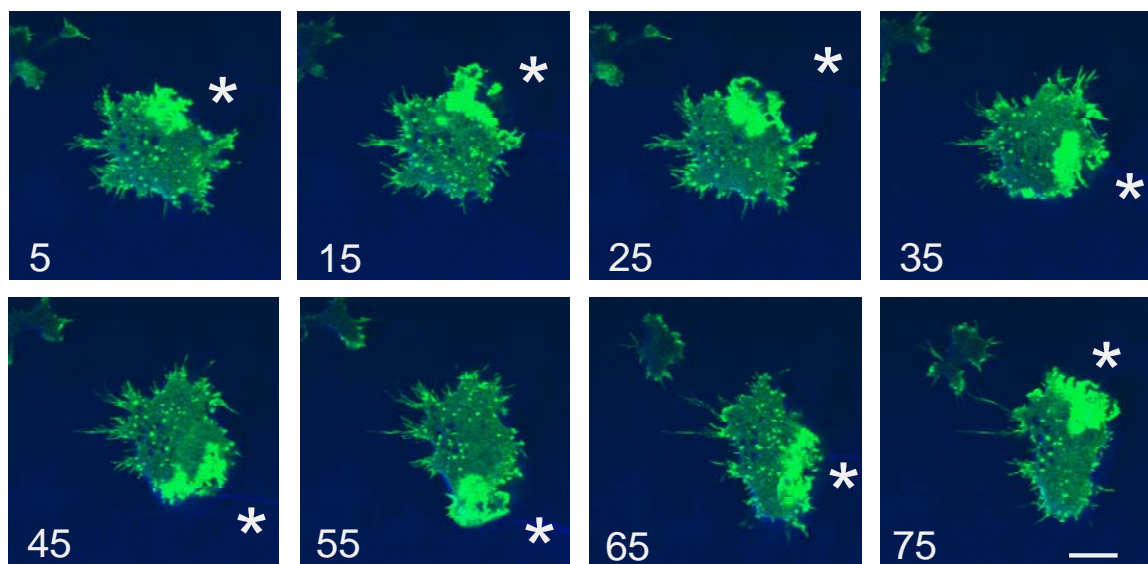


Figure 3.7. A CorA/Aip1-null cell showing re-orientation of its actin cytoskeleton towards a cAMP gradient. The double-mutant cell expressing GFP-LimE Δ was visualized by confocal microscopy. After 8 hours of development the mutant cell shows accumulation of filamentous actin at a new front evoked by a cAMP stimulus, although the cell is still exhibiting a non-elongate shape. The position of the micropipette containing cAMP is indicated by asterisks. Time is indicated in seconds. Scale bar, 10 μ m.

Results

Movie 3).

As shown by the previous results, wild-type cells start to express the aggregation-stage marker *csA* after 6 hours and *CorA/Aip1*-null cells after 10 hours of starvation. Therefore, to study wild-type and mutant cells in comparable stages of development, starvation was started 4 hours earlier in the double-mutants than in wild-type cells. Subsequently, both cell type were mixed (in equal cell numbers) and stimulated with cAMP through a micropipette. As can be seen from the direct comparison in Figure 3.8 and Movie 4, the cells lacking both *CorA* and *Aip1* moved much slower than wild-type cells towards the cAMP source, as

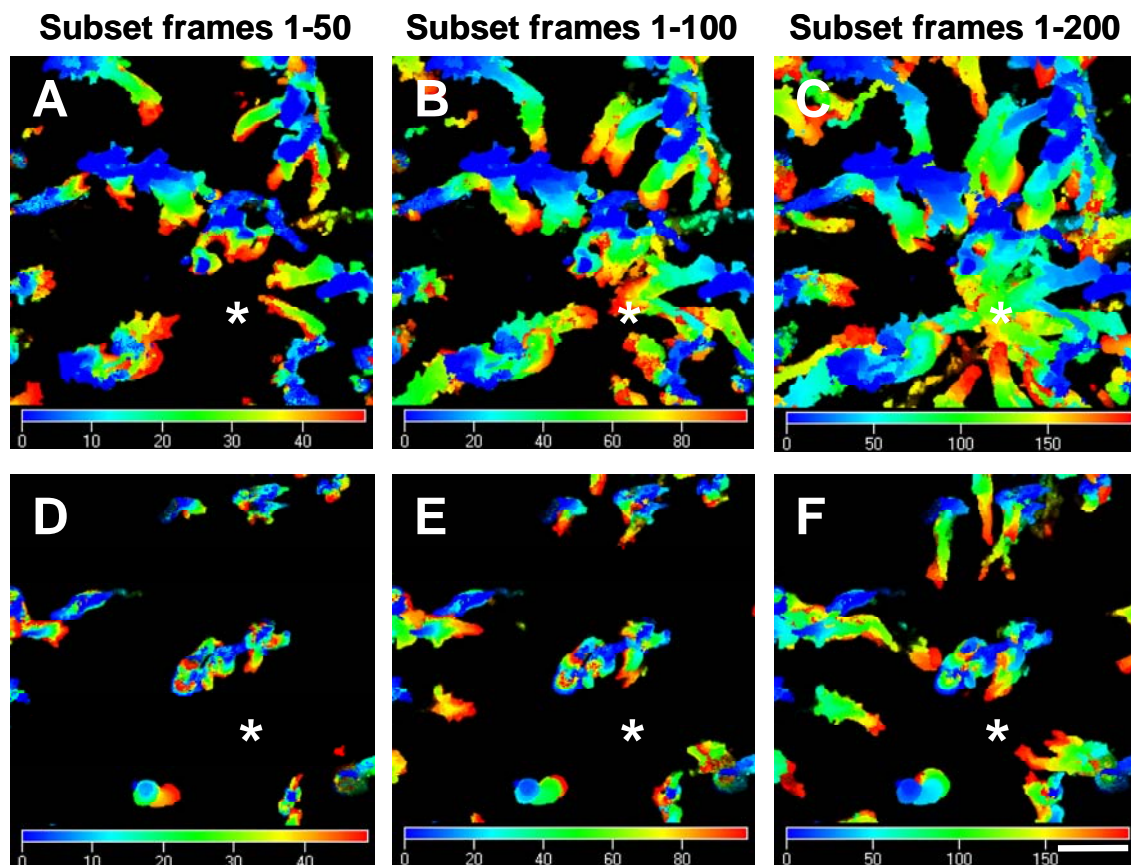


Figure 3.8. The chemotactic movement of *CorA/Aip1*-null cells is impaired. Wild-type cells labeled with mRFP-LimE Δ (A-C) and *CorA/Aip1*-null cells labeled with GFP-LimE Δ (D-F) were subjected to development in shaking culture for 6 hours and 10 hours, respectively. The cells were mixed and exposed to a gradient of cAMP. The color coding shows the superimposed first 50 frames (A, D), 100 frames (B, E), and 200 frames (C, F) of the recording, illustrating the migration trajectories of the cells. Wild-type (A-C) cells showed a faster migration in direction of the micropipette (asterisks) than double-mutant cells (D-F) as indicated by the length of individual migration trajectories. Numbers on the color scale indicate the frame number. The images were processed using the LSM 510 META software. Scale bar, 50 μ m.

Results

Table III. Velocity of cell migration

Cell strain	Velocity ($\mu\text{m}/\text{min}$)	Velocity ($\mu\text{m}/\text{min}$)
	Vegetative state	Developmental stage
AX2	6.62 \pm 0.504 (n=52)	7.34 \pm 0.421 (n=43)
CorA-null	3.12 \pm 0.476 (n=48)	3.54 \pm 0.545 (n=45)
Aip1-null	2.89 \pm 0.359 (n=46)	3.29 \pm 0.523 (n=42)
CorA/Aip1-null	1.32 \pm 0.349 (n=48)	1.83 \pm 0.511 (n=40)

Number of cells (n) and mean values over n cells \pm standard error of mean are given.

indicated by much shorter migration trajectories over the same period of time.

To explore the role of CorA and Aip1 in cell motility during growth and early development, the speed of unstimulated wild-type and mutants cells was quantified. During the growth phase wild-type, CorA-null, Aip1-null and CorA/Aip1-null cells were analyzed in confocal live-cell experiments. For early development wild-type, CorA-null, and Aip1-null cells were starved for 6 hours and CorA/Aip1-null cells for 10 hours. All cell lines expressed GFP-LimE Δ and were recorded for 30 minutes with one image every 30 seconds.

In the growth phase (vegetative stage) the velocity of locomotion was reduced in CorA-null, Aip1-null, and CorA/Aip1 double-null cells to 47%, 44% and 20%, respectively as compared to wild-type cells. In the aggregation-competent (developmental) stage the velocity of CorA-null, Aip1-null, and CorA/Aip1-null cells was reduced to 48%, 45% and 25% respectively (Table III). In both stages the double-mutants displayed the strongest reduction in migration speed.

The impairment of cell motility observed in the absence of CorA and/ or Aip1 might be a direct consequence of the increased amount of polymerized actin, resulting in an excessive accumulation of actin filaments at the leading edge, as observed in live-cells expressing GFP-LimE Δ and in fixed cells labeled with phalloidin as shown in Figure 3.1.

4 Results

*Well-defined chemoattractant stimuli modulate protein recruitment to the cell cortex of *D. discoideum**

The chemoresponsive cells of *D. discoideum* are useful models to study the function of actin-binding proteins in the control of actin dynamics. The first steps of the chemotactic signaling cascade take place within only a few seconds (Parent and Devreotes, 1999) and time scales for the dynamics of the actin cytoskeleton were found to be even shorter (Diez *et al.*, 2005).

Actin-binding proteins like CorA and Aip1 are recruited to the cell cortex upon a global upshift of the chemoattractant cAMP (Etzrodt *et al.*, 2006). However, previous experimental setups had several disadvantages for those types of experiments. In particular, the precise timing and spatial control of the release of chemoattractant turned out to be a problem. In flow chamber experiments the release of chemoattractant can not be controlled precisely and the transient time for building-up and switching of gradient profiles was found to be around 2.5 seconds (Etzrodt *et al.*, 2006). In addition, in conventional flow chambers only one experiment can be done at a time and only the cells in one field of view (at a given magnification) can be recorded for later analysis. Recently, attempts have been made to generate dynamically changing gradient signals in microfluidic chambers (Lin *et al.*, 2004). In these studies the uncaging technique of cAMP application to cells situated in a microfluidic channel has been employed to bypass the disadvantages of the flow chamber technique (Beta *et al.*, 2007). This way, the cAMP stimulus could be controlled very precisely in space and time (Figure 4), and up to 20 single-cell experiments could be performed in one experimental setup. This technique was used to investigate the temporal recruitment of proteins to the cell cortex. Furthermore, the actin assembly and disassembly in the presence or in the absence of CorA and Aip1 could be recorded in high temporal resolution and on a single cell level.

Wild-type cells have been subjected to a short pulse or to a continuous cAMP stimulus in order to study the recruitment of CorA or Aip1 to the cell cortex in response to temporal patterns of chemoattractant (Figure 4.1). The time course

Results

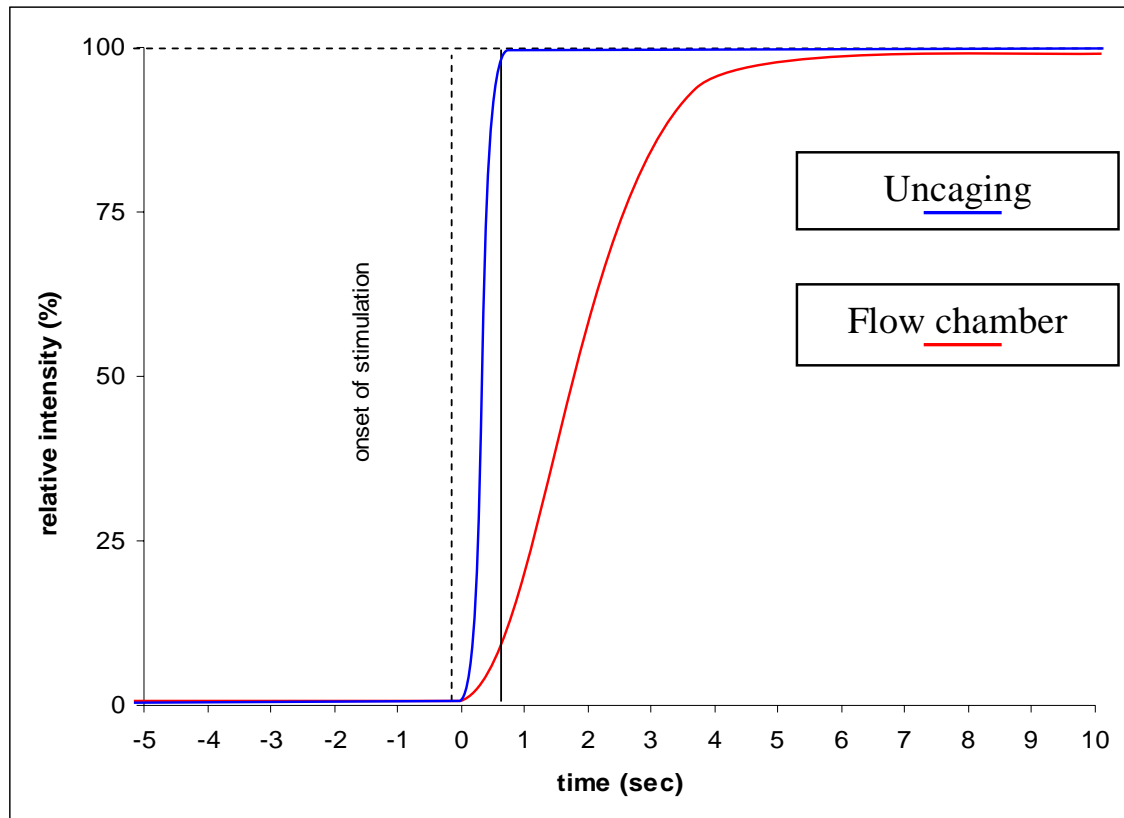


Figure 4.1 Uncaging allows a precisely controlled onset of stimulation. The red curve represents the onset of stimulation in flow chamber experiments, where the first detectable peak was 2.5 seconds after the onset of stimulation (Etzrodt *et al.*, 2006). In contrast, the blue curve shows the onset of stimulation in uncaging experiments with the first detectable peak already 0.6 seconds after the onset of stimulation (Beta *et al.*, 2007). Thus, in uncaging experiments even the early fast cell reactions can be detected and analyzed with high temporal resolution.

of CorA or Aip1 recruitment is affected by the pattern of the cAMP stimulus applied to the cells. Under continuous stimulation, the rate of CorA and Aip1 translocation is decreased in comparison to its responses to a short pulse (Tables IV and V). Thus, the cAMP conditions delivered to the cells modulate the rate of protein translocation to the cell cortex.

These two conditions of stimulation were then applied to cells deficient in the CorA or/and Aip1 and the rate of actin assembly and disassembly was analyzed (Figures 4.2 and 4.3). In the absence of CorA and Aip1 the rate of actin assembly and disassembly at the cell cortex is decreased in comparison to wild-type (Tables VI and VII). In particular the rate of actin disassembly seems to be strongly affected under both conditions of cAMP stimuli, which is in agreement with the proposed role of both proteins in promoting actin depolymerization.

In another set of experiments repetitive pulses of cAMP with different intervals between the pulses were applied to wild-type and to mutant cells lacking CorA and/or Aip1 (Figures 4.4, 4.6 and 4.7). When pulses with intervals of 20 or 40 seconds were applied to wild-type cells, they elicit a kind of resonance in the actin response after ceasing of external stimulation. However, mutant cells lacking those proteins do not (or only very rudimentary) show this response at 20 second pulse intervals. This finding may indicate that in the presence of both proteins the repetitive cAMP pulses induce the assembly and disassembly of actin to oscillate with a maximal amplitude at a certain frequency characterizing the resonance process.

In conclusion, the cAMP stimulation pattern modulates the rate of protein recruitment to the cell cortex. In the absence of CorA and Aip1 the rate of actin assembly and disassembly is altered, indicating the participation of these proteins in the spatiotemporal regulation of actin.

4.1 The temporal pattern of cAMP stimulation affects CorA and Aip1 translocation to the cell cortex

To examine the temporal pattern of cAMP-induced protein recruitment to, and release from the cell cortex, wild-type cells expressing GFP-CorA or GFP-Aip1 were exposed to a continuous cAMP stimulus or to a single pulse of 1 second duration.

The translocation of GFP-CorA or GFP-Aip1 from the cytoplasm to the cell cortex (Movies 5 and 6) was plotted as the ratio of fluorescence intensity at the cortex over the intensity in the interior of a cell, as described in Materials and Methods and shown in Figure 4.1. As an estimate of translocation rate, the first derivative was calculated of the ratio of fluorescence intensity at the cortex over the interior of the cell (Figures 4.1A', B', C', D').

The translocation of CorA as well as Aip1 after a single short pulse of cAMP was characterized by a rapid increase in fluorescence ratio with a maximum rate of about 0.5/sec, as indicated by the peak in the first derivative. The release from the cortex or decrease in the fluorescence ratio took longer and the rate was lower with about -0.3/sec as a maximal rate. Upon continuous cAMP stimulation the

Results

Table IV. Rate of CorA recruitment and release from the cell cortex after a short pulse or in response to continuous cAMP stimulation as measured by the changes in fluorescence intensities

	Rate of CorA recruitment to the cell cortex (sec ⁻¹)	Rate of CorA release from the cell cortex (sec ⁻¹)
Single pulse of 1 second (n=24)	~0.50	~0.30
Continuous stimulation (n=25)	~0.30	~0.15

n, number of cells recorded.

Table V. Rate of Aip1 recruitment and release from the cell cortex after a short pulse or in response to a continuous cAMP stimulation as measured by changes in fluorescence intensities

	Rate of Aip1 recruitment to the cell cortex (sec ⁻¹)	Rate of Aip1 release from the cell cortex (sec ⁻¹)
Single pulse of 1 second (n=25)	~0.50	~0.30
Continuous stimulation (n=24)	~0.35	~0.15

n, number of cells recorded.

translocation rate for both CorA and Aip1 was lower. The recruitment to the cortex took place with a rate of about 0.3/sec, whereas the release from the cortex took longer and had a rate of about 0.15/sec (Tables IV and V and Figure 4.1).

Thus, the rate of protein translocation to and of the release from the cell cortex is lower upon continuous stimulation than with a single short pulse. Hence, the type of cAMP stimulus can modulate the recruitment of CorA and Aip1 to, and their release from the cell cortex.

Results

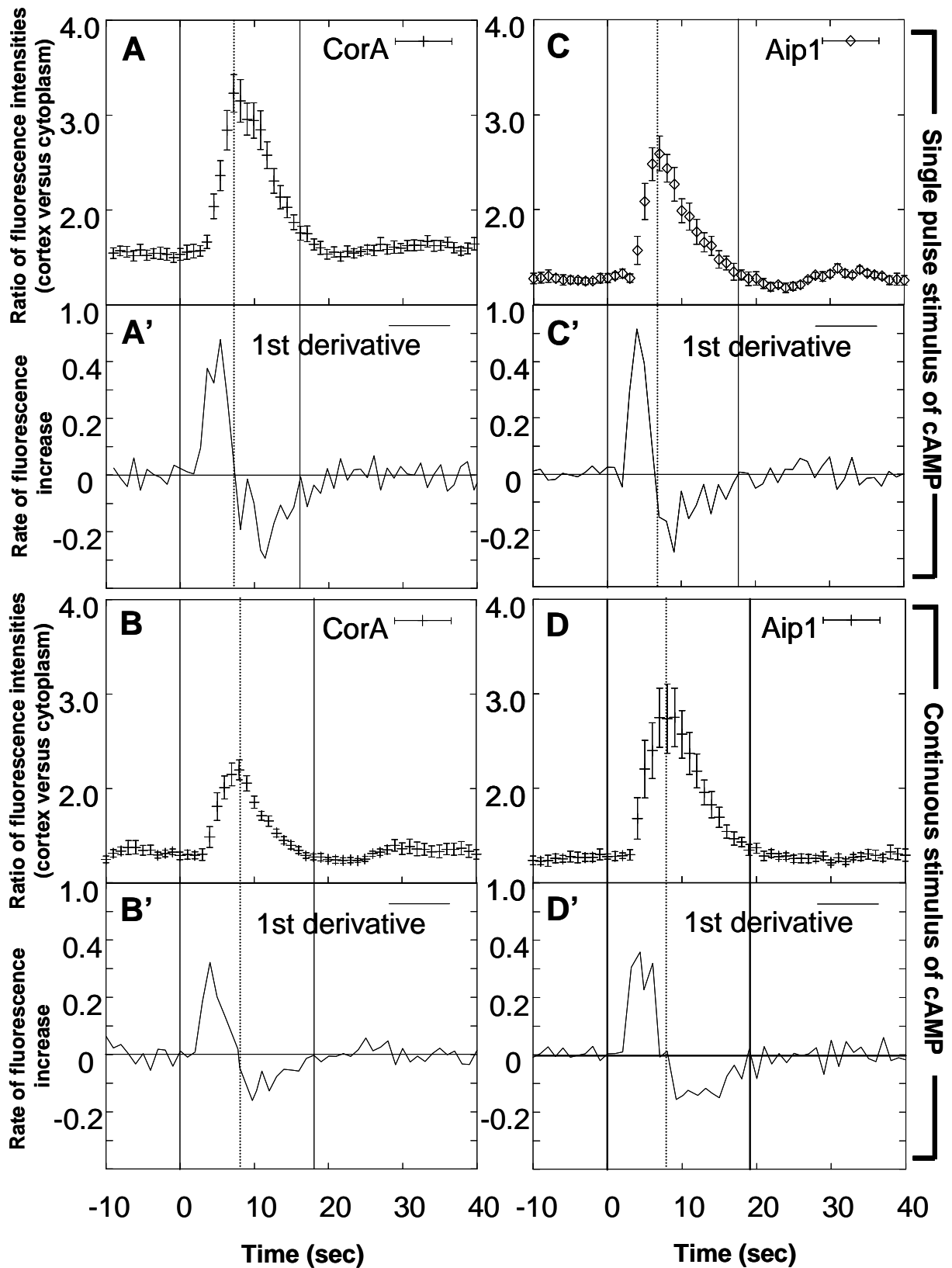


Figure 4.1, legend viewed on the following page.

Figure 4.1. The rate of CorA and Aip1 translocation to the cell cortex is altered under a continuous cAMP stimulus. *D. discoideum* wild-type cells expressing GFP-tagged CorA or Aip1 were stimulated continuously or with one single pulse of 1 second duration. Uncaging of cAMP started at 0 seconds. (A, B, C and D) The graphs show the maximal peak of cortical accumulation under single pulse or continuous stimulation with cAMP. Standard errors of the mean are indicated. (A', B', C' and D') The graphs show the temporal changes in fluorescence as given by the first derivative of fluorescence intensity (cell cortex over cytoplasm). The first derivative gives the rate of protein translocation between the cytoplasm and the cortex (recruitment or release). The CorA or Aip1 translocation to the cell cortex is lower under a continuous stimulus than in response to a single pulse (Tables IV and V). From left to right, the first vertical bar indicates the beginning of the response, the second vertical bar (dashed) indicates the peak of maximal cortical response and the third vertical bar indicates the end of the response.

4.2 The rates of actin assembly and disassembly are affected in the absence of CorA and Aip1

The immediate conversion of net polymerization of actin into net depolymerization takes place within the first 10 seconds following stimulation (Etzrodt *et al.*, 2006).

Here, the rate of actin assembly and disassembly in the absence of CorA or/and Aip1 has been explored by calculating the first derivative of the ratio of GFP-LimE Δ fluorescence intensity at the cortex over the interior of the cell (Figures 4.2 A', B', C' and D' and 4.3 A', B', C' and D'). Since GFP-LimE Δ binds specially to F-Actin, it served here as a reporter for the presence of F-actin in wild-type and mutant cells. Figures 4.2 and 4.3 (A, B, C and D) show the rise and fall in cortical fluorescence intensities as a result of actin assembly and disassembly. A rise in the fluorescence signal indicates net polymerization, whereas a fall indicates net depolymerization. The peak of the response marks the point at which polymerization and depolymerization are in equilibrium.

After a single short pulse of cAMP, wild-type cells react with a rapid actin response. The fluorescence intensity indicating polymerized actin at the cortex *versus* cytoplasm is rapidly increasing with a maximal rate of 0.8/sec. The actin depolymerization at the cortex is a slower process with a maximum rate of 0.4/sec. In mutant cells lacking CorA, Aip1 or both proteins, actin polymerization as well as depolymerization at the cortex is impaired. With a rate of 0.5/sec to 0.6/sec the actin assembly is still faster than the disassembly with a rate of about 0.2/sec in all

Results

the mutants. However, in particular the disassembly process is strongly prolonged in all mutants as compared to wild-type cells when stimulated with a single short pulse (see Tables VI, VII and Figure 4.2).

When applying a continuous cAMP stimulus the rates of actin assembly and disassembly are in general slightly below the single-short pulse values. This holds true for the wild-type and the mutants. However, the tendency in all mutants for decreased rates of actin assembly and strongly decreased rates of disassembly can also be observed upon continuous cAMP stimulation (see Tables VI, VII and Figure 4.3).

These findings demonstrate the participation of both CorA and Aip1 in the control of actin dynamics, in particular in actin depolymerization that brings F-actin back to resting level. Both proteins have been proposed to promote actin disassembly (Gerisch *et al.*, 1995; Brieher *et al.*, 2006; Aizawa *et al.*, 1999; Rodal *et al.*, 1999; Okada *et al.*, 1999). Thus, cells lacking these proteins have been predicted to display a less efficient actin depolymerization process. This impairment of actin depolymerization may be the cause responsible for the increased polymerized F-actin content observed in CorA/Aip1-double mutants (Figures 3.1 and 3.2).

Single pulse stimulus of cAMP

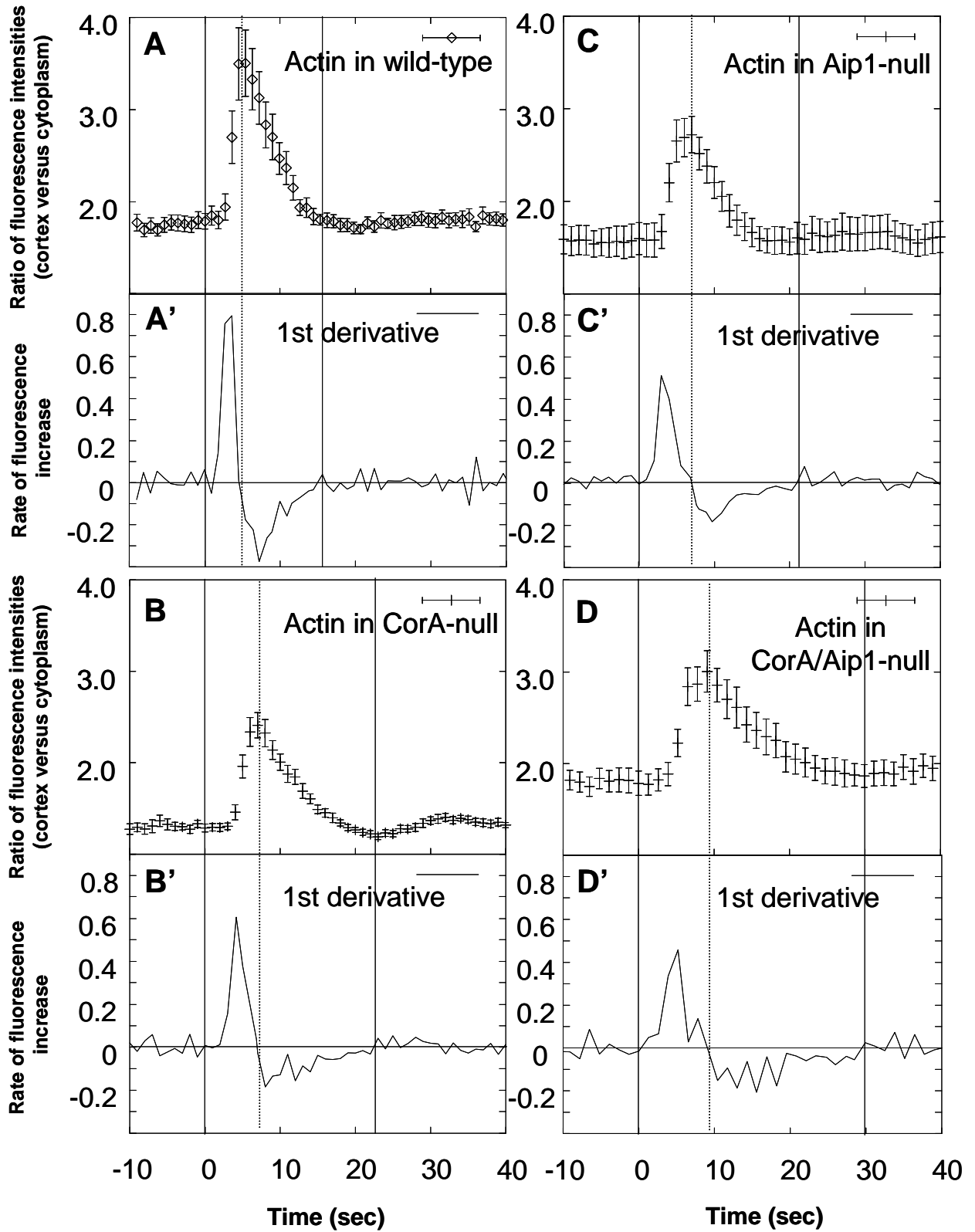


Figure 4.2, legend viewed on the following page.

Results

Figure 4.2. The rate of actin assembly and disassembly under a single cAMP stimulus is decreased in the absence of CorA or/and Aip1. *D. discoideum* wild-type or null-mutant cells expressing GFP-tagged LimE Δ were stimulated with a single pulse of 1 second duration by the uncaging of cAMP starting at 0 seconds. (A, B, C and D) The graphs show a maximal peak of cortical actin accumulation in wild-type cells. Standard errors of the mean are indicated. (A', B', C' and D') The graphs show the temporal changes in fluorescence intensity of cell cortex over cytoplasm. From left to right, the first vertical bar indicates the beginning of the response, the second vertical bar (dashed) indicates the peak of maximal cortical response and the third vertical bar indicates the end of the response.

Table VI. Rate of actin assembly (sec⁻¹) in the presence or absence of CorA or/and Aip1 under a short pulse or in response to a continuous cAMP stimulation

	Actin in wild-type	Actin in CorA-null	Actin in Aip1-null	Actin in CorA/Aip1-null
Single pulse of 1 second duration	~0.80 (n = 22)	~0.60 (n = 20)	~0.50 (n = 20)	~0.50 (n = 20)
Continuous stimulation	~0.70 (n = 30)	~0.50 (n = 20)	~0.40 (n = 30)	~0.40 (n = 20)

n, number of cells recorded.

Table VII. Rate of actin disassembly (sec⁻¹) in the presence or absence of CorA or/and Aip1 under a short pulse or in response to a continuous cAMP stimulation

	Actin in wild-type	Actin in CorA-null	Actin in Aip1-null	Actin in CorA/Aip1-null
Single pulse of 1 second duration	~0.40 (n = 22)	~0.20 (n = 20)	~0.20 (n = 20)	~0.20 (n = 20)
Continuous stimulus	~0.30 (n = 30)	~0.15 (n = 20)	~0.15 (n = 30)	~0.15 (n = 20)

n, number of cells recorded

Continuous stimulus of cAMP

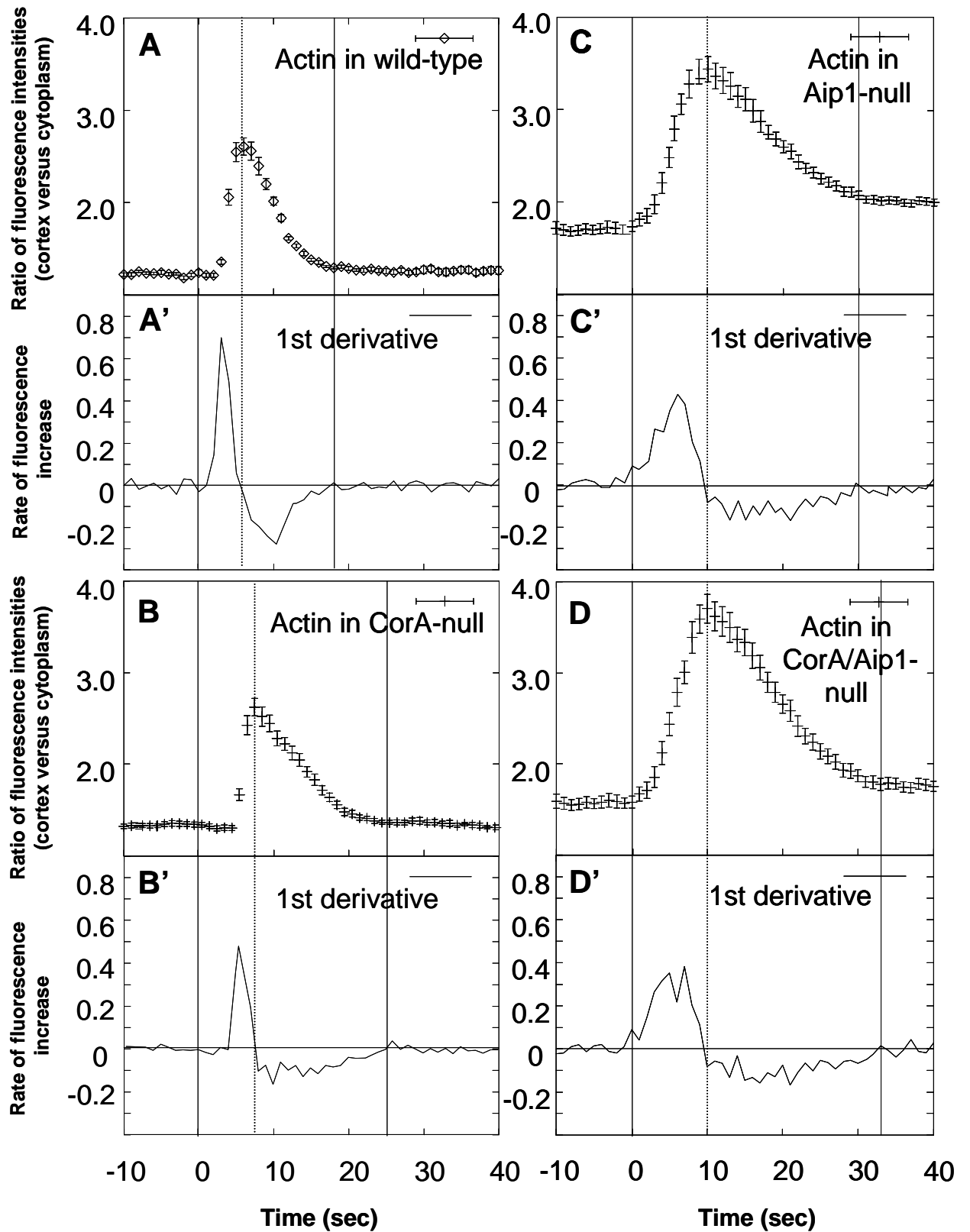


Figure 4.3, legend viewed on following page.

Figure 4.3. The rate of actin assembly and disassembly under a continuous cAMP stimulus is decreased in the absence of CorA or/and Aip1. *D. discoideum* wild-type or null-mutant cells expressing GFP-tagged LimE Δ , were stimulated with a continuous stimulus by the uncaging of cAMP starting at 0 seconds. (A, B, C and D) The graphs show a maximal peak of cortical actin accumulation. Standard errors of the mean are indicated. (A', B', C' and D') show the temporal changes in fluorescence as given by the first derivative of fluorescence intensity in the cell cortex over cytoplasm. In the absence of CorA and/or Aip1 the actin disassembly and probably also the assembly, is decreased under a continuous cAMP stimulus, as shown in Tables VI and VII. From left to right, the first vertical bar indicates the beginning of the response, the second vertical bar (dashed) indicates the peak of maximal cortical response and the third vertical bar indicates the end of the response.

4.3 Pulses of cAMP promote resonant actin responses with periods of 20 or 40 seconds

To investigate the time required for recovery to the resting state after stimulation with repetitive pulses of cAMP, wild-type cells expressing GFP-LimE Δ were stimulated with cAMP pulses of 1 second duration at different intervals. Figure 4.4 shows that in all cases the first peak of the actin response was observed about 6 seconds after the first stimulation. If the interval between the cAMP pulses was 8 or 10 seconds, the following actin responses could not recover to the resting state. In contrast, if the intervals between the pulses were 15 seconds or longer the following actin responses showed a full recovery to the resting state before the next response (Figure 4.4).

At pulse intervals of 20 and 40 seconds the cells showed a resonance response with a periodic accumulation of actin in the cell cortex after stimulation was ceased. This resonance had a period of 20 seconds in case of stimulation with a 20-seconds pulse interval, and a period of 40 seconds in case of stimulation with a 40-seconds pulse interval. In the latter case, however, the periodic actin accumulation was strongly damped (Figure 4.4).

Results

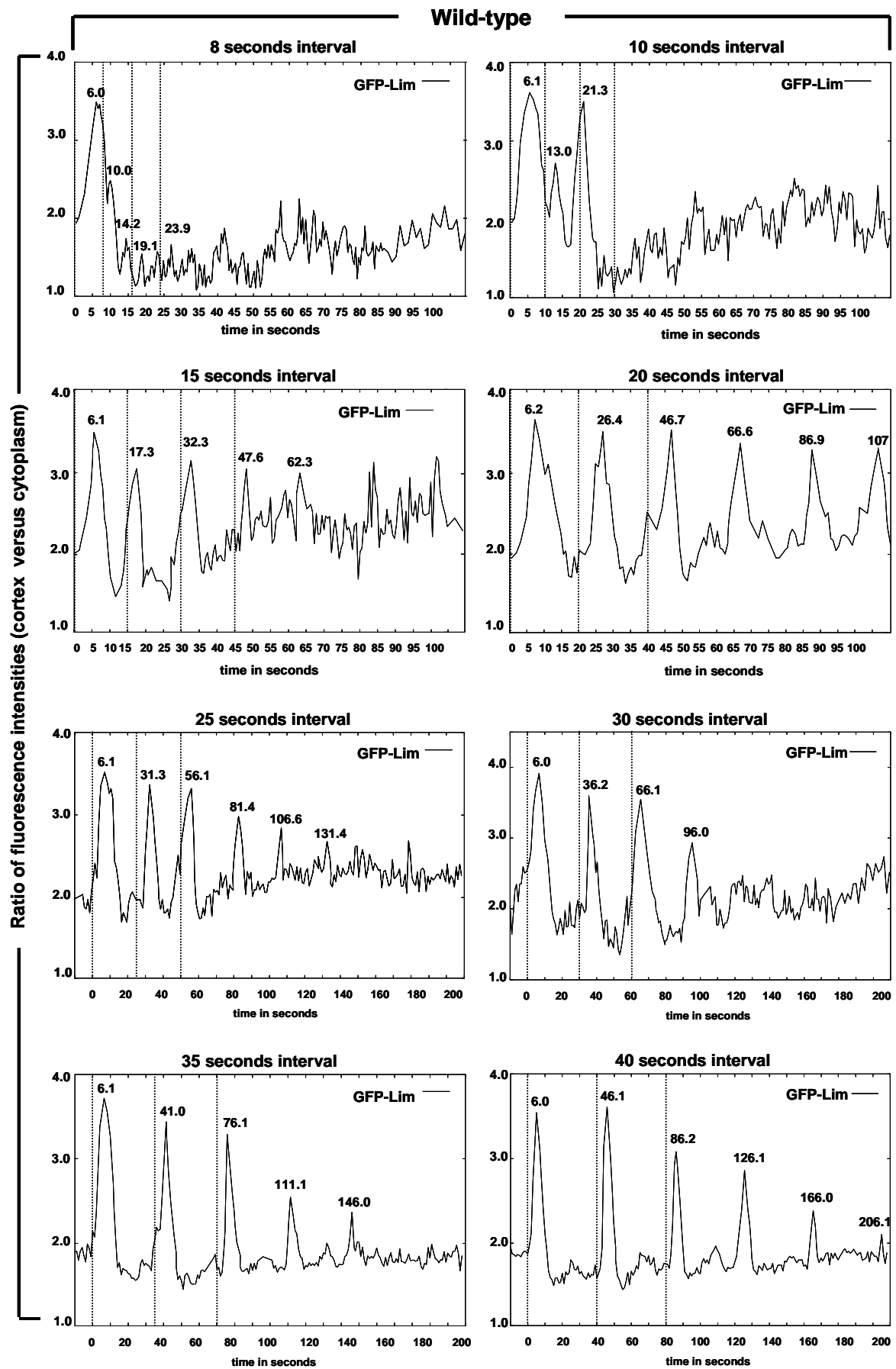


Figure 4.4, legend viewed on following page.

Results

Figure 4.4. Pulses of cAMP stimulation with 20 or 40 second intervals promote a resonant actin response. Wild-type cells expressing GFP-LimE Δ were stimulated by the uncaging of cAMP in pulses of 1 second duration and intervals of 8, 10, 15, 20, 25, 30, 35, and 40 seconds. The average response of wild-type cells (n=17) is displayed. The start of the cAMP uncaging pulses is indicated by the vertical dashed lines. The time of maximal actin accumulation in the cell cortex is indicated. Note that after cessation of the external stimulation, repetitive pulses at certain frequencies elicit resonance, inducing the actin response to oscillate.

To analyze the difference in resonance period, the responses of individual cells were analyzed (Figure 4.5). In a total of 10 cells exposed to cAMP pulses with an interval of 20 seconds, 4 cells showed similar responses as in Figures 4.5A, and 5 cells showed similar responses as in Figure 4.5B. Therefore, it appears that the stimulation with 20 or 40 second intervals entrain the cells to oscillate with a similar period of 40 seconds (Figure 4.4). The superposition of two populations with a period of 40 seconds results in the apparent period of 20 seconds seen when cell populations are stimulated with a 20 second interval.

In conclusion, cAMP pulses with 20 or 40 seconds interval entrain actin to fall into a synchronized oscillatory response.

Results

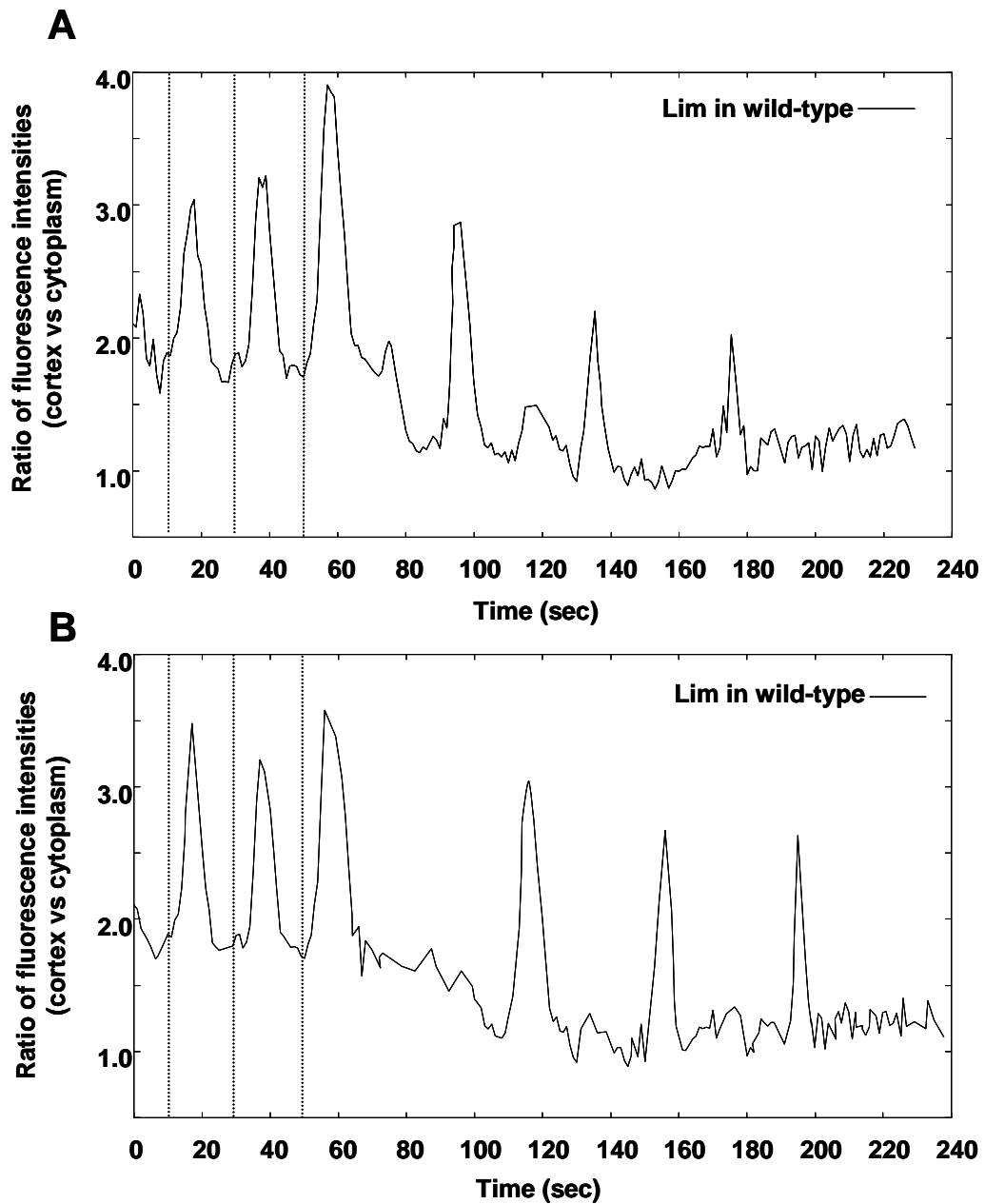


Figure 4.5. The actin response of individual cells under cAMP pulses of 20 second intervals shows a cellular entrainment with a period of 40 seconds. Wild-type cells expressing GFP-LimEΔ were stimulated by cAMP uncaging in pulses of 1 second duration and intervals of 20 seconds. After cessation of the cAMP stimuli, both cells showed a resonance response with different periods. However, when these two populations with different periods were summarized they have assumed a same period. This process whereby two interacting oscillating system, which have different periods assume the same period is denominated entrainment. The dashed vertical lines represent the cAMP uncaging pulse starting times.

4.4 Resonant actin response is promoted in the presence of CorA and Aip1, but not in their absence

To investigate the role of CorA and Aip1 during recovery of the actin response to the resting state after stimulation with pulses of cAMP, repetitive pulses with different intervals were applied to CorA-null, Aip1-null or CorA/Aip1-null cells expressing GFP-LimE Δ .

The actin response in CorA-null and Aip1-null mutants stimulated with periodic pulses of cAMP is shown in Figure 4.6. In CorA-null cells, the first peak of cortical actin accumulation appeared at about 8 seconds after the first cAMP pulse, about 2 seconds later than in wild-type cells (compare with Figure 4.4). At pulse intervals of 8 and 10 seconds no synchronized response to the consecutive pulses could be observed. The responses were irregular in amplitude and phase. However, in case of longer intervals i.e. 15 or 20 seconds between the stimuli the responses became more regular.

In Aip1-null cells the actin response showed the first peak of cortical actin accumulation at about 8 seconds after the first cAMP stimulus. Thus, similar to the CorA-null mutant, the Aip1-null mutant showed a response shift of about 2 seconds as compared to wild-type (compare with Figure 4.4). In Aip1-null cells the actin response to repetitive pulses was strongly impaired at intervals of 8 and 10 seconds between the cAMP pulses. There was no direct actin response to the second stimulus. As in CorA-null cells, longer intervals of 15 and 20 seconds between the cAMP pulses resulted in a regular response in cortical actin accumulation.

Importantly, in both CorA-null and in Aip1-null cells at 20 second pulse intervals no clear resonant actin response could be observed after the cessation of cAMP stimulation (Figure 4.6).

Results

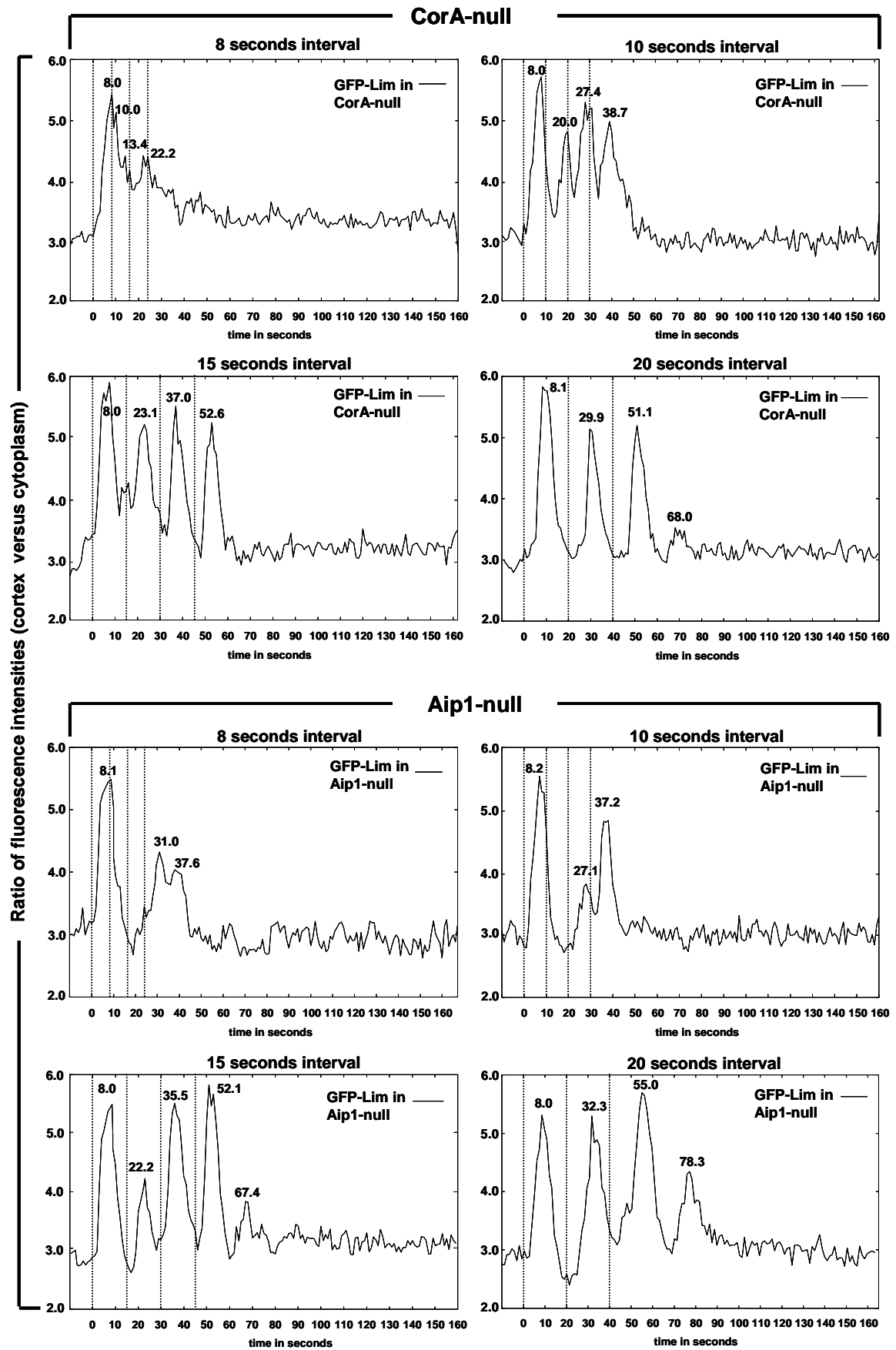


Figure 4.6, legend viewed on the following page.

Results

Figure 4.6. In the absence of CorA or Aip1 the cortical actin recruitment does not show resonant actin responses upon cAMP pulses. CorA or Aip1 single-mutant cells expressing GFP-LimE Δ were stimulated by the uncaging of cAMP in pulses of 1 second duration and intervals of 8, 10, 15, and 20 seconds. The average response of CorA-null (n=15) and Aip1-null (n=16) cells is displayed. The start of the cAMP pulses is indicated by the vertical dashed lines. Note that in the absence of CorA or Aip1, no resonant actin response was observed upon cAMP pulses with intervals of 20 or 40 seconds, as shown for wild-type cells in Figure 4.4. The time of maximal actin accumulation in the cell cortex is indicated.

In the absence of both CorA and Aip1 the first and only actin accumulation peak at the cell cortex was observed about 10 seconds after cAMP stimulation at 8 and 10 second intervals (Figure 4.7). Thus, in double-mutant cells the response was delayed by 2 seconds relative to the single-mutants or by 4 seconds relative to wild-type cells. In the absence of CorA and Aip1 the recovery of the actin response after repetitive pulses of cAMP could be observed only with intervals longer than 15 seconds (Figure 4.7). However, this recovery of actin in the double-mutant cells was delayed and not regular suggesting the participation of both proteins in adaptation and de-adaptation of the response. Repetitive pulses with 20 seconds interval also did not promote a resonant actin response in the absence of both proteins (Figure 4.7)

In conclusion, CorA and Aip1 are involved in adaptative responses, and are essential to promote the resonant actin response after stimulation by repetitive cAMP pulses.

Results

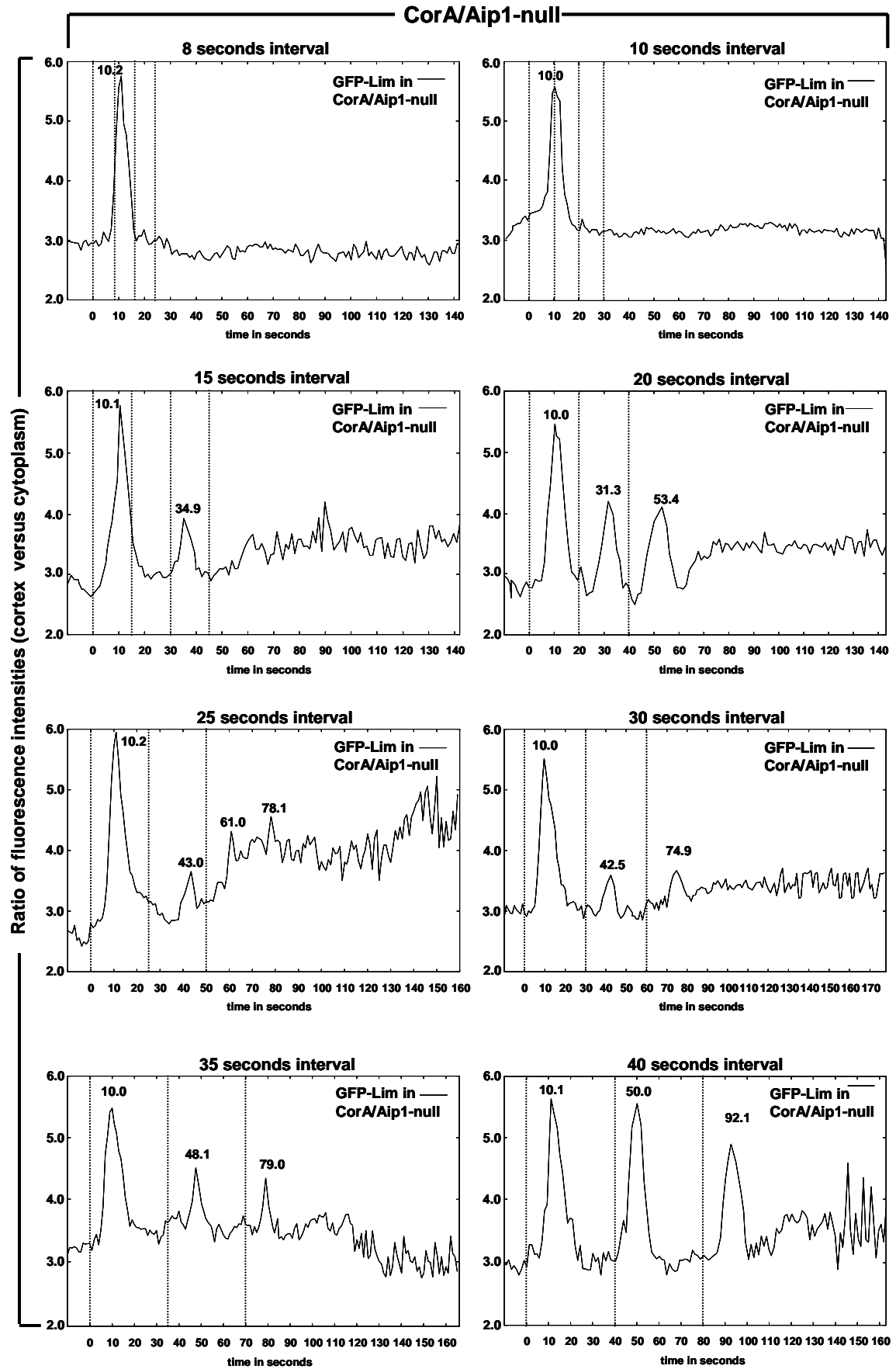


Figure 4.7, legend viewed on the following page.

Results

Figure 4.7. CorA and Aip1 might regulate adaptation of the actin response to cAMP pulses. CorA/Aip1 double-mutant cells expressing GFP-LimE Δ were stimulated by the uncaging of cAMP in pulses of 1 second duration and intervals of 8, 10, 15, 20, 25, 30, 35, and 40 seconds. The average response of CorA/Aip1 (n=15) cells is displayed. Note that in the absence of both proteins no resonance response at 20 or 40 seconds was observed. This result suggests a participation of CorA and Aip1 in adaptation and de-adaptation of the actin response. The start of the cAMP pulses is indicated by the vertical dashed lines. The time of maximal actin accumulation in the cell cortex is indicated.

5 Results

Cell-autonomous oscillations of actin polymerization in the cortex of SCAR-deficient cells

A key player in the formation of a dense cortical actin network is the seven-subunit Arp2/3 complex (Machesky *et al.*, 1994; Welch *et al.*, 1997) that nucleates the polymerization of actin filaments *de novo* and initiates branches on existing filaments (Volkman *et al.*, 2001; May, 2001). Its activity is controlled by SCAR/WAVE proteins of the WASP (Wiscott-Aldrich Syndrome Protein) family that are downstream effectors of receptor-mediated signaling pathways (Smith and Li, 2004). SCAR protein forms a complex with four other proteins: PIR121 (p53-inducible mRNA), NAP125 (Nck associated protein), Abi1 or 2 (Abl-interactor), and HSPC300 (hematopoietic stem-cell progenitor) (Eden *et al.*, 2002; Goley *et al.*, 2006).

Here, evidence of oscillatory actin instability in the cortex of mutant cells lacking members of the pentameric SCAR complex is provided. SCAR-deficient *D. discoideum* cells exhibit self-sustained, cell-autonomous oscillations of cortical actin polymerization with periods of about 20 seconds, while a steady state of polymerization with only slight fluctuations is observed in wild-type cells.

Stimulation with the chemoattractant cAMP does not suppress the actin oscillations, but it promotes a phase shift. Thus, the oscillatory system must be linked to the chemosensory pathway, and signals are transmitted from cAMP receptors to the actin machinery even if SCAR is missing. As chemotaxis is strongly impaired in SCAR-null mutants (Bear *et al.*, 1998; Caracino *et al.*, 2007), suppression of these oscillations by SCAR appears to be required for efficient directional responses in chemotactic cells.

In conclusion, SCAR prevents the transition from steady-state polymerization in wild-type cells to periodic alternating phases of polymerization and depolymerization observed in SCAR-deficient cells.

5.1 Autonomous and periodic fluctuations of actin polymerization in the cortex of SCAR-deficient cells

In wild-type cells the fluctuations of actin polymerization in the cell cortex and cytoplasm have small amplitudes and are non-periodic (see Figure 5.1 for example and Movie 7).

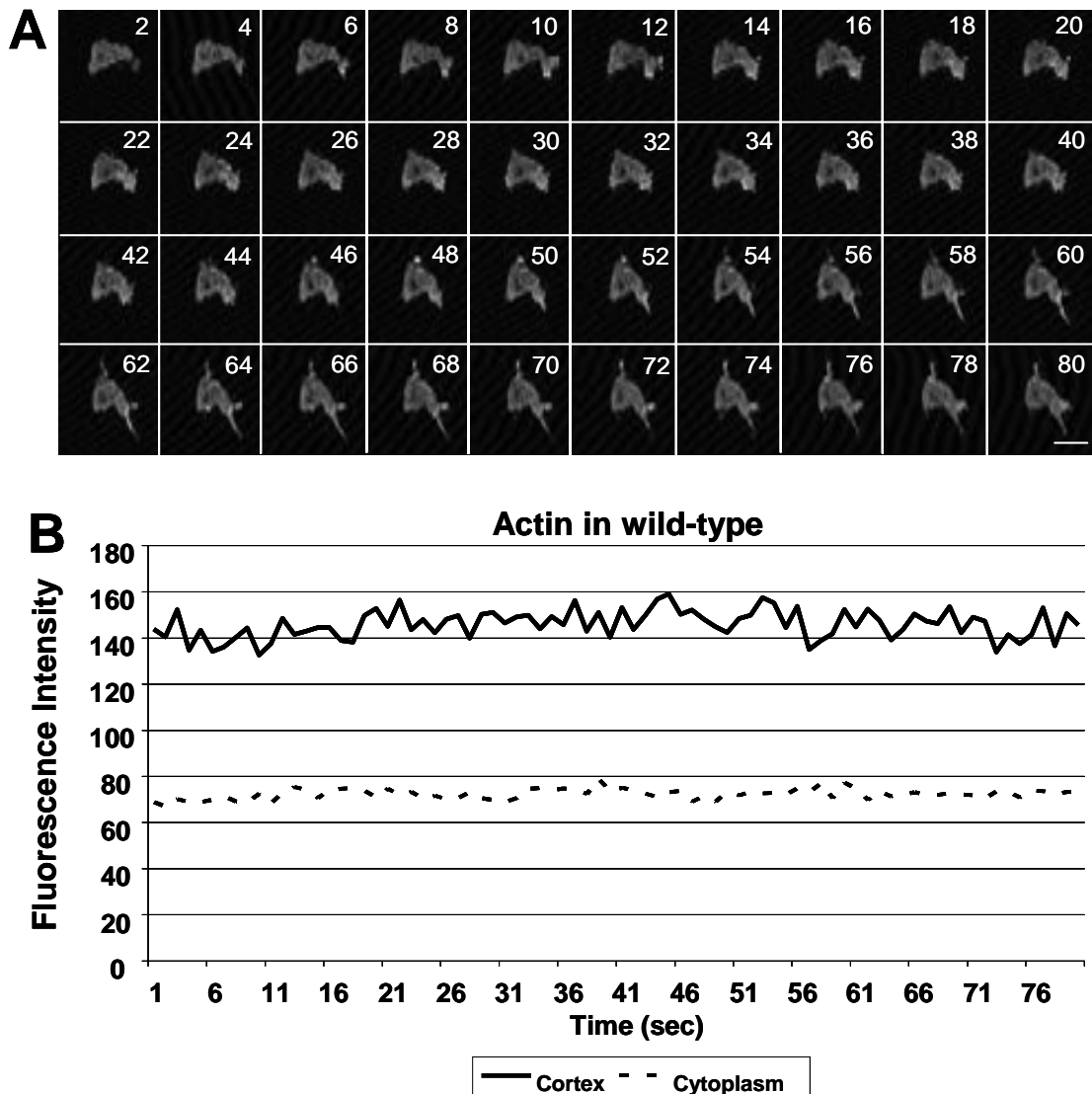


Figure 5.1. A wild-type cell of *D. discoideum* shows small, non-periodic actin fluctuations at the cell cortex and in the cytoplasm. (A) Time series of the wild-type cell expressing GFP-LimE Δ . 80 frames were recorded with a time interval of 1 second/frame. The time in seconds is indicated. (B) the fluorescence intensity of GFP-LimE Δ at the cell cortex (solid line) and in the cytoplasm (dashed line), fluctuates with small amplitudes and is non-periodic. Scale bar, 10 μ m.

Results

In contrast, SCAR-deficient cells show autonomous periodic fluctuations of actin polymerization in the cell cortex (see Figure 5.2 for example and Movies 8, 9 and 10) with high amplitudes in comparison to wild-type cells. Note that the phases

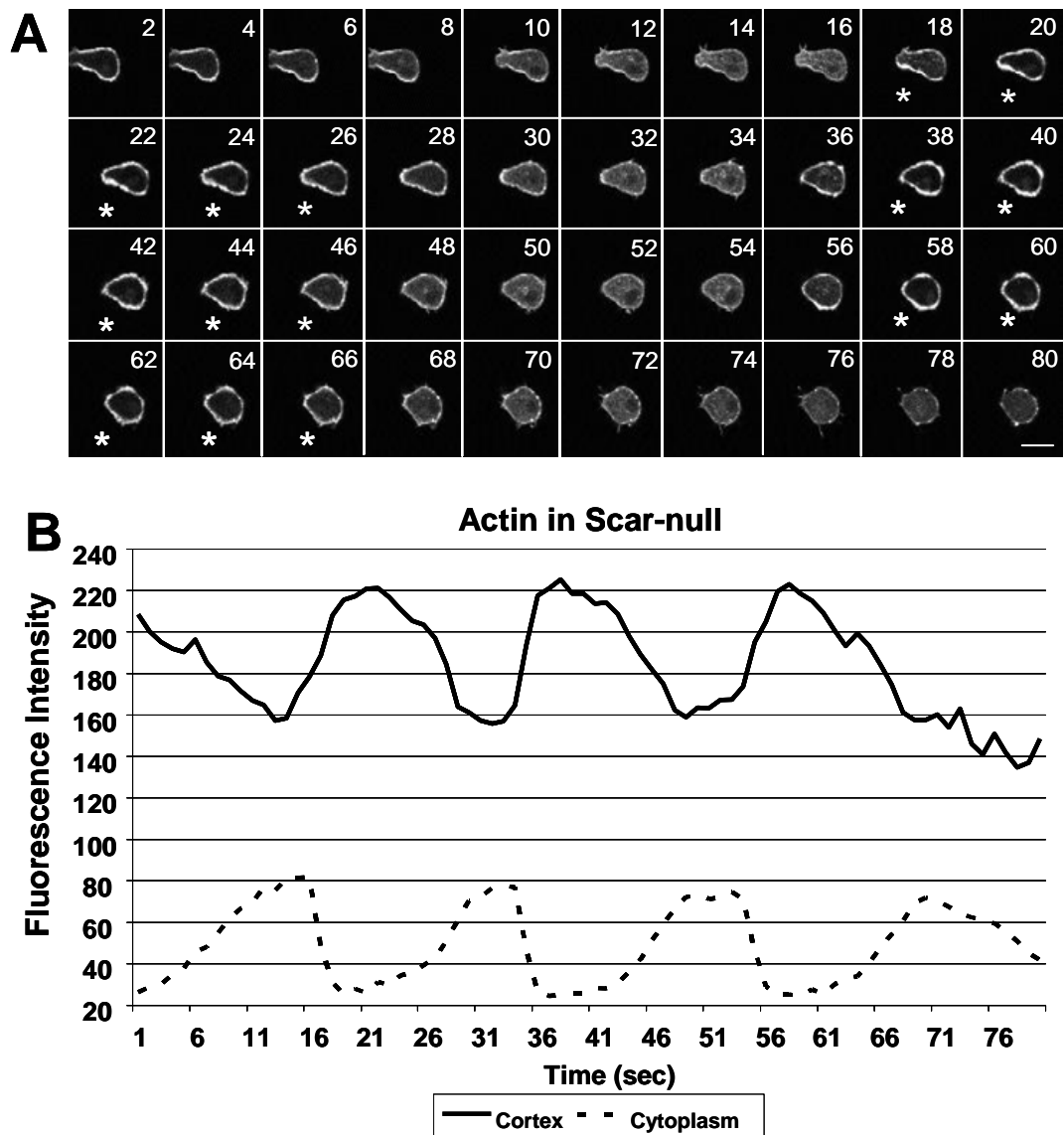


Figure 5.2. Unstimulated *D. discoideum* SCAR-null cell showing free running actin oscillations with high amplitudes at the cell cortex and in the cytoplasm. (A) Time series of the SCAR-null cell expressing GFP-LimE Δ . 80 frames were recorded with a time interval of 1 second/frame. The time in seconds is indicated. The asterisks indicate frames where most actin has been translocated from the cytoplasm to the cell cortex. **(B)** Measurements of the fluorescence intensity establish fluctuations of LimE Δ fluorescence in the cell cortex (solid line) and in the cytoplasm (dashed line) of the cell shown in (A). The actin fluctuations in the SCAR-null cell have much higher amplitudes than in the wild-type cell shown in Figure 5.1 and are clearly periodic. Scale bar, 10 μ m.

Results

of actin polymerization between cell cortex and cytoplasm are alternating (Figure 5.2B). When the level of cytoplasmic actin (G-actin) is high, the level of the cortical actin (F-actin) is low. *Vice-versa*, when the level of the cortical F-actin is high, the cytoplasmic actin level is low. Thus, the G-actin is recruited periodically from the cytoplasm to polymerize the filamentous actin at the cell cortex.

These autonomous oscillations of actin polymerization do not only take place in SCAR-deficient cells, but also in PIR121 and SCAR/PIR121 double-mutant cells. However, since PIR121 is known to protect SCAR protein from degradation (Blagg *et al.*, 2003), cells deficient of PIR121 most probably have very low amounts of functional SCAR protein, leading to a similar phenotype as in SCAR-null mutants. To analyze the periodicity of these actin oscillations in SCAR-null, PIR121-null and SCAR/PIR121-null cells the frequency spectra have been determined (Figure 5.3).

Apart from one exception wild-type cells did not exhibit any detectable periodic activities of actin polymerization (Figure 5.3A), whereas in all three mutant strains a period of about 20 seconds (0.05 Hz) was prominent (Figure 5.3B-D).

The magnitude of the dominant frequency peak demonstrates that oscillations are most pronounced in mutant cells deficient in both SCAR and PIR121. This difference between SCAR-null and SCAR/PIR121-null mutants suggests that PIR121 has an impact on the actin regulatory system independent of its role as a regulator of SCAR activity.

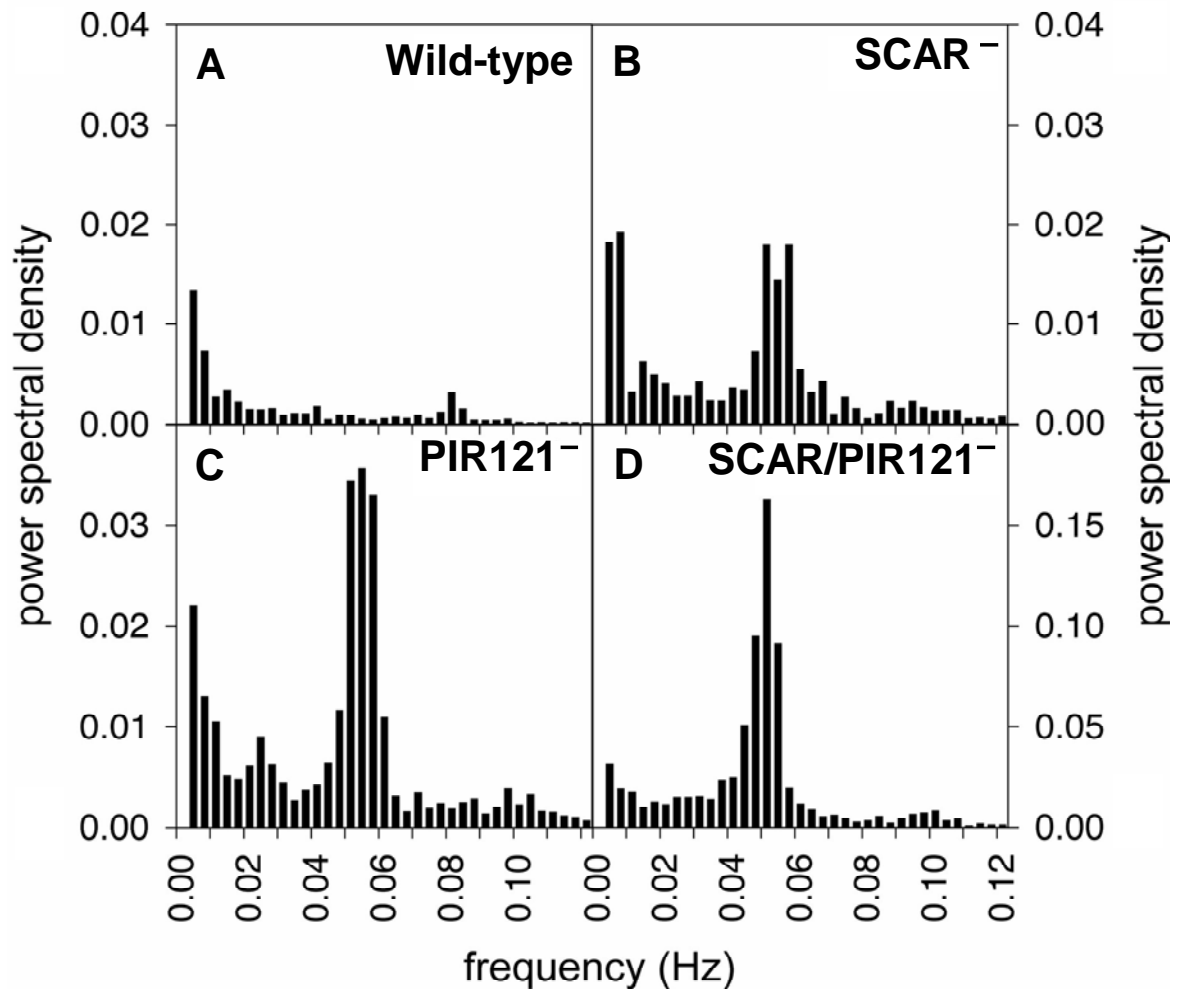


Figure 5.3. Autonomous actin translocation to the cell cortex of SCAR and PIR121-null cells is periodic. Frequency spectra summarizing the periodic activity in populations of (A) wild-type cells, (B) SCAR-null, (C) PIR121-null, and (D) SCAR/PIR121 double-null mutants are shown. The spectra result from averaging over the frequency distributions of individual cells. The data are based on recordings of 27 wild-type, 12 SCAR-null, 14 PIR121-null, and 24 SCAR/PIR121-null cells. 7 of the 12 recorded SCAR-null cells exhibited periodic activities as shown in Figure 5.2. The other cells showed less regular or no obvious oscillations. 11 of the 14 PIR121-null cells and 16 cells of the 24 SCAR/PIR121-null mutants exhibited a clear periodicity. In all three mutants an oscillation period of around 20 seconds (0.05 Hz) was observed. Note the different scale on the ordinate of panel D.

5.2 The developmental stage of SCAR-deficient cells has no influence on autonomous fluctuations of actin polymerization in the cell cortex

D. discoideum cells have strictly separated growth and aggregation stages. Therefore, the question was whether oscillations of actin polymerization and depolymerization in SCAR-deficient cells are observed in both stages and in wild-type cells in none of the two stages.

D. discoideum cells kept in nutrient medium stay in the growth phase, but when the medium is substituted by buffer, starvation drives the cells into development. Wild-type and mutant cells expressing GFP-LimE Δ were recorded in the growth phase and aggregate stage. In Figure 5.4A-H each curve represents the time course of cortical actin accumulation in a single wild-type or mutant cell in the absence of external stimulation. Whereas fluctuations were minute and non-periodic in the wild-type cell in growth and development (Figure 5.4A and 5.4E), regular oscillations with large amplitudes were observed in all three mutants in both the growth phase (Figure 5.4B-D) and developmental stage (Figure 5.4F-H). Thus, in cells deficient of SCAR, PIR121 or both proteins, actin polymerization oscillates independent of the cell stage, whereas it does not oscillate in wild-type in any of the two stages.

In order to determine whether the observed oscillations in the actin system are cell-autonomous, several cells located in the same field of view were recorded. The phases of their oscillations did not coincide and the frequencies varied slightly, as in the example shown in Figure 5.4H and Movies 11a and 11b. These data indicate that the oscillations are independent and free-running in each individual cell.

Results

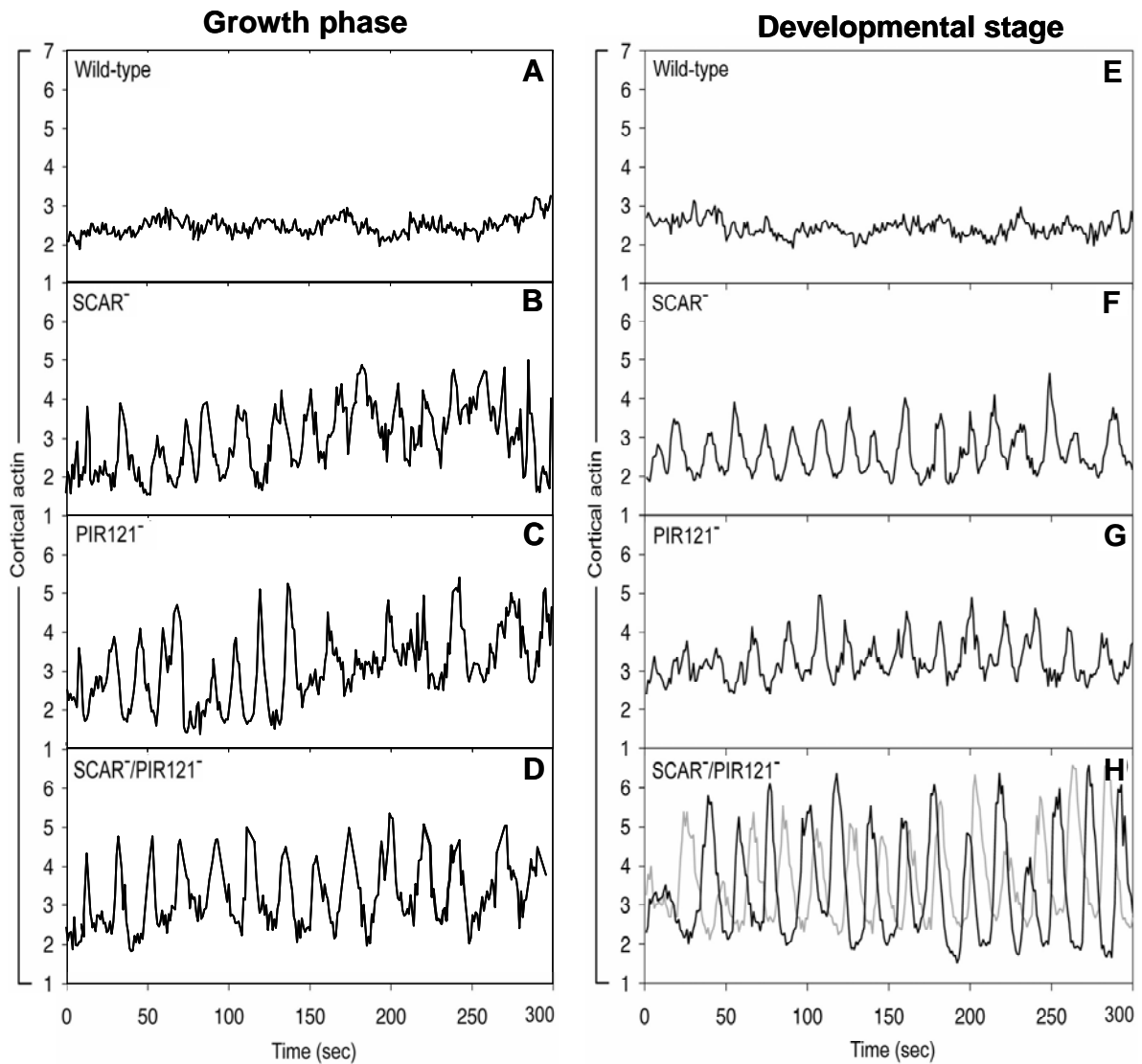


Figure 5.4. SCAR-null, PIR121-null and SCAR/PIR121-null cells show autonomous actin fluctuations in the cell cortex in growth and development. Time series of confocal recordings through the middle of the cell body were acquired at intervals of 1 second. The enrichment of GFP-LimE Δ in the cell cortex was normalized by calculating the ratio of fluorescence intensity in the cortex over that in the interior of a cell. Cells in the growth phase (A-D) and developmental stage (E-H) were analyzed. (A, E) Examples of small and non-periodic fluctuations in wild-type cells. SCAR-null (B, F), PIR121-null (C, G), and SCAR/PIR121-null (D, H) cells showed in growth and development free-running oscillations at the cell cortex. In (H) independent oscillations in two individual SCAR/PIR121 double-mutant cells were recorded simultaneously (black and grey curve). These cells were located in the same field of view at a distance of 23 μ m from each other. No liquid flow was applied in this experiment, which means that any chemical signals that might be exchanged between cells were retained.

5.3 Development of *D. discoideum* appears not to be affected by the absence of SCAR and PIR121

During the early period of *D. discoideum* development the starvation conditions activate genes implicated in cell aggregation. One of these genes encodes the contact site A (csA) glycoprotein (Müller and Gerisch, 1978). This gene is activated during starvation in response to pulsative cAMP signals (Faix *et al.*, 1992). The csA glycoprotein is not detected in the growth-phase, but shows a maximal accumulation in the aggregation stage (Noegel *et al.*, 1986). Therefore, this protein can serve as an indicator for development towards aggregation (see 1.2). To investigate the development in the absence of SCAR and PIR121, the expression of the csA glycoprotein was monitored in wild-type and SCAR/PIR121-null cells by *Western blot* analysis. Both cell lines were starved in shaking culture under cAMP pulses for 12 hours to induce aggregation. Every 2 hours aliquots of wild-type and mutant cells were collected and prepared for *Western blot* analysis. The data show that the expression of csA in wild-type and in mutant cells starts after 4 hours of starvation. Thus, no major difference could be observed in respect to the time of development between wild-type and SCAR/PIR121-deficient cells (Figure 5.5).

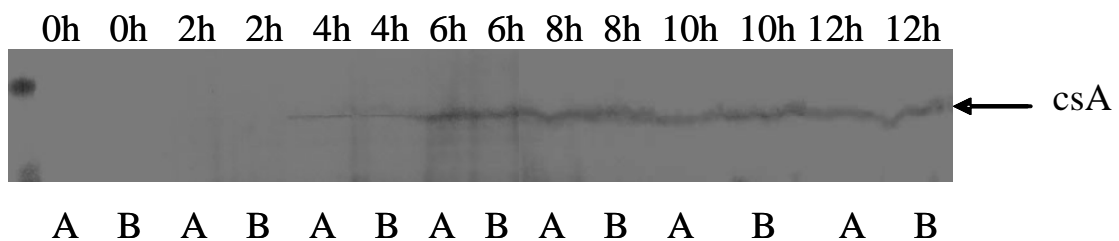


Figure 5.5. Development of *D. discoideum* cells to the aggregation stage is not affected in the absence of SCAR and PIR121 as shown by *Western blot* analysis of contact site A (csA). Expression of this protein is used as a marker for development towards the aggregation stage. Wild-type (A) and SCAR/PIR121-null cells (B) were kept in shaking culture at a density of 1×10^7 cells/ml and received pulses of cAMP every 6 minutes for the stimulation of development. Every 2 hours aliquots of both cell lines were collected and analyzed by SDS-PAGE and immunoblot analysis using anti-csA antibody (33-294-17).

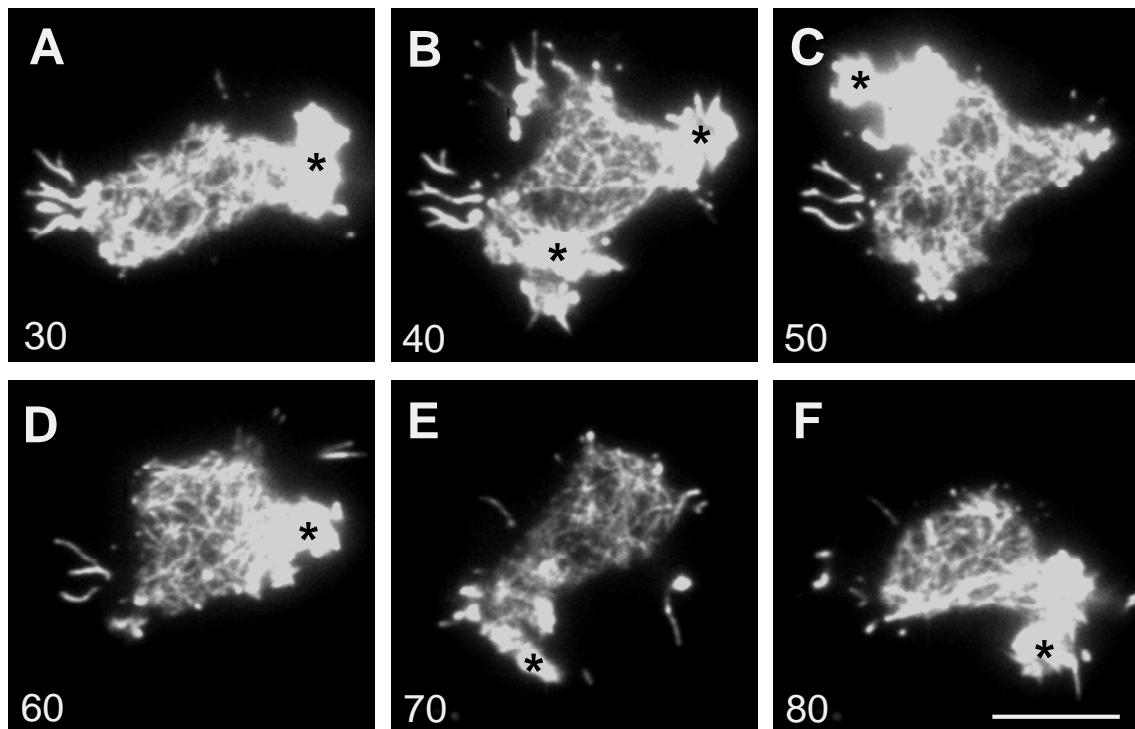


Figure 5.6. Wild-type *D. discoideum* cell showing patterns of strong actin enrichment in cell surface extensions. The TIRF images show patterns formed by GFP-LimE Δ at the substrate-attached surface of a wild-type cell. Actin accumulations were observed at the leading edge of the cell (asterisks). The time series of the cell moving on a glass surface was acquired with intervals of 1 second and 100 ms exposure time for each image. Time is indicated in seconds. Scale bar, 10 μ m.

5.4 Actin redistribution at the basal cell cortex exhibits different patterns in the absence of SCAR or PIR121

The widefield microscopy technique TIRF (Total Internal Reflection Fluorescence) selectively excites fluorescently labeled structures within an evanescent field extending only about 150 nm from the substrate into the substrate-near surface of the cell. In *D. discoideum* cells the membrane-anchored actin filament network has a thickness of 100-200 nm (Hanakam *et al.*, 1996), meaning almost its entire structure is amenable to visualization by TIRF. Therefore, TIRF microscopy has been used to analyze the actin organization close to the substrate-attached surface of *D. discoideum* cells. TIRF images of a wild-type cell expressing GFP-LimE Δ shows actin network structures and prominent actin accumulation at leading edges and in foci at the substrate-attached cell surface (Figure 5.6 and Movie 12).

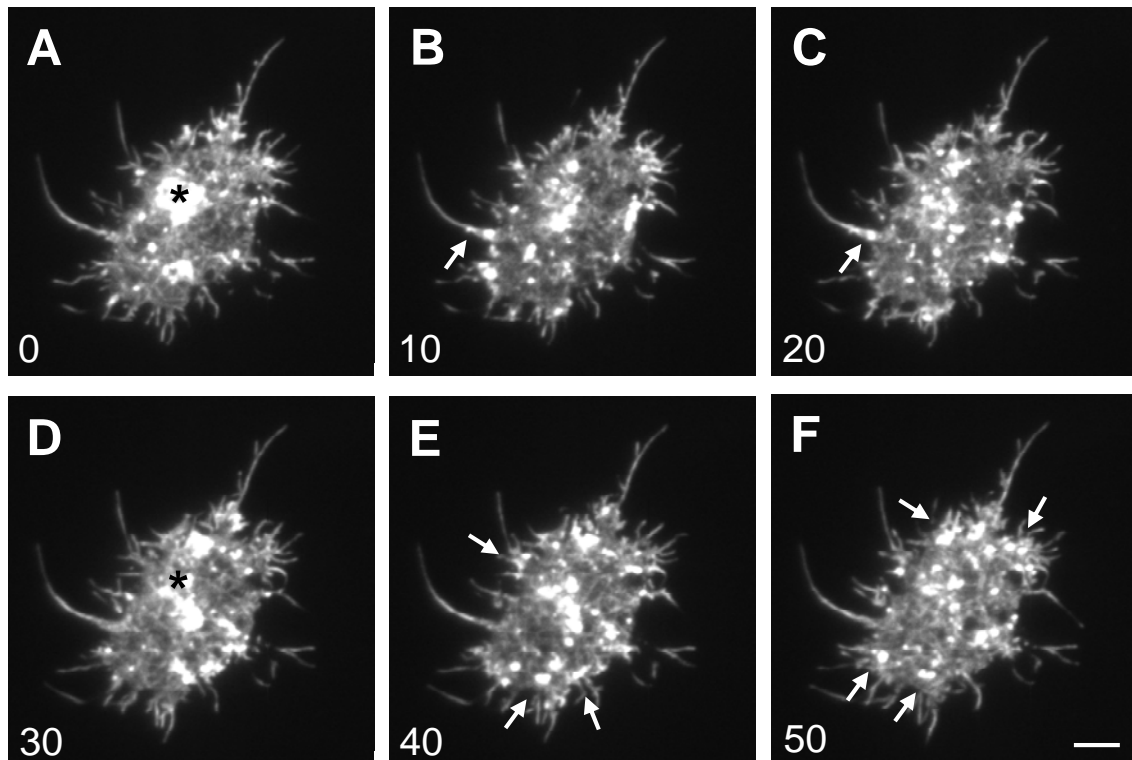


Figure 5.7. *D. discoideum* cell lacking PIR121 shows dynamic patterns of actin enrichment in the cell body and cell extensions. TIRF images of patterns formed by GFP-LimE Δ at the substrate-attached surface of a PIR121-null cell that moves on a glass surface were acquired with intervals of 1 second and 100 ms exposure time for each image. (A) The GFP-LimE Δ label visualized actin accumulation at the cell body (asterisks), which in B and C started to redistribute from the cell body into long extensions (arrows). (D) Actin accumulated at the cell body (asterisks) in a similar pattern as shown in A, E and F, redistributed in small granules towards the cell periphery (arrows). Note that this cell is larger than the wild-type cell shown in Figure 5.6. The time is indicated in seconds. Scale bar, 10 μ m.

In PIR121-null, SCAR-null, and SCAR/PIR121-null cells the actin showed different patterns of organization (Figures 5.7, 5.8 and 5.9). In the absence of PIR121 the cells appeared large, with extensive protrusions. At the basal cell cortex close to substrate, the actin redistributed from large actin clumps to smaller clumps at the periphery and along cell protrusions (Figure 5.7 and Movie 13). In SCAR and SCAR/PIR121-null cells the actin also redistributed periodically from the surface of the cell body to the cell periphery, but the large clumps are missing (Figures 5.8 and 5.9A-F and Movies 14 and 15). In SCAR/PIR121-null cells a mixture of SCAR-null and PIR121-null patterns was observed: small cells with short protrusions like SCAR-null cells and large cells with extensive protrusions like PIR121-null cells (Figure 5.9G-I and Movie 16).

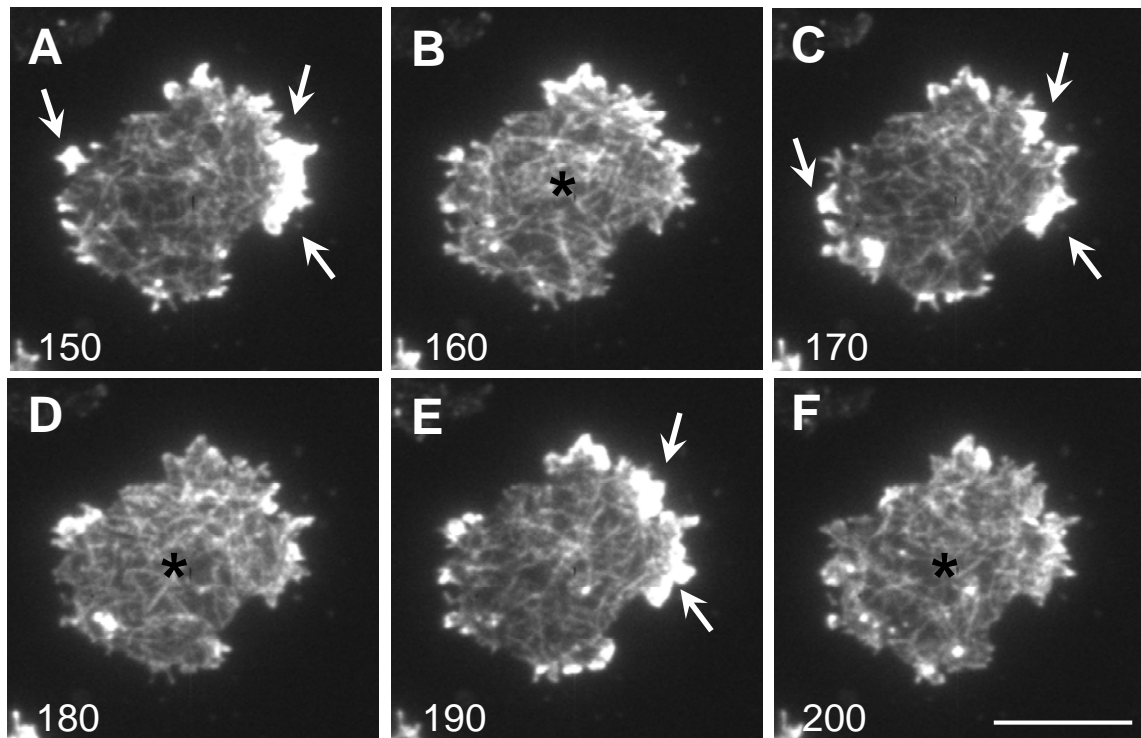


Figure 5.8. *D. discoideum* cell lacking SCAR shows dynamic patterns of actin enrichment with a periodic redistribution from the center of the substrate-attached surface cell body to the periphery. TIRF images of patterns formed by GFP-LimE Δ in a SCAR-null cell moving on a glass surface were acquired with intervals of 1 second and 100 ms exposure time for each image. (A, C, E) the GFP-LimE Δ label visualized strong actin accumulations in the cell periphery (arrow). (B, D, F) This label became weaker at the cell periphery and distributed more homogeneously over the cell surface (asterisks). A periodic redistribution of actin to the cell periphery is observed with period about 20 seconds. The time is indicated in seconds. Scale bar, 10 μ m.

The actin dynamics at the cell cortex observed by TIRF in wild-type and mutant cell contributes to the understanding of actin oscillations seen by laser scanning confocal microscopy. The actin oscillations observed in mutant cells could also be caused by the dynamic pattern of actin reorganization at the cell cortex.

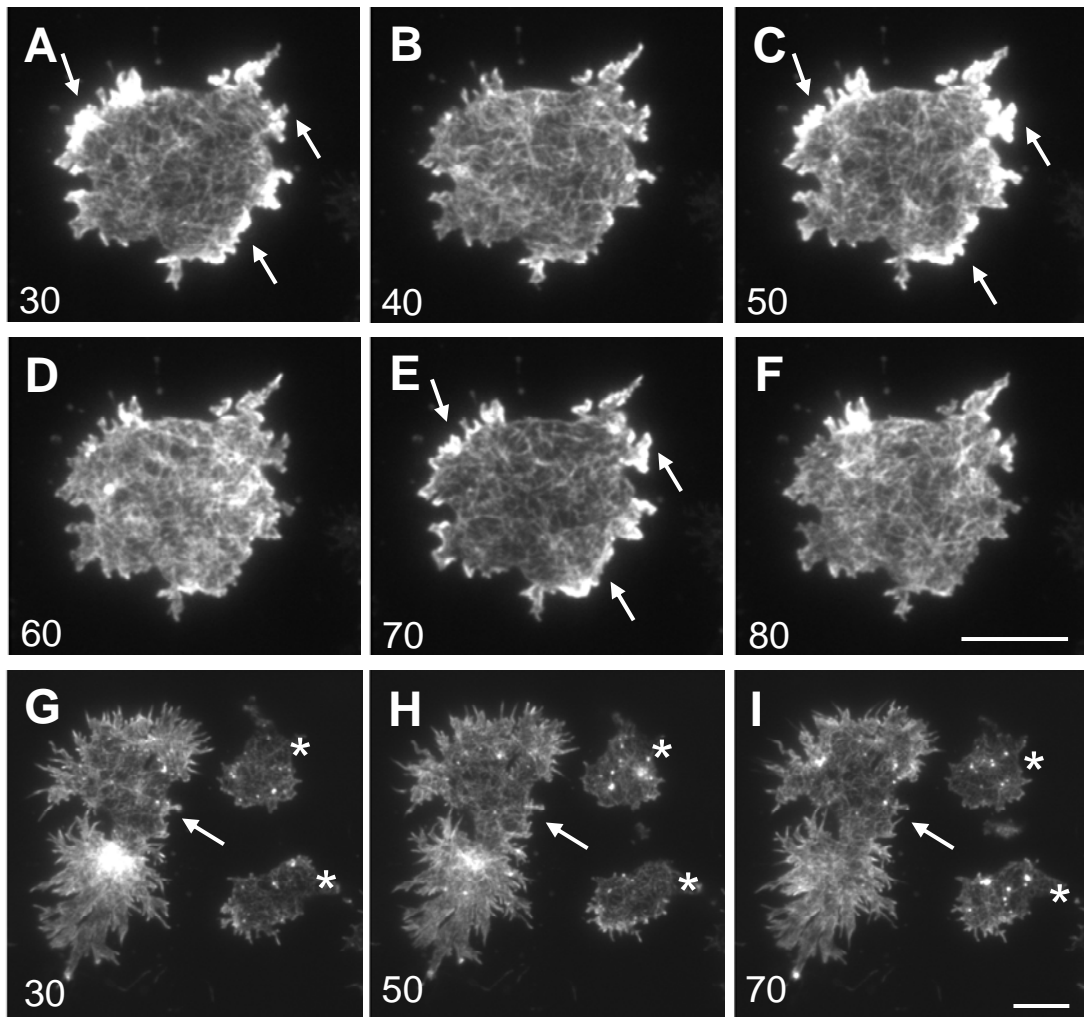


Figure 5.9. *D. discoideum* cells lacking both SCAR and PIR121 show dynamic patterns of actin enrichment with a periodic redistribution from the center of the substrate-attached surface to the cell border. TIRF images of patterns formed by GFP-LimE Δ at the substrate-attached surface of a SCAR/PIR121-null cell moving on a glass surface were acquired with an interval of 1 second and 100 ms exposure time for each image. The GFP-LimE Δ label indicated stronger actin accumulation at the cell border (A, C, E); (arrows) and weaker accumulation at the border (B, D, F). When the actin accumulation was stronger at the border it was weaker at the cell body. The redistribution of GFP-LimE Δ from the cell body to the border appears to be periodic with an interval of about 20 seconds. (G-I) Double-mutant cells showing characteristics of SCAR as well as PIR121 mutants. The asterisks indicate two small cells with short extensions similar to SCAR-null cells (Figure 5.8). The arrows indicate a large cell with long extensions and morphology similar to PIR121-null cells (Figure 5.7). The time is indicated in seconds. Scale bar, 10 μ m.

5.5 Localization of the Arp2/3 complex is not disturbed in the absence of SCAR

The Arp2/3 complex possesses little activity on its own. However, when engaged by nucleation promoting factors, proteins like WASP or SCAR complex, it is activated to nucleate actin polymerization (Goley and Welch, 2006).

To investigate whether Arp2/3 complex localization is affected by the absence of the SCAR protein, wild-type and SCAR-null cells expressing GFP-Arp3 or mRFP-ArpC-p41 and mRFP-LimE Δ or GFP-LimE Δ were studied by confocal and TIRF microscopy. In wild-type and SCAR-null cells the Arp2/3 complex was distributed throughout the cytoplasm and at the leading edge (Figure 5.10A and D). Actin was localized mainly at the leading edge (Figure 5.10B and E) and co-localizes with the Arp2/3 at the leading edge in both cell lines (Figure 5.10C and F). Hence, localization of the Arp2/3 complex is still observed in the absence of SCAR.

To visualize the distribution of the Arp2/3 complex with higher resolution at the substrate-near base of the cell, TIRF microscopy has been used. TIRF image series of SCAR-null cells expressing mRFP-ArpC-p41 subunit of the Arp2/3 complex and GFP-LimE Δ showed co-localization of Arp2/3 complex with actin at the leading edge (Figure 5.10G-I). This finding reinforces the data obtained by confocal microscopy indicating that the Arp2/3 complex is localized at the leading edge even in the absence of SCAR.

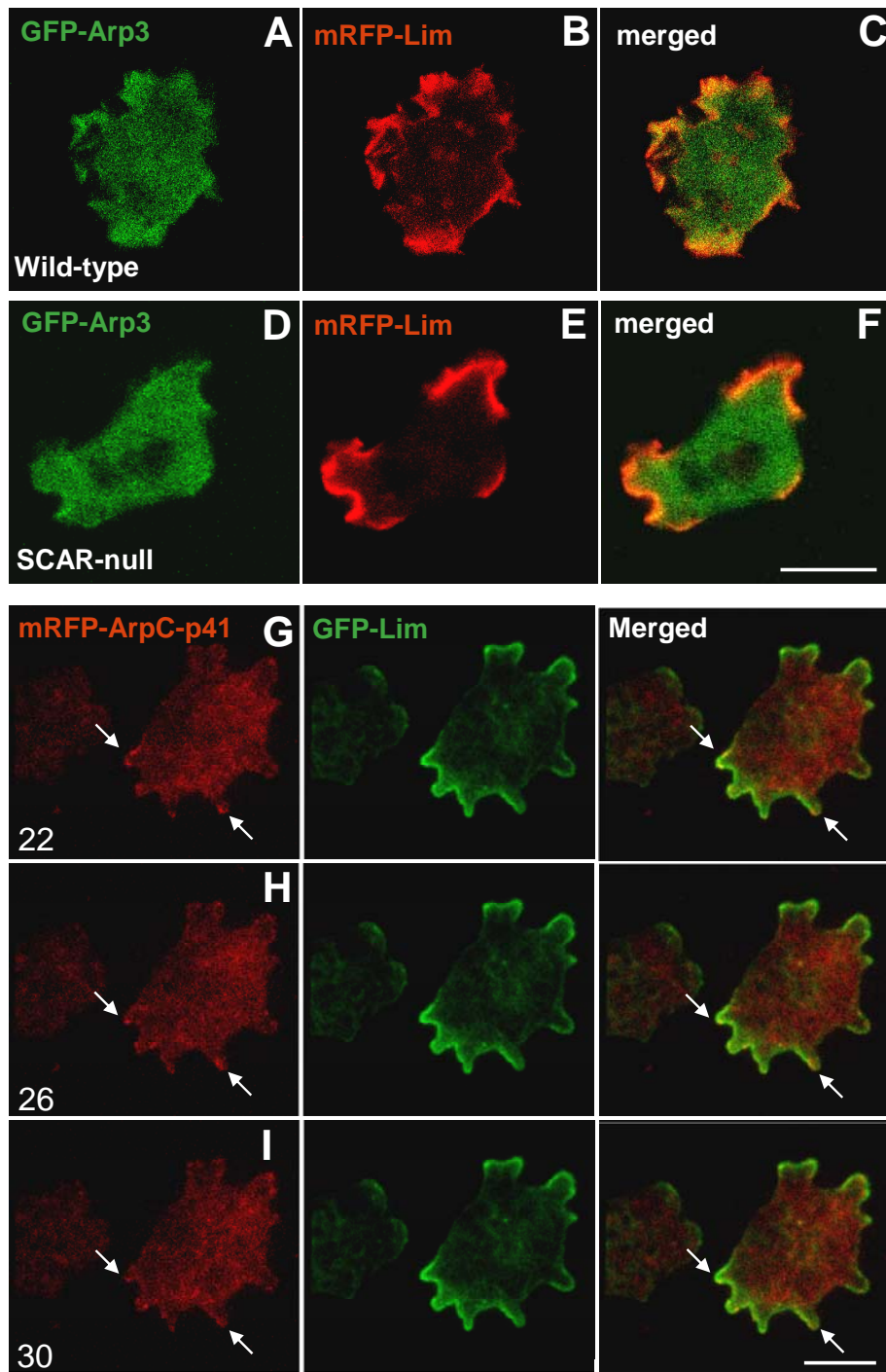


Figure 5.10. The Arp2/3 complex is localized to the leading edge in cells lacking SCAR. Confocal images of a wild-type cell showed localization of GFP-Arp3 (as a marker for the Arp2/3 complex) and mRFP-LimEΔ. (A-C) Wild-type (D-F and further down G-I) SCAR-null cells showed the Arp2/3 localization in the cytoplasm and at leading edges. The Arp2/3 complex and mRFP-LimEΔ co-localized at the leading edge in both cell lines (C and F). (G-I) TIRF images of patterns formed by mRFP-ArpC-p41 (subunit used as a marker for the Arp2/3 complex) and GFP-LimEΔ at the substrate-attached surface of a SCAR-null cell moving on a glass surface. Images were acquired with 1 second interval and 100 ms exposure time for each image. The arrows show localization of the Arp2/3 complex at the leading edge. At the merged panels, the arrows show the places where the Arp2/3 complex co-localizes with actin. Scale bar, 10 μm.

5.6 CorA is recruited to the leading edge in the absence of SCAR

Arp2/3 complex is regulated by activation of the SCAR complex and inhibited by coronin (Bear *et al.*, 1998; Humphries *et al.*, 2002). Since the localization of the Arp2/3 complex seems to be not affected in the absence of SCAR and is still localized at the leading edge, an obvious next step was to study the localization of CorA in the absence of SCAR.

Figure 5.11C shows the CorA localization in wild-type cell just behind actin. In the absence of SCAR, CorA is still recruited to the leading edge, but co-localizes there with actin as shown in Figure 5.11F.

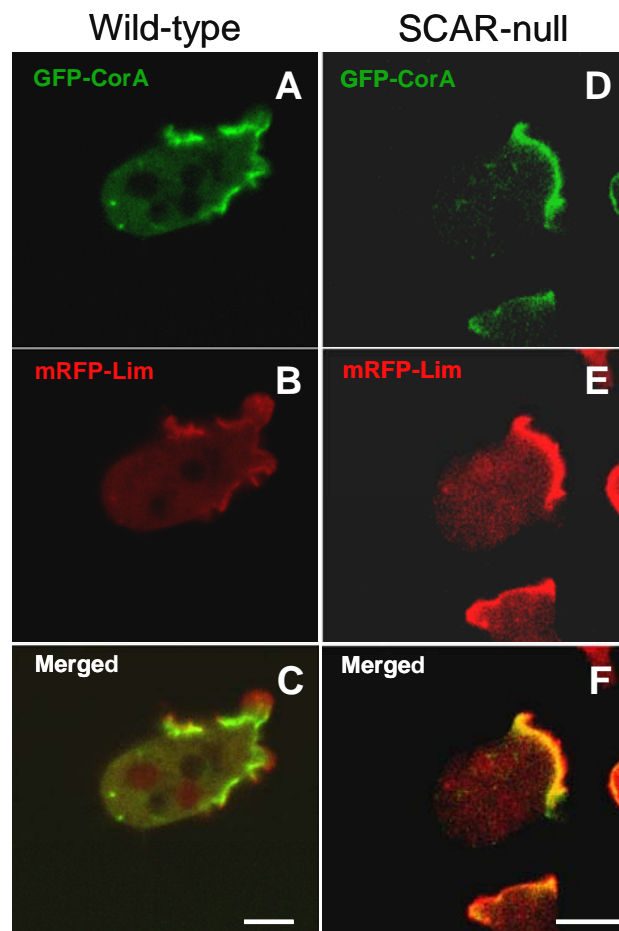


Figure 5.11. CorA is localized at the leading edge in cells lacking SCAR. Wild-type (A-C) and SCAR-null (D-F) cells expressing GFP-CorA and mRFP-LimE Δ were recorded by confocal microscopy. The wild-type cell showed CorA localization (A) directly behind the LimE Δ label (B) with little overlap (C). In the SCAR-null cell CorA (D) as well as LimE Δ (E) were localized at the leading edge and co-localized there (F). Scale bar, 5 μ m.

5.7 External cAMP stimulation promotes a shift in the phase of actin oscillations in SCAR and PIR121-deficient cells

A spatial gradient of the chemoattractant cAMP induces actin cytoskeleton reorganization in *D. discoideum* cells (Franca-Koh and Devreotes, 2004). Therefore, to explore whether cAMP influences the actin oscillations observed in the absence of SCAR, PIR121 and double-mutant cells were allowed to settle on a coverslip with a plastic ring of 5 cm diameter. The cells were incubated with 0.5 μ M caged cAMP for 15 minutes and covered with a piece of agar of 0.5 x 0.5 cm. After incubation the excess of caged cAMP solution was removed.

One area was selected to apply the laser for uncaging the cAMP. The active cAMP was released from this area and attracted the surrounding cells to move in its direction. Actin dynamics could be observed during migration of the double-mutant cells by monitoring the GFP-LimE Δ (Figure 5.12). The double-mutant cells respond to the stimulation and migrate towards the cAMP source showing actin oscillations at the cell cortex (Movie 17). Thus, the cAMP chemoattractant does not suppress the actin oscillations in the absence of SCAR and PIR121 and the cells are capable to respond to the stimulus.

To study whether a cAMP pulse shifts the phase of the actin oscillations, wild-type and double-mutant cells were exposed to a single cAMP pulse of 2 seconds duration. In this case, the peak concentration of cAMP was about 2 μ M.

Wild-type cells showed only small actin fluctuations before the cAMP stimulus and a distinct peak of actin accumulation after the stimulus (Figure 5.13A). In SCAR/PIR121-null cells the amplitudes of spontaneous actin oscillations had a similar size as the responses to cAMP in wild-type cells. In some cases the cAMP pulse caused a shift in the phase of oscillations in the double-mutant cells. Figure 5.13B and 5.13C display typical examples of a phase shift. The peaks that are shifted in response to the cAMP pulse show similar amplitudes as the spontaneous oscillations. Even in cases where the cAMP stimulus was initiated in phase with the intrinsic oscillations, no increase in the amplitude could be observed (Figure 5.13D). Also in cases of less regular or disordered actin

Results

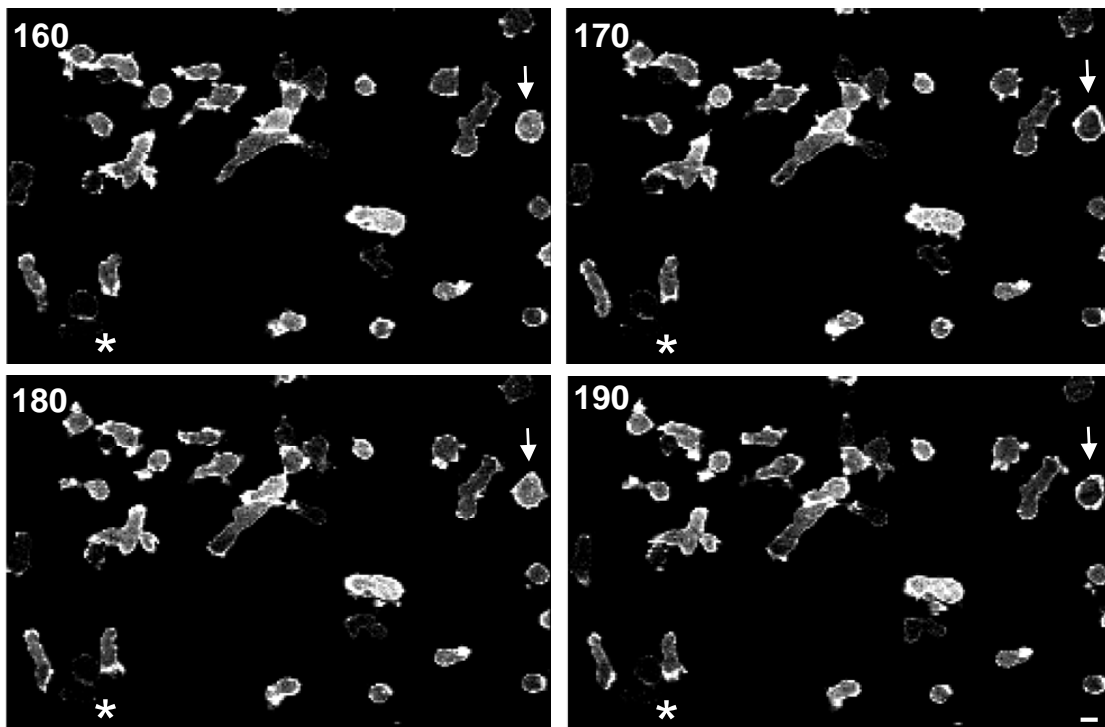


Figure 5.12. The chemoattractant cAMP does not suppress the autonomous oscillations of actin to the cell cortex in SCAR/PIR121 double-null cells. SCAR/PIR121-null cells expressing GFP-LimE Δ were settled in a chamber, incubated with 0.5 μ M of caged cAMP and covered with a piece of agar. After incubation the excess liquid was removed with a piece of paper tissue. cAMP uncaging was performed in a selected area (asterisks). The peak concentration of cAMP was about 6.0×10^{-2} μ M. The double-mutant cells showed actin oscillations in the cell cortex and the cytoplasm in the presence of a chemoattractant gradient. The complete time series can be seen in the Movie 17. Frame numbers are indicated. The time interval of each frame is 1 second. Scale bar, 10 μ m.

fluctuations no sharp actin response to a cAMP stimulus was observed (Figure 5.13E).

To investigate whether a cAMP pulse shifts the phase of the actin oscillations at the cortex and cytoplasm, the fluorescence intensities of GFP-LimE Δ were separately plotted (Figure 5.13.1). The plots showed a clear phase-shift effect on the alternating peaks of actin polymerization between cortex and cytoplasm.

These data indicate that cAMP may synchronize the phases of autonomous actin oscillations by shifting the actin peaks at cell cortex and cytoplasm. However, the cAMP stimulus does not influence the amplitude of the actin peak and does not suppress the actin oscillations.

Results

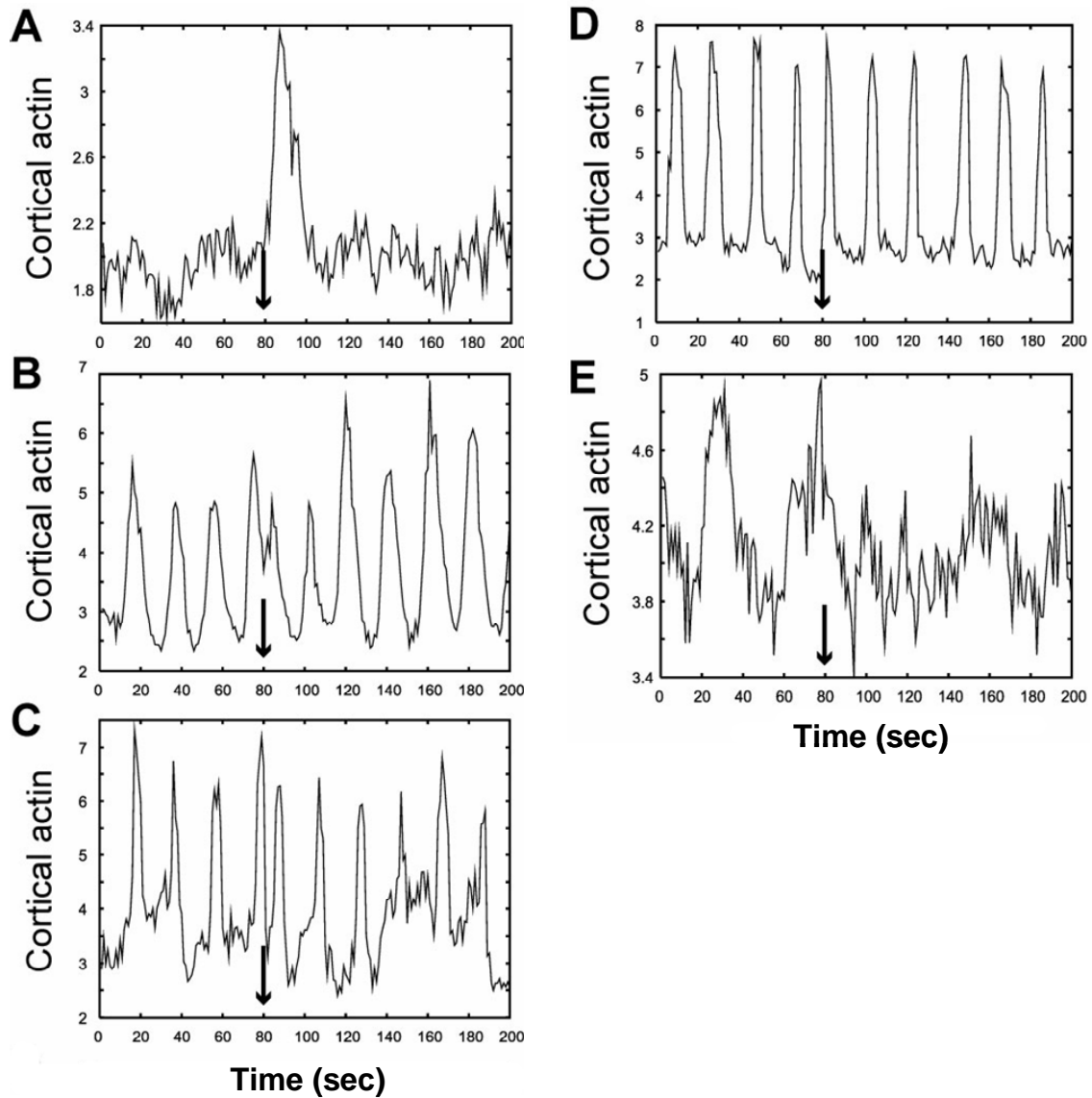


Figure 5.13. A cAMP stimulus promotes phase-shifts of actin oscillations in mutant cells lacking SCAR and PIR121. In a microfluidic channel, cells were exposed under flow conditions for about 2 seconds to a spatial stimulus of cAMP that was generated by flow photolysis of caged cAMP. The peak concentration of cAMP was about 2 μ M. The cAMP stimulus was supplied after 80 seconds of recording, as indicated by the arrow in each panel. Confocal recordings through the middle of the cell bodies were acquired at intervals of 1 second. The measured response was the transient accumulation of actin in cortical regions of the cells. The intensity of GFP-LimE Δ fluorescence at the cell cortex was normalized by calculating the ratio of fluorescence intensity in the cortex over that in the interior of a cell. In (A) a single wild-type cell exhibited the typical peak in cortical actin accumulation, demonstrating that the normal response to cAMP clearly exceeds the range of intrinsic fluctuations. In (B-E) single SCAR/PIR121 double-mutant cells were analyzed. In (B) and (C), the cAMP pulse resulted in a shift in the phase of oscillations. No additive effect on the amplitude was observed, even when a cAMP pulse was supplied right at the onset of a spontaneous peak as shown in (D). In (E), an extreme case of strong and disordered fluctuations that persisted both before and after stimulation of the cell is presented.

Results

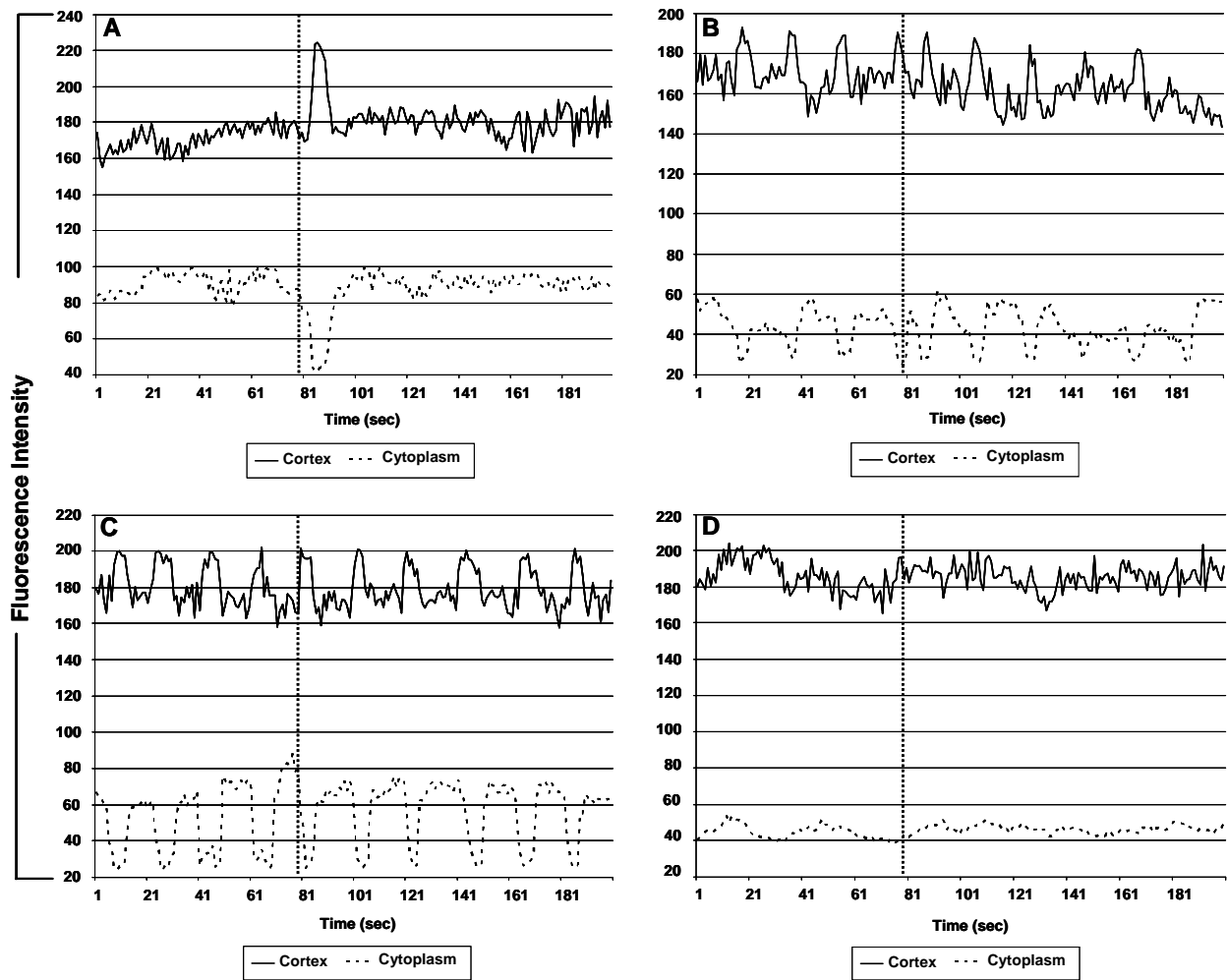


Figure 5.13.1. The phase-shift of the actin oscillations at the cell cortex and the cytoplasm. The same cells described in Figure 5.13 (A, C, D and E), were re-plotted here. The ratios of fluorescence intensity in the cortex over the cytoplasm showed in Figure 5.13 (A, C, D and E), where split and separately plotted. (A) The wild-type cell shows a clearly increased peak of actin polymerized at the cortex and a decreased peak at the cytoplasm, only after short cAMP pulse (vertical dashed line). (B and C) SCAR/PIR121-mutant cells, show alternating peaks of actin polymerization/depolymerization between cortex and cytoplasm before and after cAMP pulse. A phase-shift is observed after cAMP pulse (B and C). In (B) the phase is delayed and in (C) the phase is advanced. (D) An extreme case of the double-mutant cell showing a strong disordered fluctuations of actin polymerization at the cell cortex and cytoplasm that persist both before and after cAMP stimuli.

5.8 The Arp2/3 complex is poorly recruited to the leading edge in the absence of SCAR in a gradient of cAMP

To investigate the recruitment of the Arp2/3 complex to the leading edge during chemotaxis in the absence of SCAR, wild-type and SCAR-null cells expressing GFP-Arp3 and mRFP-LimE Δ were starved in shaking culture for 6 hours and then subjected to the chemoattractant cAMP released from a micropipette.

Figure 5.14 shows that in the presence of SCAR the Arp2/3 complex is clearly recruited to the leading edge of the cells during chemotaxis. In the absence of SCAR this recruitment of the Arp2/3 complex appears to be weaker but still present (Figure 5.15). These data indicate that SCAR may improve, but it is not essential for Arp2/3 recruitment to the leading edge during a chemotactic response.

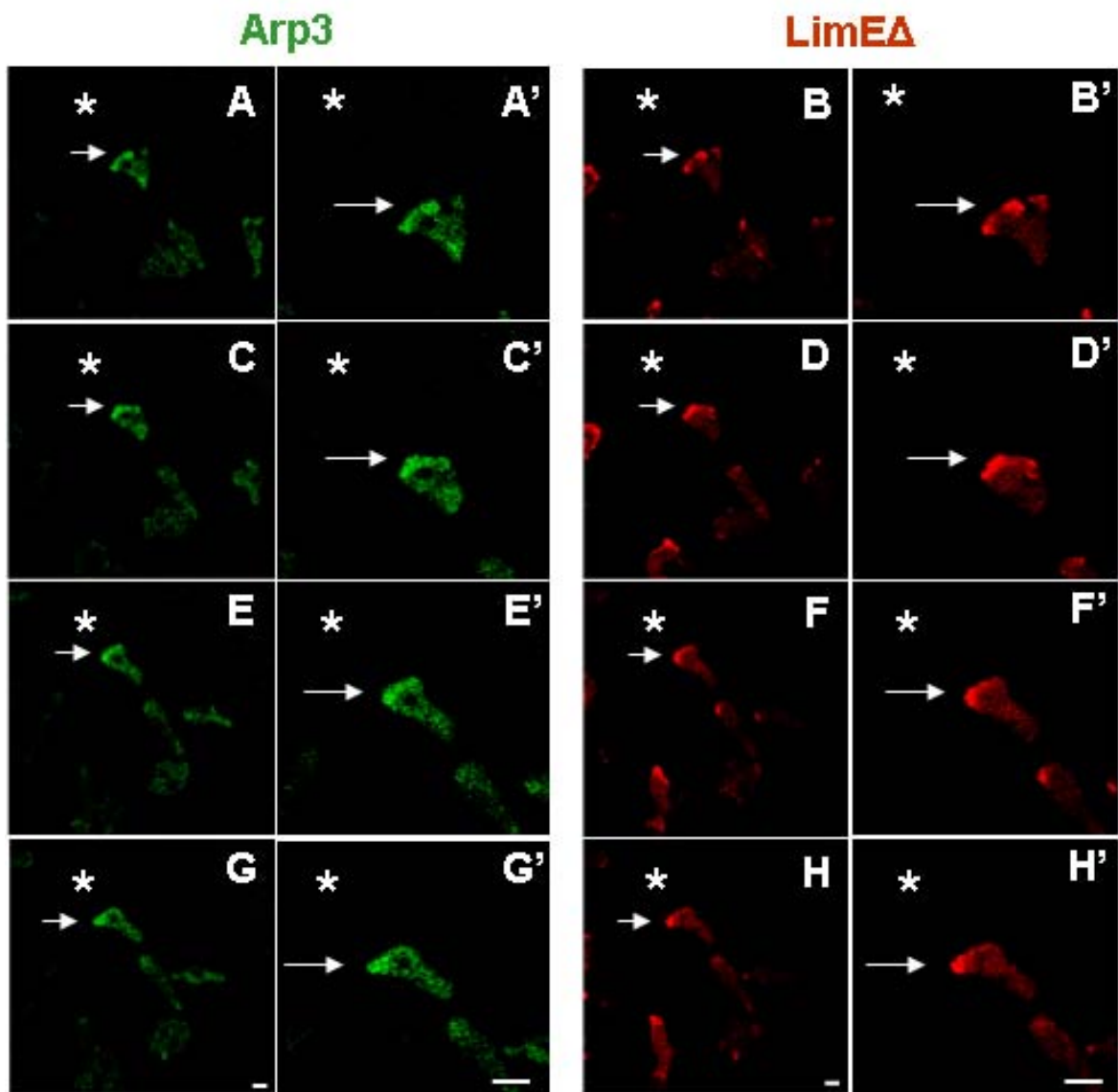


Figure 5.14. In the presence of SCAR the Arp2/3 complex is strongly recruited to the leading edge in a gradient of cAMP. Wild-type cells expressing GFP-Arp3 and mRFP-LimE Δ were kept in shaking culture for 8 hours and then subjected to chemoattractant released from a micropipette. The tip position is indicated by asterisks. Images were taken every 15 seconds. GFP-Arp3 (A, C, E, G and its magnification A', C', E', G') and mRFP-LimE Δ (B, D, F, H and its magnification B', D', F', H') were recruited to the leading edge directed towards the source of chemoattractant as indicating by arrows. Scale bars, 5 μ m.

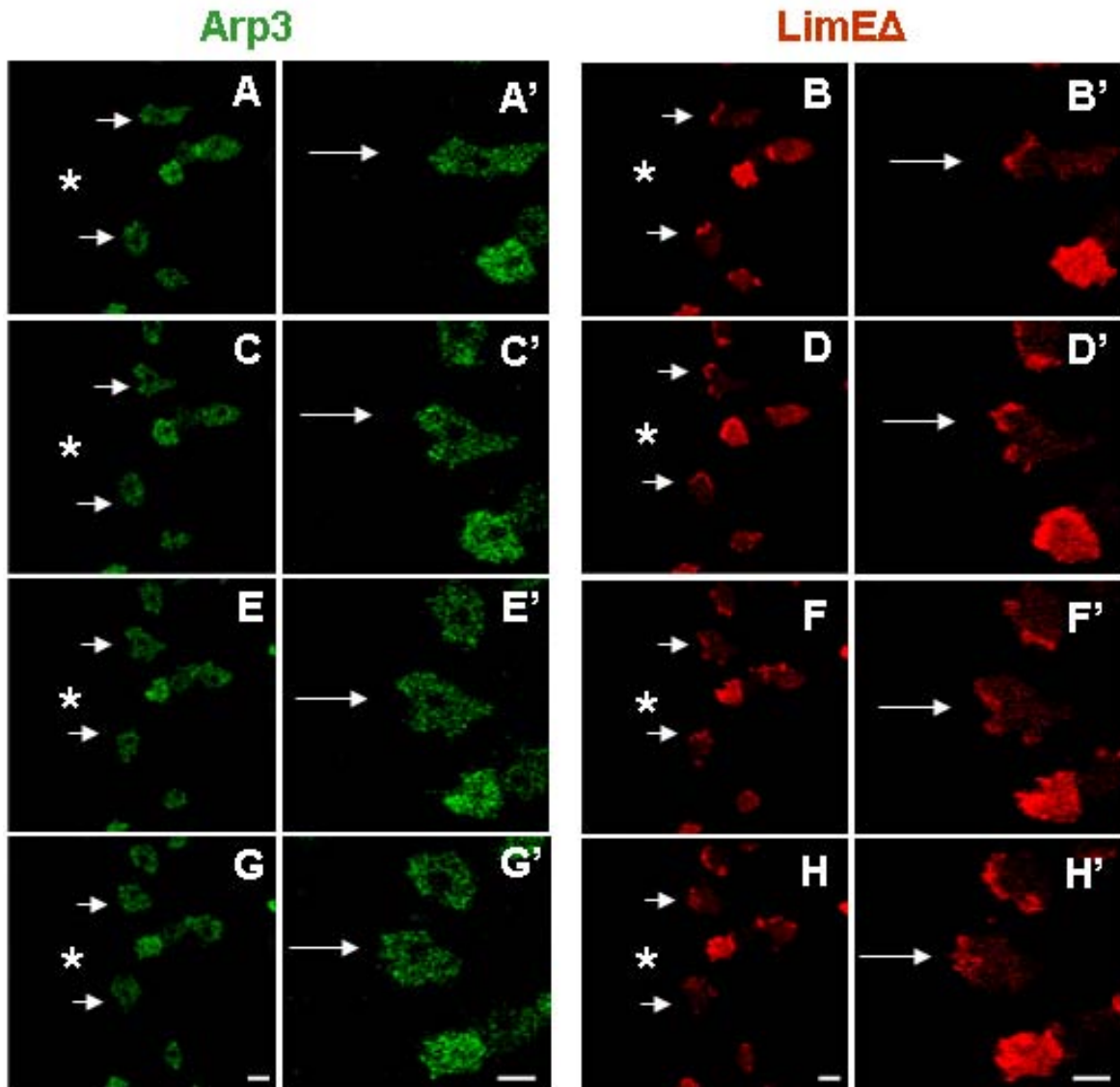


Figure 5.15. In the absence of SCAR the Arp2/3 complex is poorly recruited to the leading edge in a gradient of cAMP. SCAR-null cells expressing GFP-Arp3 and mRFP-LimEΔ were kept in shaking culture for 8 hours and then subjected to chemoattractant released from a micropipette. The tip position is indicated by asterisks. Images were taken every 15 seconds. As indicated by arrows the GFP-Arp3 (A, C, E, G and in magnification A', C', E', G') was poorly recruited to the leading edge. In contrast, mRFP-LimEΔ (B, D, F, H and in magnification B', D', F', H') was recruited to the leading edge during chemotaxis. Scale bars, 5 μ m.

6 Discussion

Many cellular processes, including cytokinesis, endocytosis and cell locomotion, require dynamic remodeling of the actin cytoskeleton. All of these processes involve proteins that regulate and control assembly, disassembly and reorganization of actin networks in response to cellular cues (Humphries *et al.*, 2002; Eichinger *et al.*, 2005). The exact mechanisms regulating these proteins are subject to current research.

In this work, *D. discoideum* has been used as a model system to study the role of CorA, Aip1 and members of the SCAR complex (Eden *et al.*, 2002 and Goley and Welch, 2006) in the regulation of processes that involve actin dynamics. Earlier studies based on single-null mutants provided already evidence of an involvement of CorA and Aip1 in cytokinesis, phagocytosis and cell motility (de Hostos *et al.*, 1991 and 1993; Maniak *et al.*, 1995; Konzok *et al.*, 1999). Here, single- and double-mutants deficient in CorA, Aip1, in the SCAR protein and PIR121 have been used in order to gain insights into their role controlling actin assembly and disassembly.

6.1 CorA and Aip1 contribute to an effective chromosome segregation and act cooperatively in cytokinesis

Mitosis in *D. discoideum* is characterized by the persistence of the nuclear envelope and the absence of a typical anaphase. *D. discoideum* has six small chromosomes. In metaphase they are arranged in the form of a ring around the midzone of the spindle. Already before the compact metaphase spindle elongates, the chromosomes are linked to the centrosomes at the spindle poles, and the spindle starts to disassemble at the midzone before the cleavage furrow ingresses (Neujahr *et al.*, 1998).

If a mitotic nucleus acquires two centrosomes it will divide normally, giving rise to a complete set of chromosomes in each of the two daughter nuclei. However, if one or more than two centrosomes attach to a nucleus, a monopolar or multipolar spindle is formed and cells will turn to poly- or aneuploidy. In Figure

3.4D and E cells lacking both CorA and Aip1 are shown with one or more than two centrosomes attached to a nucleus. The attachment of multiple centrosomes to one nucleus may result in the formation of tri-polar spindles in a cruciform configuration (Figure 3.4D-E) leading to aberrant chromosome segregation. The association of centrosomes with nuclei is reversible. It perpetuates a genetic instability, enabling a mutant cell line to survive even with an excess number of centrosomes (Gerisch *et al.*, 2004). Supernumerous centrosomes have been described earlier for Aip1 single-mutant cells (Gerisch *et al.*, 2004). It is a hallmark of tumor cells (Lingle *et al.*, 2002; Nigg, 2002). In conclusion, the deficiency of the double-mutant cells in promoting effective chromosome segregation could be a consequence of these centrosomal aberrations caused by the absence of CorA and Aip1.

The elimination of both CorA and Aip1 results also in severe cytokinesis defects in the double-mutant cells. Cells lacking CorA or Aip1 are characterized by a moderate impairment of cytokinesis. The disorder is, however, much more pronounced in the double-mutant (personal communication by Annette Müller-Taubenberger). During continuous growth CorA/Aip1-null cells become extremely large and multinucleate (Figure 3.5D-E), which might be the result of a deficiency in cytokinesis.

Aip1 and CorA are localized in *D. discoideum* at the poles of dividing cells and do not co-localize with actin or myosin II at the contractile ring during cytokinesis (de Hostos *et al.*, 1993; de Hostos, 1999; Konzok *et al.*, 1999). Aip1-null cells become multinuclear when grown attached on to a glass surface (Konzok *et al.*, 1999). When CorA-null cells are grown attached to a solid substratum a higher number of multinuclear cells can be observed than in shaking suspension (de Hostos *et al.*, 1993). Therefore, the attachment of Aip1-null or CorA-null cells to a surface does not favor cell division.

However, in CorA/Aip1-null cells cytokinesis is proceeding much better when the cells are attached to a solid substratum than in shaking suspension (personal communication by Annette Müller-Taubenberger). This is similar to the behavior of myosin II mutants (Neujahr *et al.*, 1997). Therefore, under attached conditions the double-mutant cells are able to undergo cytokinesis more frequently or to perform cytofission, a traction-mediated process first described in myosin II-null mutants (Fukui *et al.*, 1999).

In conclusion, in the absence of the individual proteins CorA or Aip1 the cells might divide by cytokinesis A, which is independent of cell-to-substrate adhesion and is dependent on myosin II (Nagasaki *et al.*, 2002). However, in the absence of both proteins the cells might divide by cytokinesis B, a myosin II-independent kind of cytokinesis which depends on cell-to-substrate adhesion (Neujahr *et al.*, 1997).

Many of the proteins constituting the actin system in *D. discoideum*, including Aip1 and CorA studied in this work, are related to mammalian proteins (Glöckner *et al.*, 2002). Therefore, it is tempting to speculate that mutations in genes encoding actin-binding proteins like CorA and Aip1 may contribute to genomic instability in mammalian cells and might be considered as one of the factors involved in cancer progression (Boveri, 1914; Nigg, 2002).

6.2 CorA and Aip1 participate in actin turnover during phagocytosis and cell motility

Phagocytosis is a first line of defense against invading pathogens, and is performed by macrophages and leukocytes that migrate to the site of infection. The internalized pathogen is contained in a membrane-limited vacuole termed the phagosome that interacts via fission and fusion reactions with the endo-lysosomal system, leading to the death of the microbe. Paradoxically, many pathogens actually stimulate cells to initiate phagocytosis, and once inside use the intracellular environment to allow for their own growth. The continued survival of these intracellular pathogens often involves disruption of the normal endo-lysosomal to phagosomal membrane trafficking pathways (Stuart and Ezekowitz, 2005).

Dictyostelium is an organism well suited for studies of the phagocytosis process. This free-living soil amoeba is a professional phagocyte in its vegetative state and can internalize particles at higher rates than macrophages or neutrophils. The organization of the actin cytoskeleton, cell motility, membrane trafficking, and internalization events are comparable to those observed for neutrophils and macrophages. Also, phagosomal maturation in *Dictyostelium*

appears comparable to phagosomal maturation in mammalian phagocytes (Rupper and Cardelli, 2001). *Dictyostelium* uses similar mechanisms as mammalian phagocytes during internalization of particles, interactions between the endo-lysosomal system and during phagosome maturation (Aderem and Underhill, 1999). Once a particle has been internalized, membrane trafficking events rapidly modify the nascent phagosome and provide it with the ability to degrade its contents. Actin and actin-binding proteins are removed from the nascent phagosomes and interact again with the late endo-lysosomal system (Drengk *et al.*, 2003).

Actin contributes to internalization at the plasma membrane (Apodaca, 2001; Qualmann and Kessels, 2002) and to subsequent trafficking steps like propulsion through the cytoplasm (Merrifield *et al.*, 1999; Taunton *et al.*, 2000), fusion of phagosomes with early endosomes (Guerin and de Chastellier, 2000), and transition from early to the late endosomes (van Deurs *et al.*, 1995; Brown and Song, 2001). Thus, the endocytic pathway depends on the actin cytoskeleton and actin-binding proteins.

Rauchenberger *et al.* (1997) showed in *D. discoideum* that CorA is present transiently on endocytic vesicles after acidification. Schmauch and Maniak (2008) demonstrated through hybrid proteins the association of CorA and Aip1 with actin at the cell cortex and in the late endosomes. Interestingly, the authors describe different localization of these proteins. CorA having a preferential actin-binding affinity localized to the cell cortex more than to the endosomal actin coat, whereas Aip1 and cofilin having a stronger affinity to the endosomal actin coat than to the cell cortex and are localized at the endosomal vacuoles as a kind of cluster. Thus, the authors concluded that Aip1 and cofilin function as enhancers of F-actin-depolymerization activity resulting in the breakdown of the endosomal actin coat causing subsequent agglutination of endosomal vacuoles.

At the initial step of phagocytosis, during the formation of phagocytic cups, CorA and Aip1 are also present (Maniak *et al.*, 1995; Hacker *et al.*, 1997; Konzok *et al.*, 1999). Thus, to investigate the functional contribution of both proteins to early phagocytosis, wild-type and double-mutant cells deficient in both CorA and Aip1 have been fed with killed-yeast particles. The formation of phagocytic cups has been recorded with a confocal microscope, using GFP-LimE Δ as a marker for filamentous actin.

Discussion

In wild-type cells, the formation of a phagocytic cup, from inception until the complete engulfment of a yeast particle, took 40 seconds. In the CorA/Aip1-double mutant cells, the duration of the uptake process was prolonged to 120 seconds (Figure 3.6A). This is similar to values measured earlier for the single-mutants (Maniak *et al.*, 1995; Konzok *et al.*, 1999).

During engulfment of a particle in double-mutant cells, a strong label of GFP-LimE Δ was observed around the phagocytic cup (Figure 3.6B). A phagocytic cup needs to precisely follow the shape of the particle during protrusion (Hacker *et al.*, 1997). Therefore, if existing actin filaments do not depolymerize fast enough during this process, the engulfment of a particle might be delayed as shown in Figure 3.6C.

In conclusion, CorA and Aip1 contribute to an effective actin-turnover allowing a fast growth of phagocytic cups. The understanding of how CorA and Aip1 might be involved in phagocytosis is a contribution for a potential therapeutic intervention against for example, pathogens that disrupt the normal phagosomal maturation leading to diseases.

Chemotaxis is a pivotal response of many cell types to external spatial cues. It plays important roles in diverse functions such as finding nutrients in prokaryotes, forming multicellular organisms in *D. discoideum*, tracking bacterial infections in neutrophils, and organizing the embryonic cells in metazoa (Baggiolini, 1998; Campbell and Butcher, 2000; Crone and Lee, 2002). In *D. discoideum* cells, extracellular cAMP functions as a chemoattractant that is detected by specific G-protein coupled surface receptors. Chemotaxis is achieved by coupling gradient sensing to basic cell movement. During migration pseudopod extension at the leading edge is mediated by the formation of new actin filaments, whereas actomyosin filaments at the rear of the cell inhibit pseudopod formation and retract the uropod (Parent and Devreotes, 1999).

In a gradient of the chemoattractant cAMP, *D. discoideum* cells are orientated with a distinct front directed toward the source and their tail pointing into the opposite direction. The front region is specified by the polymerization of actin and by the accumulation of proteins like the Arp2/3 complex, CorA and Aip1 that regulate actin disassembly into a dense network of filaments (Gerisch *et al.*, 1995; Brieher *et al.*, 2006; Konzok *et al.*, 1999). The tail is distinguished by the

recruitment of filamentous myosin-II (Fukui *et al.*, 1997; Laevsky and Knecht, 2003; Etzrodt *et al.*, 2006).

Here, the aim was to investigate the participation of CorA and Aip1 in actin dynamics during cell migration. CorA/Aip1-double mutant cells are unable to move properly in a chemotactic gradient although they are still able to sense a cAMP gradient (Figure 3.8). The impact on the velocity of cell migration is much stronger in the absence of both proteins than in the absence of individual proteins (Table II), suggesting that CorA and Aip1 act cooperatively in actin dynamics at the front of the cells.

Since the double-mutants migrate slowly but are still capable of reorganizing the actin cytoskeleton (Figure 3.7), the next question was whether the temporal actin organization is affected in cells missing CorA and Aip1 under patterns of cAMP stimulation.

6.3 CorA and Aip1 regulate the temporal dynamics of actin polymerization and depolymerization

After a global upshift of the chemoattractant cAMP *D. discoideum* cells show a peak of actin polymerization and depolymerization within 10 seconds of stimulation. This peak is linked to the recruitment of proteins that activate or inhibit actin polymerization. CorA and Aip1, two proteins involved in either the termination of actin polymerization or in enhancement of actin depolymerization, show such a sharp cAMP-induced increase and decrease of their cortical localization in flow chamber experiments (Etzrodt *et al.*, 2006). However, the precise control of cAMP delivery to the cells could not be obtained with this experimental technique.

By employing a new experimental setup for chemotaxis experiments based on light-induced cAMP uncaging in a microfluidic system under confocal inspection, the limitation of the flow chamber to precisely control the stimulus was overcome (Beta *et al.*, 2007). This approach has been applied to investigate the spatiotemporal translocation of CorA and Aip1 to the cell cortex and the contribution of these proteins to temporal actin assembly and disassembly.

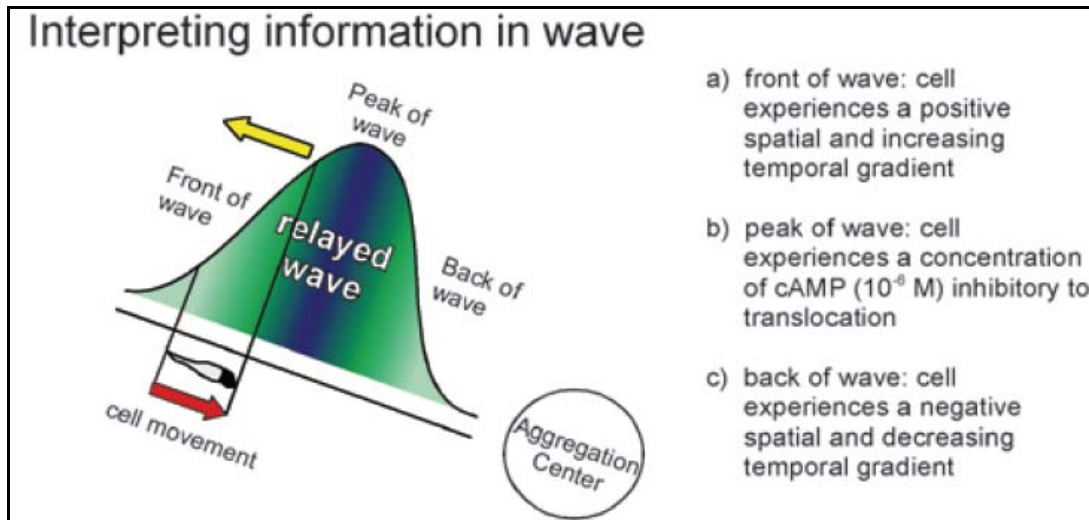


Figure 6.1. Model of chemotaxis in *Dictyostelium* proposed by Soll *et al.* 2002. In the front of the cAMP wave each cell experiences an increasing temporal gradient and a positive spatial gradient of cAMP, at the peak of the wave the cell experiences a cAMP concentration inhibitory to locomotion, and in the back of the wave the cell experiences a decreasing temporal and negative spatial gradient of cAMP.

Two different conditions of stimulation, i.e. a continuous or a short pulse of cAMP, were applied and the translocation rate of CorA and Aip1 to the cortex and the release of these proteins from the cortex were determined. The rate of recruitment and the release of CorA and Aip1 from the cell cortex might be lower under a continuous cAMP stimulus in comparison to short pulses (Figure 4.1 and Tables IV and V). Thus, the cellular response can be modulated by different stimulation patterns.

These patterns of stimuli might follow the model of information phases of cAMP waves proposed by Soll *et al.* (2002). This model takes into account the different information present in each phase of a natural cAMP wave (Figure 6.1). A natural cAMP wave has three phases: the front, peak and back phase.

In the front phase of a cAMP wave each cell experiences a positive spatial and increasing temporal gradient. The back phase is characterized by a decreasing temporal and negative spatial gradient of cAMP. cAMP concentration increases as a function of time (increasing temporal gradient) through the front of the wave and decreases as a function of time (decreasing temporal gradient) through the back of the wave. The concentration at the peak of the wave is actually inhibitory to translocation and cell polarity (10^{-6} M) (Wessels *et al.*, 1989; Zhang *et al.*, 2003). Thus, when cells receive a short pulse of cAMP, they might be

Discussion

exposed to the front of the wave, where the cAMP concentration is increasing, followed by the back of the wave with decreasing cAMP concentration. Therefore, this rapidly increasing and decreasing temporal gradient is enough to provide an efficient rate of the cellular responses.

Under conditions of a continuous cAMP stimulation with no decline of cAMP concentration, the cells experience not only the front, but also a prolonged peak phase of a wave. At the peak of a wave the cells experience a cAMP concentration inhibitory to locomotion ($>10^{-6}$ M concentration applied during the experiments). Therefore, the actin dynamics might be slowed down at this point leading to a decreased rate of protein responses.

Upon a chemoattractant stimulus, the initial steps of the chemotactic signaling cascade take place within only a few seconds (Parent and Devreotes, 1999) and time scales for the dynamics of the actin cytoskeleton were found to be even shorter (Diez *et al.*, 2005). The aim here was to analyze whether and how the temporal dynamics of actin assembly and disassembly would be affected in the absence of CorA and Aip1.

In short, in live-cell experiments the rates of increase and decrease of F-actin assembly in the cell cortex was measured by fluorescently labeled LimE Δ . The rate for actin assembly and disassembly in cells lacking CorA or/and Aip1 is impaired and the stimulus pattern applied to the cells might modulate this impairment (Figures 4.2 and 4.3). In the absence of CorA and/or Aip1 the rate of actin disassembly is much more disturbed than the rate of actin assembly (Tables VI and VII), suggesting a stronger contribution of both proteins in promoting actin disassembly. This is in agreement with previous work. Gerisch *et al.* (1995) proposed a role of CorA in promoting the disassembly of actin filaments, 'balancing' the activities of proteins that nucleate actin polymerization. Briehner *et al.* (2006) reported that coronin stimulates cofilin activity indirectly by binding to actin filaments and altering their structure in a way that facilitates the binding of cofilin, reinforcing evidence that coronin promotes actin disassembly.

Konzok *et al.* (1999), Okada *et al.* (1999), Rodal *et al.* (1999), Aizawa *et al.* (1999) reported that Aip1 collaborates with ADF/cofilin to disassemble actin filaments by enhancing monomer dissociation from the pointed ends. If CorA and Aip1 assist in promoting actin disassembly, then in the absence of both proteins

the turnover of actin filaments should be slowed down, resulting in a reduced rate of actin disassembly. This is observed in the experiments reported here (Table VII). The rate of actin disassembly is decreased in the absence of Aip1 and CorA but it is much more reduced in the absence of both proteins.

In conclusion, these findings support the notion that both CorA and Aip1 are involved in the regulation of actin disassembly. They play a role in actin turnover and in providing the balance between actin assembly and disassembly. The decreased rates of actin assembly and disassembly in cells missing CorA and/or Aip1 might be responsible for the observed impairments of the actin-related processes observed, as an ineffective cytokinesis and a decreased rate of phagocytosis and cell motility.

6.4 cAMP pulses promote an actin resonance response in wild-type but not in CorA or/and Aip1-null cells

The pattern of cAMP stimulation modulates protein translocation and actin dynamics. Thus, the next step was to analyze how pulses of cAMP influence actin recovery to the resting state in the absence of CorA and/or Aip1.

Cells were exposed to consecutive cAMP pulses with different intervals between the pulses. Wild-type cells exhibited sharp and distinct actin response peaks upon cAMP pulses with intervals of 15, 20, 25, 30, 35 and 40 seconds, and irregular and ineffective responses upon intervals of less than 10 seconds (Figure 4.3). Thus, the de-adaptation response upon a new stimulus needs an interval longer than 10 seconds. This is in agreement with the data from Yang and Iglesias (2006) and Etzrodt *et al.* (2006), where the actin response adapts within 10 seconds after cAMP stimulation.

An interesting phenomenon observed here was a resonant actin response following three consecutive pulses of cAMP stimulation applied to wild-type cell populations. After the cessation of cAMP stimulation, additional cycles of actin accumulation were observed when pulses with an interval of 20 or 40 seconds were applied. When stimulated with a pulse interval of 20 seconds, the resonance period was also 20 seconds. When stimulated with a pulse interval of 40 seconds, the resonance period was also 40 seconds. However, analyses of single cells

stimulated with cAMP pulses of 20 second intervals has clarified that the difference in the resonance period is due to the superposition of two cell populations both responding with a 40 second period but temporally shifted. Thus, cAMP pulses with 20 or 40 seconds interval entrain actin to fall into a synchronized oscillatory response with a periodicity of 40 seconds. However, the amplitude of these additional actin accumulations decreases with each cycle as if there is a damping factor inhibiting oscillations in the actin system. In cells lacking CorA and/or Aip1, this cAMP-induced oscillatory response can hardly be observed. Therefore, CorA and Aip1 might be essential to promote the resonant actin response.

A similar phenomenon of actin response with an oscillatory character, but not induced by any apparent external stimulation or entrainment, was observed in the absence of SCAR and PIR121, two proteins involved in actin nucleation. This phenomenon will be discussed below. However, the results presented so far indicate that the actin system has the capability to act as an oscillator with a certain frequency.

6.5 SCAR and PIR121 suppress intrinsic actin oscillations

Since CorA and Aip1 have been found to promote actin depolymerization, proteins involved in the process of actin polymerization and its regulation were investigated in the next part of this work.

Nucleation of new actin filaments is the polymerization of monomers *de novo*. This process is a key event in any cellular process relying on the dynamic assembly of actin filaments. Actin nucleation is promoted by nucleators like the Arp2/3 complex, spire and formins. Here, the focus is on the regulation of the Arp2/3 complex. The Arp2/3 complex nucleates the formation of dendritic actin filament arrays, which are especially prominent at the leading edges of motile cells. WASP/SCAR family proteins regulate the activity of the Arp2/3 complex, and also link its activity to several signaling pathways (Vartiainen and Machesky, 2004).

In vivo the SCAR complex exists as a heteropentameric complex containing SCAR protein, PIR121, NAP1, Abi1 or 2, and HSPC300 (Eden *et al.*, 2002).

Discussion

Recent biochemical and genetic studies have provided contradictory evidence as to the nature and regulation of the SCAR complex *in vivo* (Eden *et al.*, 2002; Steffen *et al.*, 2004; Blagg *et al.*, 2003 and 2004; Kunda *et al.*, 2003; Rogers *et al.*, 2003; Deeks *et al.*, 2004; Innocent *et al.*, 2004). There is no consensus whether the complex functions as an unchanging unit or alters its composition in response to stimulation, as originally proposed by Eden *et al.* (2002). It is also unclear whether the complex members exclusively regulate SCAR or if they have additional targets (Gautreau *et al.*, 2004; Ibarra *et al.*, 2006; Weiner *et al.*, 2006). Here, more evidence for the role of the SCAR complex, as one of the major regulators of Arp2/3 complex mediated actin nucleation and polymerization, has been obtained using mutant cells lacking members of the SCAR complex.

Cells missing either SCAR protein, PIR121 protein (single-mutants) or both proteins (double-mutant) expressing GFP-LimE Δ were monitored by confocal microscopy to analyze their actin dynamics. In SCAR-deficient cells, an intriguing phenomenon became apparent. In a wild-type cell fluctuations of actin polymerization in the cell cortex and cytoplasm have small amplitudes and are non-periodic (Figure 5.1). In contrast, single- and double-mutant cells lacking SCAR and/or PIR121 showed autonomous fluctuations of actin polymerization in the cortex, with high amplitudes and a regular periodicity (Figure 5.2).

In order to identify the underlying base of the autonomous actin oscillations observed in SCAR-null mutants, effects of an external cAMP stimulus were analyzed. cAMP is the key external stimulus in *D. discoideum* development. During aggregation the cells in the center release cAMP in regular and periodic intervals and the surrounding cells respond by chemotactic movement and the relay of cAMP signals (Robertson *et al.*, 1972; Shaffer, 1975) before they become unresponsive to further cAMP pulses for several minutes. In case of the SCAR-deficient cells a short cAMP stimulus can reset the phase of the oscillatory actin response. The phase-shifts in the actin oscillation in response to chemoattractant stimuli (Figures 5.13 and 5.13.1) indicate that the oscillatory system is linked to the chemosensory pathway. The activity of a cAMP receptor results in dissociation of the G-protein complex, which can then activate downstream effectors and subsequently induce actin polymerization (Kimmel and Parent, 2003 and Manahan *et al.*, 2004). Therefore, in the absence of SCAR the signals from the cAMP receptor are still transmitted to the actin machinery.

Discussion

To investigate if external cues could induce the actin oscillations, the effect of light was analyzed. If the onset of light would promote these oscillations, it should synchronize the phases of oscillations. However, in several cases, cells in the same field of view were recorded simultaneously but oscillated in different phases (Figure 5.4H and Movies 11a and 11b). Oscillations with the same autonomous periodicity were observed with different conventional laser scanning confocal microscopes and at different imaging rates. To determine whether the light from the confocal imaging system initiates the oscillations, the first peaks of actin oscillations in 49 SCAR/PIR121-null cells were analyzed (data not shown). The first recorded images showed the cells in different phases of actin oscillation, either at/or closer to the peak or at the valley of the phases. These data indicate that the oscillations are present already before image acquisition has started and most probably are not induced by light from the microscope.

However, so far this clear phenomenon of actin oscillation could not be observed by use of spinning disk confocal microscopy. What is different in a spinning disk system? The spinning disk microscope, instead of scanning a single point across the specimen (like in the conventional laser scanning confocal microscope), builds an image by passing light through a spinning mask of pinholes, thereby simultaneously illuminating many discrete points. The light travels through the thousands of pinholes and onto the specimen and the returning light passes through the same pinholes for optical sectioning. As the disk spins, the entire specimen is covered several times in a single rotation (Sheppard and Shotton, 1997). Therefore, the cells receive light several times but in a smaller dose (depending on the detector sensitivity). In conventional laser scanning confocal systems the cells are usually imaged with a higher laser dose but with a lower frequency. Whether these differences in imaging modality are the cause for not observing the actin oscillations in spinning disk systems so far, remains to be investigated.

Various dynamic cellular behaviors have been successfully modeled in terms of elementary circuitries showing particular characteristics such as sustained oscillations and their inhibition (Murray, 2002). The finding of autonomous actin oscillations observed in SCAR-deficient cells lead to the conclusion that the actin

system functions as a self-sustained oscillator modulated through the SCAR protein.

Spontaneous oscillations occur in non-linear dynamic systems that are open i.e. there is a continuous flow of energy through the system from its environment (Strogatz, 1994). Oscillations in cytoskeletal structures have been reported, such as the axonemes of cilia. Spontaneous oscillations of mechanosensitive hair bundles have been shown to give frequency selectivity and amplification to mechano-sensation (Kruse and Jülicher, 2005).

The actin system can oscillate in the presence of two actin-binding proteins (CorA and Aip1) but not in their absence (Figure 4.4), suggesting that CorA and Aip1 are essential to promote oscillations. CorA and Aip1 bind to actin at the poles of a cell in division (de Hostos *et al.*, 1993; Konzok *et al.*, 1999), probably to generate force to separate the daughter cells. This force-generating mechanism could induce spontaneous oscillations in the actin system promoted by CorA and Aip1.

Grill *et al.* (2001) reported oscillations of cytoskeleton structures observed during unequal cell division. When the mitotic spindle is positioned away from the center of the cell before cell cleavage, this repositioning is accompanied by oscillatory movements of the spindle. These spindle movements result from the cooperative attachment and detachment of cortical force generators to astral microtubules that lead to spontaneous oscillations.

Periodic actin oscillations in the absence of SCAR and PIR121 reported here, are similar to periodic actin tail formation of the *Listeria* bacteria that lack ActA protein. The ActA protein induces actin nucleation on the bacterial surface and promotes a continuous process of actin elongation. Deletion of the ActA C-region leads to discontinuous actin tail formation in these bacteria. Therefore, in the absence of the ActA C-region, the formation of actin tails undergoes periodic cycles of actin polymerization (Lasa *et al.*, 1997). These findings support the notion that cytoskeletal structures like microtubules and the actin system can function as biological oscillators.

SCAR-null cells are characterized by a small cell size with reduced F-actin levels and deficiencies in movement (Bear *et al.*, 1998). PIR121-null cells have an exceptionally high proportion of F-actin, severe defects in movement and chemotaxis, and very low amounts of full-length SCAR protein. The

Discussion

SCAR/PIR121-double mutant cells have reduced F-actin levels and also deficiencies in movement (Blagg *et al.*, 2003). In addition, the actin redistribution at the substrate-near cell cortex exhibited patterns in these three mutants that differ from the wild-type patterns (Figures 5.6, 5.7, 5.8 and 5.9). NAP1 and Abi1 are two other members of the SCAR complex. NAP1-null *D. discoideum* cells are small and round with reduced actin polymerization and small pseudopods, and have reduced SCAR protein activity. Furthermore, deficiencies evoked by elimination of NAP1 are more severe than those in the absence of either SCAR or PIR121 proteins (Ibarra *et al.*, 2006). In addition, Pollitt and Insall (2008) have demonstrated that in *D. discoideum* the absence of Abi1 causes less severe defects in motility than the absence of SCAR, indicating that the SCAR protein retains partial activity in the absence of Abi1.

In short, not only the lack of SCAR and/or PIR121 results in an impairment of F-actin formation, but also the absence of other members of the SCAR complex. These findings raise the question whether the other SCAR complex members are also important in suppressing actin oscillations and which role they play in this process. Lack of function mutants and observation of actin fluctuations would be a suitable approach to answer this question.

In Figure 6.2 a schema of the protein network involved in the generation of actin oscillations observed in SCAR-deficient cells is presented.

The SCAR complex is suggested to be the major activator of Arp2/3 complex mediated actin nucleation. This raises the question how actin nucleation and polymerization is promoted in cells lacking SCAR and/or PIR121 protein. In the absence of a complete SCAR complex, CorA and Arp2/3 complex are recruited to the cell cortex (Figures 5.10 and 5.11). As reported by Humphries *et al.* (2002) the yeast coronin recruits the Arp2/3 complex to the cell cortex. Thus, in the absence of SCAR protein, CorA translocated to the cell cortex might recruit the Arp2/3 complex (Figures 5.10 and 5.15). Arp2/3 complex is then activated either by an incomplete SCAR complex or by other Arp2/3 activators such as WASP. As a result of Arp2/3 complex activation, actin nucleation and polymerization is promoted at the cell cortex. These suggestions are not unlikely, as *in vitro* evidence shows that PIR121 and NAP1 alone can form an independent complex that has some activity in the absence of SCAR protein (Gautreau *et al.*, 2004).

Discussion

Myers *et al.* (2005) reported that WASP in *D. discoideum* is responsible for F-actin organization and polarity during cell migration. The WASP function in promoting actin polymerization at the cell cortex and its relationship to the Arp2/3 complex is still not fully understood. Other candidates for promoting actin polymerization in the absence of a complete SCAR complex are nucleators bypassing the Arp2/3 complex like formins. Formins, which constitute the second

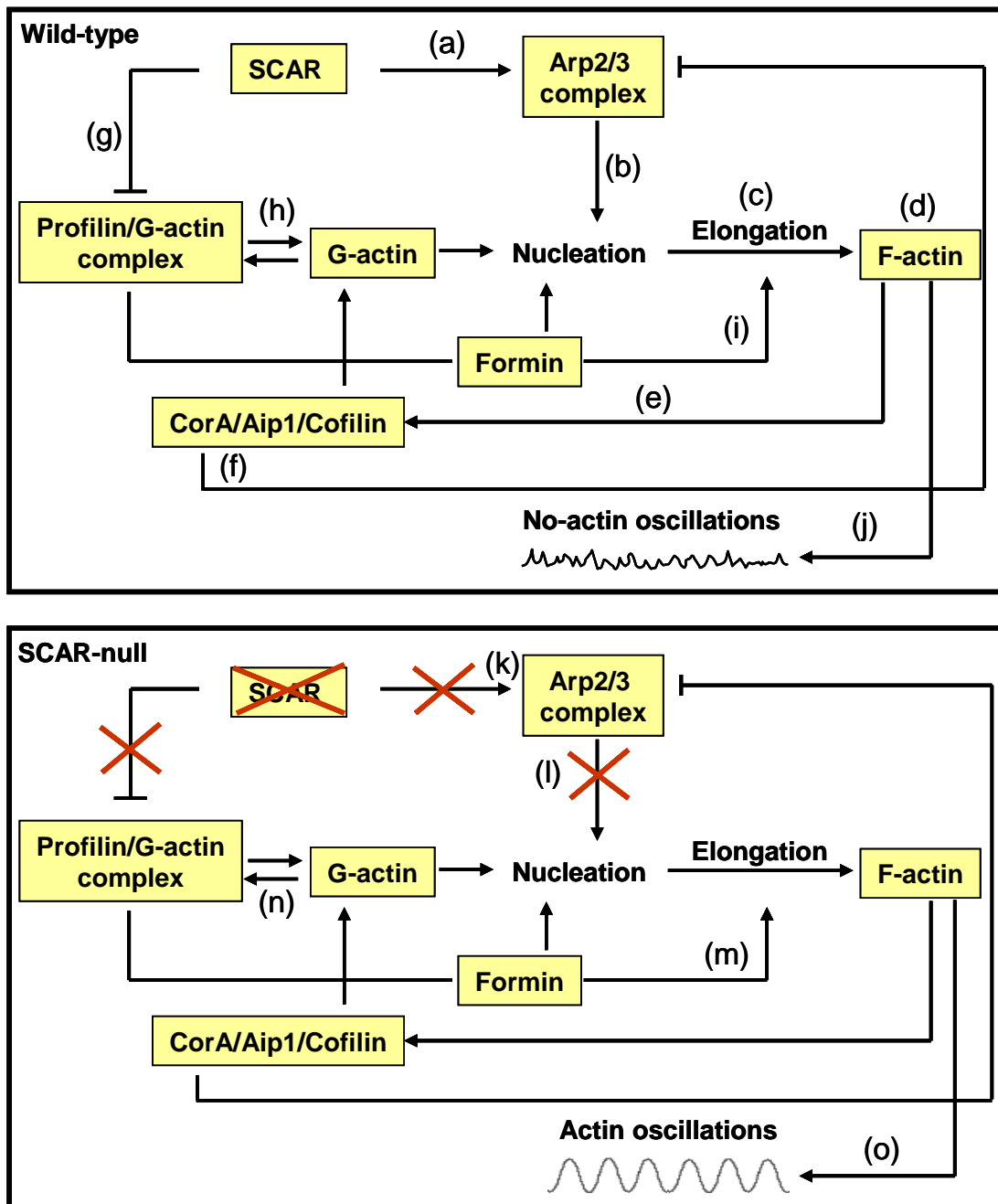


Figure 6.2, legend viewed on the following page.

Discussion

Figure 6.2. Scheme of the protein network involved in the generation of actin oscillations. In wild-type cells, (a) SCAR activates the Arp2/3 complex to promote nucleation (b), followed by elongation (c) and F-actin formation (d) (Machesky *et al.*, 1998 and 1999). (e) CorA, Aip1 and cofilin contribute to actin depolymerization (Gerisch *et al.*, 1995; Briehner *et al.*, 2006; Konzok *et al.*, 1999; Okada *et al.*, 1999; Rodal *et al.*, 1999; Aizawa *et al.*, 1999; Table VII). CorA inhibits the activity of the Arp2/3 complex (f) (Humphries *et al.*, 2002). SCAR also interacts physically with profilin, probably negatively regulating its function (g) (Seastone *et al.*, 2001; Kovar *et al.*, 2006). SCAR-null cells have a decreased amount of F-actin, while profilin-null cells have an increased F-actin content (Haugwitz *et al.*, 1994; Bear *et al.*, 1998), suggesting that SCAR inhibits the profilin activity to promote a balanced equilibrium of actin polymerization and depolymerization. Profilins prevent actin polymerization by sequestering G-actin (h) (Carlsson *et al.*, 1977; Vinson *et al.*, 1998). On the other hand, profilins also bind to formins to accelerate actin elongation (i) (Kovar *et al.*, 2006). Therefore, the regulated profilin-binding to G-actin and to formin might control the equilibrium between actin polymerization and depolymerization in the presence of SCAR; thus no actin oscillations are observed (j). However, in SCAR-null cells, Arp2/3 complex activation might be impaired (k) leading to a slowdown of the nucleation process (l). Less Arp2/3 complex is recruited to the cell cortex in the absence of SCAR (Figure 5.15), leading to the decreased F-actin content observed in SCAR-null cells (Bear *et al.*, 1998). Therefore, in the absence of SCAR, non-regulated profilin activity might promote F-actin formation through formins (m), and contribute to actin depolymerization by sequestering G-actin monomers (n). Consequently, the activity of profilin in the absence of SCAR might generate an instable balance between actin polymerization and depolymerization that could result in actin oscillations (o). Thus, SCAR suppresses actin oscillations in wild-type cells.

major class of actin nucleators of eukaryotic cells, possess the biochemical properties for generating unbranched actin filaments that are prominent in actin cables, stress fibers and filopodia (Zigmond, 2004). The mammalian formin (mDia2) as well as its homolog in *Dictyostelium* (dDia2) localize to filopodial tips and are candidates to be involved in the nucleation of filopodial actin filaments (Peng *et al.*, 2003; Pellegrin *et al.*, 2005; Schirenbeck *et al.*, 2005). Vlahou and Rivero (2006) showed that over-expression of dDia2 leads to longer and more stable filopodia and to reduced motility as compared with wild-type cells. Interestingly, PIR121-null cells have a strikingly similar phenotype. PIR121-null cells are large with long filopodia and impaired cell motility. Thus, in the absence of PIR121 an inefficient activation of the Arp2/3 complex might lead to an over-expression of formins, causing these effects in mutant cells. Formins are candidates for being involved in the periodic actin re-organization in SCAR-deficient cells. However, future experiments would be needed to investigate the expression of formins in these mutants, in particular in PIR121-null cells.

Formins contain two highly conserved formin-homology domains, FH1 and FH2. The FH2 domain is sufficient to mediate nucleation and the FH1 domain binds profilin, an actin-monomer-binding protein that delivers actin to the growing

barbed end of filaments. The FH1-profilin interaction enhances nucleation (Evangelista *et al.*, 2003). Formins also contribute to actin elongation, and the profilin/actin-binding to formins increases the barbed-end elongation rate (Kovar *et al.*, 2003 and 2006).

Profilin is able to drastically stimulate the ADP/ATP exchange in the actin monomer (Mockrin and Korn, 1980; Nishida, 1995; Goldschmidt-Clermont *et al.*, 1991). After addition of ATP-actin to filament ends, the ATP hydrolyzes, rendering filaments largely composed of ADP-actin. In comparison to ATP-actin, ADP-actin monomers released during depolymerization have a decreased affinity for filament ends and are not as easily available for renewed elongation (Pollard, 1996). The nucleotide exchange activity of profilin will again produce ATP-actin and thus, quickly increase the potency of the cell to stimulate F-actin formation. Along this line, it seems consistent that increased levels of profilin are found in zones of highly dynamic F-/G-actin turnover (Buß *et al.*, 1992; Cao *et al.*, 1992; Finkel *et al.*, 1994). However, profilin sequesters G-actin monomers thus, removes polymerizable G-actin from the equilibrium (Haugwitz *et al.*, 1994). It is known that profilin stimulates actin assembly at low concentrations (Vinson *et al.*, 1998), while at high concentrations it acts as an actin monomer sequestering protein and prevents F-actin assembly (Carlsson *et al.*, 1977).

SCAR and profilin interact physically to regulate F-actin polymerization during endocytosis (Seastone *et al.*, 2001). *D. discoideum* profilin-null cells have an increased F-actin content, while SCAR-null cells have a decreased amount of F-actin (Haugwitz *et al.*, 1994; Bear *et al.*, 1998). These opposite effects suggest that SCAR negatively regulates profilin activity.

In the absence of SCAR the activated profilins sequester G-actin monomers, resulting in decreased F-actin formation. The generation of profilin/G-actin complex might stimulate profilin-binding formins to promote actin nucleation and elongation. Therefore, in the absence of SCAR the equilibrium between actin polymerization and depolymerization might be disturbed resulting in the actin oscillations, mainly caused by unregulated profilin activity.

In conclusion, the loss of a major regulator in a balanced system, give space to secondary regulators that might provide delayed cellular responses, responsible for intrinsic oscillations.

7 References

- Aderem, A.; Underhill, D.M. (1999). Mechanisms of phagocytosis in macrophages. *Annu Rev Immunol.* **17**, 593-623.
- Aizawa, H.; Sutoh, K.; Tsubuki, S.; Kawashima, S.; Ishii, A.; Yahara, I. (1995). Identification, characterization, and intracellular distribution of cofilin in *Dictyostelium discoideum*. *J. Biol Chem.* **270**, 10923-10932.
- Aizawa, H.; Fukui, Y.; Yahara, I. (1997). Live dynamics of *Dictyostelium* cofilin suggests a role in remodeling actin latticework into bundles. *J Cell Sci.* **110**, 2333-2344.
- Aizawa, H.; Katadae, M.; Maruya, M.; Sameshima, M.; Murakami-Murofushi, K.; Yahara, I. (1999). Hyperosmotic stress-induced reorganization of actin bundles in *Dictyostelium* cells over-expressing cofilin. *Genes Cells.* **4**, 311-324.
- Amberg, D.C.; Basart, E.; Botstein, D. (1995). Defining protein interactions with yeast actin *in vivo*. *Nat Struct Biol.* **2**, 28-35.
- Apodaca, G. (2001). Endocytic traffic in polarized epithelial cells: role of the actin and microtubule cytoskeleton. *Traffic.* **2**, 149-159.
- Appleton, B.A.; Wu, P.; Wiesmann, C. (2006). The crystal structure of murine coronin-1: a regulator of actin cytoskeletal dynamics in lymphocytes. *Structure.* **14**, 87-96.
- Ashworth, J.M.; Watts, D.J. (1970). Metabolism of the cellular slime mould *Dictyostelium discoideum* grown in axenic culture. *Biochem J.* **119**, 175-82.
- Baggiolini, M. (1998). Chemokines and leukocyte traffic. *Nature.* **392**, 565-568 .
- Balcer, H.I.; Goodman, A.L.; Rodal, A.A.; Smith, E.; Kugler, J.; Heuser, J.E.; Goode, B.L. (2003). Coordinated regulation of actin filament turnover by a high-molecular-weight Srv2/CAP complex, cofilin, profilin and Aip1. *Curr Biol.* **13**, 2159-2169.
- Bamburg, J.R. (1999). Proteins of the ADF/cofilin family: essential regulators of actin dynamics. *Annu Rev Cell Dev Biol.* **15**, 185-230.
- Bamburg, J.R.; McGough, A.; Ono S. (1999). Putting a new twist on actin: ADF/cofilins modulate actin dynamics. *Trends Cell Biol.* **9**, 364-370.
- Bear, J.E.; Rawls, J.F.; Saxe, C.L. (1998). SCAR, a WASP-related protein, isolated as a suppressor of receptor defects in late *Dictyostelium* development. *J. Cell Biol.* **142**, 1325-1335.
- Bertholdt, G.; Stadler, J.; Bozzaro, S.; Fichtner, B.; Gerisch, G (1985). Carbohydrate and other epitopes of the contact site A glycoprotein of *Dictyostelium discoideum* as characterized by monoclonal antibodies. *Cell Differ.* **16**, 187-202.
- Berks, M.; Kay, R.R. (1988). Cyclic AMP is an inhibitor of stalk cell differentiation in *Dictyostelium discoideum*. *Dev Biol.* **126**, 108-114.
- Beta, C.; Wyatt, D.; Rappel, W.-J.; Bodenschatz, E. (2007). Flow-photolysis for spatiotemporal stimulation of single cells. *Analytical Chemistry.* **79**, 3940-3944
- Blagg, S.L.; Stewart, M.; Sambles, C.; Insall, R.H. (2003). PIR121 regulates pseudopod dynamics and SCAR activity in *Dictyostelium*. *Curr. Biol.* **13**, 1480-1487.

References

- Blagg, S.L.; Insall, R.H. (2004). Control of SCAR activity in *Dictyostelium discoideum*. *Biochem. Soc. Trans.* **32**, 1113-1114.
- Boveri, Th. (1914). Zur Frage der Entstehung maligner Tumoren. Fischer, Jena.
- Breslauer, D.N.; Lee, P.J.; Lee, L.P. (2006). Microfluidics-based systems biology. *Mol Biosyst.* **2**, 97-112
- Bretschneider, T.; Diez, S.; Anderson, K.; Heuser, J.; Clarke, M.; Müller-Taubenberger, A.; Köhler, J.; Gerisch, G. (2004). Dynamic actin patterns and Arp2/3 assembly at the substrate-attached surface of motile cells. *Curr. Biol.* **14**, 1-10.
- Brieher, W.M.; Kueh, H.Y.; Ballif, B.A.; Mitchison, T.J. (2006). Rapid actin monomer insensitive depolymerization of *Listeria* actin comet tails by cofilin, coronin and Aip1. *J. Cell Biol.* **175**, 315-324.
- Brokaw, C.J. (1975). Molecular mechanism for oscillation in flagella and muscle. *Proc Natl Acad Sci USA.* **72**, 3102-3106.
- Brokaw, C.J. (2002). Computer simulation of flagellar movement VIII: coordination of dynein by local curvature control can generate helical bending waves. *Cell Motil Cytoskeleton.* **53**, 103-124
- Brown, B.K.; Song, W. (2001). The actin cytoskeleton is required for the trafficking of the B cell antigen receptor to the endosomes. *Traffic.* **2**, 414-427.
- Buß, F.; Temm-Grove, C.; Henning, S.; Jockusch, M. (1992). Distribution of profilin in fibroblasts correlates with the presence of highly dynamic actin filaments. *Cell Motil. Cytoskel.* **22**, 51-61.
- Cai, L.; Holoweckyj, N.; Schaller, M.D.; Bear, J.E. (2005). Phosphorylation of coronin 1B by protein kinase C regulates interaction with Arp2/3 and cell motility. *J Biol Chem.* **280**, 31913-31923.
- Cai, L.; Marshall, T.W.; Uetrecht, A.C.; Schafer, D.A.; Bear, J.E. (2007). Coronin 1B coordinates Arp2/3 complex and cofilin activities at the leading edge. *Cell.* **128**, 915-929.
- Camalet, S.; Jülicher, F. (2000). Generic aspects of axonemal beating. *N J Phys.* **2**, 1-23.
- Campbell, J.J.; Butcher, E.C. (2000). Chemokines in tissue-specific and microenvironment-specific lymphocyte homing. *Curr. Opin. Immunol.* **12**, 336- 341
- Cao, L.; Babcock, G. G.; Rubenstein, P. A.; Wang, Y. (1992). Effects of profilin and profilactin on actin structure and function in living cells. *J. Cell Biol.* **777**, 1023-1029.
- Caracino, D.; Jones, C.; Compton, M.; Saxe III, C. L (2007). The N-terminus of *Dictyostelium* Scar interacts with Abi and HSPC300 and is essential for proper regulation and function. *Mol Biol Cell.* **18**, 1609-1620
- Cardelli, J. (2001). Phagocytosis and macropinocytosis in *Dictyostelium*. Phosphoinositide-based processes, biochemically distinct. *Traffic.* **2**, 311-320.
- Carlier, M.F.; Ressad, F.; Pantaloni, D. (1999). Control of actin dynamics in cell motility. Role of ADF/cofilin. *J Biol Chem.* **274**, 33827-33830.
- Carlsson, L.; Nystrom, L. E.; Sundkvist, I.; Markey, F.; Lindberg, U. (1977). Actin polymerizability is influenced by profilin, a low molecular weight protein in non-muscle cells. *J. Mol. Biol.* **115**, 465-483.

References

- Charo, I.F.; Taubman, M.B. (2004). Chemokines in the pathogenesis of vascular disease. *Circ Res.* **95**, 858-866.
- Chen, Y.; Takizawa, N.; Crowley, J.L.; Oh, S.W.; Gatto, C.L.; Kambara, T.; Sato, O.; Li, X.D.; Ikebe, M.; Luna, E.J. (2003). F-actin and myosin II binding domains in supervillin. *J Biol Chem.* **278**, 46094-46106.
- Chisholm, R.L.; Firtel, R.A. (2004). Insights into morphogenesis from a simple developmental system. *Nat Rev Mol Cell Biol.* **5**, 531-541.
- Chiu, D.T.; Jeon, N.L.; Huang, S.; Kane, R.S.; Wargo, C.J.; Choi, I.S.; Ingber, D.E.; Whitesides, G.M. (2000). Patterned deposition of cells and proteins onto surfaces by using three-dimensional microfluidic systems. *Proc Natl Acad Sci U S A.* **97**, 2408-2413.
- Clarke, M.; Maddera, L. (2006). Phagocyte meets prey: uptake, internalization, and killing of bacteria by *Dictyostelium amoebae*. *Eur J Cell Biol.* **85**, 1001-1010.
- Crone, S.A.; Lee, K.F. (2002). The bound leading the bound: target-derived receptors act as guidance cues. *Neuron.* **36**, 333-335.
- Deeks, M.J.; Kaloriti, D.; Davies, B.; Malho, R.; Hussey, P.J. (2004). Arabidopsis NAP1 is essential for Arp2/3-dependent trichome morphogenesis. *Curr. Biol.* **14**, 1410-1414.
- Defacque, H.; Egeberg, M.; Habermann, A.; Diakonova, M.; Roy, C.; Mangeat, P.; Voelter, W.; Marriott, G.; Pfannstiel, J.; Faulstich, H.; Griffiths, G. (2000). Involvement of ezrin/moesin in *de novo* actin assembly on phagosomal membranes. *EMBO J.* **19**, 199-212
- de Hostos, E. L.; Bradike, B.; Lottspeich F.; Guggenheim, R.; Gerisch, G. (1991). Coronin, an actin-binding protein of *Dictyostelium discoideum* localized to cell surface projections, has sequence similarities to G protein/3 subunits. *EMBO (Eur. Mol. Biol. Organ.)*. **10**, 4097-4104.
- de Hostos, E.L.; Rehfuss, C.; Bradtke, B.; Waddell, D.R.; Albrecht, R.; Murphy, J.; Gerisch, G. (1993). *Dictyostelium* mutants lacking the cytoskeletal protein coronin are defective in cytokinesis and cell motility. *J Cell Biol.* **120**, 163-173.
- de Hostos, E.L. (1999). The coronin family of actin-associated proteins. *Trends Cell Biol.* **9**, 345-350.
- Devreotes, P.N.; Steck, T.L. (1979) Cyclic 3'5' AMP relay in *Dictyostelium discoideum*. Requirements for the initiation and termination of the response. *J Cell Biol.* **80**, 300-309.
- Diez, S.; Gerisch, G.; Anderson, K.; Müller-Taubenberger, A.; Bretschneider, T. (2005). Subsecond reorganization of the actin network in cell motility and chemotaxis. *PNAS.* **102**, 7601-7606
- Dormann, D.; Libotte, T.; Weijer, C.J.; Bretschneider, T. (2002). Simultaneous quantification of cell motility and protein-membrane-association using active contours. *Cell Motil Cytoskeleton.* **52**, 221-230
- Drengk, A.; Fritsch, J.; Schmauch, C.; Rühling, H.; Maniak, M. (2003). A coat of filamentous actin prevents clustering of late-endosomal vacuoles *in vivo*. *Curr. Biol.* **13**, 1814-1819.
- Eccles, D.M. (2004). Hereditary cancer: guidelines in clinical practice. Breast and ovarian cancer genetics. *Ann Oncol.* **15**, 133-138.
- Eden, S.; Rohatgi, R.; Podtelejnikov, A.V.; Mann, M.; Kirschner, M.W. (2002). Mechanism of regulation of WAVE1-induced actin nucleation by Rac1 and Nck. *Nature.* **418**, 790-793.

References

- Eichinger, L.; Lee, S.S.; Schleicher, M. (1999). *Dictyostelium* as model system for studies of the actin cytoskeleton by molecular genetics. *Microsc Res Tech.* **47**, 124-134.
- Eichinger, L.; Noegel, A.A. (2003). Crawling into a new era – the *Dictyostelium* genome project. *EMBO J.* **22**, 1941-1946.
- Eichinger, L.; Pachebat, J.A; Glöckner, G. (2005). The genome of the social amoeba *Dictyostelium discoideum*. *Nature.* **435**, 43-57
- Etzrodt, M.; Ishikawa, H.C.; Dalous, J.; Müller-Taubenberger, A.; Bretschneider, T.; Gerisch, G. (2006). Time-resolved responses to chemoattractant, characteristic of the front and tail of *Dictyostelium* cells. *Febs Letters.* **580**, 6707-6713
- Evangelista, M.; Zigmond, S.; Boone, C. (2003). Formins: signaling effectors for assembly and polarization of actin filaments. *J Cell Sci.* **116**, 2603-2611.
- Faix, J.; Günther, G.; Noegel, A.A. (1992). Overexpression of the csA cell adhesion molecule under its own cAMP-regulated promoter impairs morphogenesis in *Dictyostelium*. *J Cell Sci.* **102**, 203-214.
- Finkel, T.; Theriot, J. A.; Disc, K. R.; Tomaselli. G. F.; Goldschmidt-Clermont, P. J. (1994). Dynamic actin structures stabilized by profilin. *Proc. Natl. Acad. Sci. USA.* **91**, 1510-1514.
- Fischer, M.; Haase, I.; Simmeth, E.; Gerisch, G.; Müller-Taubenberger, A. (2004). A brilliant monomeric red fluorescent protein to visualize cytoskeleton dynamics in *Dictyostelium*. *FEBS Lett.* **577**, 227-232.
- Foger, N.; Rangell, L.; Danilenko, D.M.; Chan, A.C. (2006). Requirement for coronin 1 in T-lymphocyte trafficking and cellular homeostasis. *Science.* **313**, 839-842.
- Franca-Koh, J.; Devreotes, P.N. (2004). Moving forward: mechanisms of chemoattractant gradient sensing. *Physiology (Bethesda).* **19**, 300-308.
- Fukui, Y.; Yumura, S.; Yumura, T.K.; Mori, H. (1986). Agar overlay method: high-resolution immunofluorescence for the study of the contractile apparatus. *Methods Enzymol.* **134**, 573-580
- Fukui, Y.; de Hostos, E.L.; Inoué S. (1997). Dynamics of GFP-coronin and eupodia in live *Dictyostelium* observed with real-time confocal optics. *Biol Bull.* **193**, 224-225.
- Fukui, Y.; Engler, S.; Inoué, S.; de Hostos, E.L. (1999). Architectural dynamics and gene replacement of coronin suggest its role in cytokinesis. *Cell Motil Cytoskeleton.* **42**, 204-217.
- Gandhi, M.; Goode. B.L. (2008). Coronin: the double-edged sword of actin dynamics. *Subcell Biochem.* **48**, 72-87.
- Gautreau, A.; Ho, H.Y.; Li, J.; Steen, H.; Gygi, S.P.; Kirschner, M.W. (2004). Purification and architecture of the ubiquitous Wave complex. *Proc. Natl. Acad. Sci. USA.* **101**, 4379–4383.
- Gerbal, F.; Chaikin, P.; Rabin, Y.; Prost, J. (2000). An elastic analysis of *Listeria monocytogenes* propulsion. *Biophys J.* **79**, 2259-2275.
- Gerisch, G.; Fromm, H.; Huesgen, A.; Wick, U. (1975a). Control of cell contact sites by cyclic AMP pulses in differentiating *Dictyostelium* cells. *Nature.* **255**, 547-549.
- Gerisch, G.; Wick, U. (1975b). Intracellular Oscillations and Release of Cyclic-Amp from *Dictyostelium* Cells. *Bioch and Bioph Res Comm.* **65**, 364-370.

References

- Gerisch, G.; Keller, H. (1981). Chemotactic reorientation of granulocytes stimulated with micropipettes containing fMET–Leu–Phe. *J. Cell Sci.* **52**, 1-10.
- Gerisch, G.; Albrecht, R.; Heizer, C. (1995). Chemoattractant controlled accumulation of coronin at the leading edge of *Dictyostelium* cells monitored using a green fluorescent protein-coronin fusion protein. *Curr. Biol.* **5**, 1280-1285.
- Gerisch, G.; Faix, J.; Köhler, J.; Müller-Taubenberger, A. (2004). Actin-binding proteins required for reliable chromosome segregation in mitosis. *Cell Motil Cytoskeleton.* **57**, 18-25.
- Goldschmidt-Clermont, P. J., Machesky, L. M., Doberstein, S. K., Pollard, T. D. (1998). Mechanism of the interaction of human platelet profilin with actin. *J. Cell Biol.* **773**, 1081-1089.
- Goley, E.D.; Welch, M.D. (2006). The ARP2/3 complex: an actin nucleator comes of age. *Nat Rev Mol Cell Biol.* **7**, 713-726.
- Goode, B.L.; Wong, J.J.; Butty, A.C.; Peter, M.; McCormack, A.L.; Yates, J.R.; Drubin, D.G.; Barnes, G. (1999). Coronin promotes the rapid assembly and cross-linking of actin filaments and may link the actin and microtubule cytoskeletons in yeast. *J Cell Biol.* **11**, 83-98.
- Glöckner, G.; Eichinger, L.; Szafranski, K.; Pacheban, J.A.; Bankier, A.T.; Dear, P.H.; Lehmann, R.; Baumgart, C.; Parra, G.; Abril, J.F.; Guigó, R.; Kumpf, K.; Tunggal, B.; Cox, E.; Quail, M.A.; Platzer, M.; Rosenthal, A.; Noegel, A.A. (2002). Sequence and analysis of chromosome 2 of *Dictyostelium discoideum*. *Nature.* **418**, 79-85.
- Gräf R, Euteneuer U, Ueda M, and Schliwa M (1998). Isolation of nucleation-competent centrosomes from *Dictyostelium discoideum*. *Eur J Cell Biol.* **76**, 167-175.
- Gräf, R.; Brusis, N.; Dauderer, C.; Euteneuer, U.; Hestermann, A.; Schliwa, M.; Ueda, M. (2000). Comparative structural, molecular, and functional aspects of the *Dictyostelium discoideum* centrosome. *Curr Top Dev Biol.* **49**, 161-85.
- Grill, S.W.; Gonczy, P.; Stelzer, E.H.; Hyman, A.A. (2001). Polarity controls forces governing asymmetric spindle positioning in the *Caenorhabditis elegans* embryo. *Nature.* **409**, 630-633.
- Guerin, I.; de Chastellier, C. (2000). Disruption of the actin filament network affects delivery of endocytic contents marker to phagosomes with early endosome characteristics: the case of phagosomes with pathogenic mycobacteria. *Eur. J. Cell Biol.* **79**, 735-749.
- Gurney, A.M.; Lester, H.A. (1987). Light-flash physiology with synthetic photosensitive compounds. *Physiol Rev.* **67**, 583-617.
- Hacker, U.; Albrecht, R.; Maniak, M. (1997). Fluid-phase uptake by macropinocytosis in *Dictyostelium*. *J Cell Sci.* **110**, 105-112.
- Hagen, V.; Dzeja, C.; Bendig, J.; Baeger, I.; Kaupp, U.B. (1998). Novel caged compounds of hydrolysis-resistant 8-Br-cAMP and 8-Br-cGMP: photolabile NPE esters. *J Photochem Photobiol B.* **42**, 71-78.
- Hanakam, F.; Albrecht, R.; Eckerskorn, C.; Matzner, M.; Gerisch, G. (1996). Myristoylated and non-myristoylated forms of the pH sensor protein hisactophilin II: Intracellular shuttling to plasma membrane and nucleus monitored in real time by a fusion with green fluorescent protein. *EMBO J.* **15**, 2935-2943.
- Harwood, A.J.; Hopper, N.A.; Simon, M.N.; Driscoll, D.M.; Veron, M.; Williams, J.G. (1992). Culmination in *Dictyostelium* is regulated by the cAMP-dependent protein kinase. *Cell.* **69**, 615-624.

References

- Haugwitz M, Noegel AA, Karakesisoglou J, Schleicher M. (1994). *Dictyostelium* amoebae that lack G-actin-sequestering profilins show defects in F-actin content, cytokinesis, and development. *Cell*. **79**, 303-314.
- Hinchcliffe, E. H.; Sluder, G. (2001). "It Takes Two to Tango": understanding how centrosome duplication is regulated throughout the cell cycle. *Genes Dev*. **15**, 1167-1181.
- Hopper, N.A.; Anjard, C.; Reymond, C.D.; Williams, J.G. (1993a). Induction of terminal differentiation of *Dictyostelium* by cAMP-dependent protein kinase and opposing effects of intracellular and extracellular cAMP on stalk cell differentiation. *Development*. **119**, 147-154.
- Hopper, N.A.; Harwood, A.J.; Bouzid, S.; Veron, M.; Williams, J.G. (1993b). Activation of the prespore and spore cell pathway of *Dictyostelium* differentiation by cAMP-dependent protein kinase and evidence for its upstream regulation by ammonia. *EMBO J*. **12**, 2459-2466.
- Hotulainen, P.; Paunola, E.; Vartiainen, M.K.; Lappalainen, P. (2005). Actin-depolymerizing factor and cofilin-1 play overlapping roles in promoting rapid F-actin depolymerization in mammalian nonmuscle cells. *Mol Biol Cell*. **16**, 649-664.
- Howard, T.H.; Oresajo, C.O. (1985). The kinetics of chemotactic peptide-induced change in F-actin content, F-actin distribution, and the shape of neutrophils. *J. Cell Biol*. **101**, 1078-1085.
- Humphries, C.L.; Balcer, H.I.; D'Agostino, J.L.; Winsor, B.; Drubin, D.G.; Barnes, G.; Andrews, B.J.; Goode, B.L. (2002). Direct regulation of Arp2/3 complex activity by the actin binding protein coronin. *J. Cell Biol*. **159**, 993-1004.
- Ibarra, N.; Blagg, S.L.; Vazquez, F.; Insall, R.H. (2006). NAP1 regulates *Dictyostelium* cell motility and adhesion through SCAR-dependent and -independent pathways. *Curr. Biol*. **16**, 717-722.
- Ichetovkin, I.; Han, J.; Pang, K.M.; Knecht, D.A.; Condeelis, J.S. (2000). Actin filaments are severed by both native and recombinant *Dictyostelium* cofilin but to different extents. *Cell Motil Cytoskeleton*. **45**, 293-306.
- Innocenti, M.; Zucconi, A.; Disanza, A.; Frittoli, E.; Areces, L.B.; Steffen, A.; Stradal, T.E.; Di Fiore, P.P.; Carrier, M.F.; Scita, G. (2004). Abi1 is essential for the formation and activation of a WAVE2 signalling complex. *Nat. Cell Biol*. **6**, 319-327.
- Insall, R.; Müller-Taubenberger, A.; Machesky, L.; Köhler, J.; Simmeth, E.; Atkinson, S.J.; Weber, I.; Gerisch, G. (2001). Dynamics of the *Dictyostelium* Arp2/3 complex in endocytosis, cytokinesis, and chemotaxis. *Cell Motil Cytoskeleton*. **50**, 115-128.
- Irimia, D.; Geba, D.A.; Toner, M. (2006). Universal microfluidic gradient generator. *Anal Chem*. **78**, 3472-3477.
- Jiang, X.; Xu, Q.; Dertinger, S.K.; Stroock, A.D.; Fu, T.M.; Whitesides, G.M. (2005). A general method for patterning gradients of biomolecules on surfaces using microfluidic networks. *Anal Chem*. **77**, 2338-2347.
- Jülicher, F.; Prost, J. (1997). Spontaneous oscillations of collective molecular motors. *Phys Rev Lett*. **78**, 4510-4513.
- Jung, G.; Wu, X.; Hammer, J.A. 3rd. (1996). *Dictyostelium* mutants lacking multiple classic myosin I isoforms reveal combinations of shared and distinct functions. *J. Cell Biol*. **133**, 305-323.
- Kaplan, J.H.; Somlyo, A.P. (1989). Flash photolysis of caged compounds: new tools for cellular physiology. *Trends Neurosci*. **12**, 54-59.

References

- Kay, R.R. (1982). cAMP and spore differentiation in *Dictyostelium discoideum*. *Proc Natl Acad Sci USA*. **79**, 3228-3231.
- Kelleher, J.F; Atkinson, S.J; Pollard, T.D. (1995). Sequences, structural models, and cellular localization of the actin-related proteins Arp2 and Arp3 from *Acanthamoeba*. *J. Cell Biol.* **131**, 385-397.
- Kesbeke, F.; Snaar-Jagalska, B.E.; Van Haastert, P.J.M. (1988). Signal transduction in *Dictyostelium* fgd A mutants with a defective interaction between surface cAMP receptors and a GTP-binding regulatory protein. *J. Cell Biol.* **107**, 521-528.
- Kessin, R.H. (2001). *Dictyostelium*: evolution, cell biology, and the development of multicellularity. Developmental and cell biology series. *Edit. Cambridge*
- Khodjakov, A.; Rieder, C. L. (2001). Centrosomes enhance the fidelity of cytokinesis in vertebrates and are required for cell cycle progression. *J. Cell Biol.* **153**, 237-242.
- Koizumi, M.; Soukup, G.A.; Kerr, J.N.; Breaker, R.R. (1999). Allosteric selection of ribozymes that respond to the second messengers cGMP and cAMP. *Nat Struct Biol.* **6**, 1062-1071.
- Kimmel, A.R.; Parent, C.A. (2003). The signal to move: *D. discoideum* go orienteering. *Science*. **300**, 1525-1527.
- Konijn, T.M.; Van De Meene, J.G.; Bonner, J.T.; Barkley, D.S. (1967). The acrasin activity of adenosine-3,5-cyclic phosphate. *Proc Natl Acad Sci USA*. **58**, 1152-1154.
- Konzok, A.; Weber, I.; Simmeth, E.; Hacker, U.; Maniak, M.; Müller-Taubenberger, A. (1999). DAip1, a *Dictyostelium* homologue of the yeast actin-interacting protein 1, is involved in endocytosis, cytokinesis, and motility. *J. Cell Biol.* **146**, 453-464.
- Kovar, D.R.; Kuhn, J.R.; Tichy, A.L.; Pollard, T.D. (2003). The fission yeast cytokinesis formin Cdc12p is a barbed end actin filament capping protein gated by profilin. *J. Cell Biol.* **161**, 875-887.
- Kovar, D.R.; Harris, E.S.; Mahaffy, R.; Higgs, H.N.; Pollard, T.D. (2006). Control of the assembly of ATP- and ADP-actin by formins and profilin. *Cell*. **124**, 423-435.
- Kruse, K.; Jülicher, F. (2005). Oscillations in cell biology. *Curr. Biol.* **17**, 20-26.
- Kumagai, A.; Pupillo, M.; Gundersen, R.; Miake-Lye, R.; Devreotes, P.N.; Firtel, R.A. (1989). Regulation and function of Galpha protein subunits in *Dictyostelium*. *Cell*. **57**, 265-275.
- Kunda, P.; Craig, G.; Dominguez, V.; Baum, B. (2003). Abi, Sra1, and Kette control the stability and localization of SCAR/WAVE to regulate the formation of actin-based protrusions. *Curr. Biol.* **13**, 1867-1875.
- Kyhse-Anderson, J. (1984). Electroblothing of multiple gels: a simple apparatus without buffer tank for rapid transfer of proteins from polyacrylamide to nitrocellulose. *J Biochem Biophys Meth.* **10**, 203-209.
- Laemmli, U. K. (1970). Cleavage of structural proteins during the assembly of the head of bacteriophage T4. *Nature (Lond)*. **227**, 680-685.
- Laevsky, G.; Knecht, D.A. (2003). Cross-linking of actin filaments by myosin II is a major contributor to cortical integrity and cell motility in restrictive environments. *J. Cell Sci.* **116**, 3761-3770.

References

- Langanger, G.; De Mey, J.; Adam H. (1983). 1,4-Diazobicyclo-(2,2,2)-octane (DABCO) retards the fading of immunofluorescence preparations. *Mikroskopie*. **40**, 237-241.
- Lasa, I.; Gouin, E.; Goethals, M.; Vancompennolle, K.; David, V.; Vanderkerkhove, J.; Cossart, P. (1997). Identification of two regions in the N-terminal domain of ActA involved in the actin comet tail formation by *Listeria monocytogenes*. *EMBO J*. **16**, 1531-1540.
- LeClaire, L.L. 3rd.; Baumgartner, M.; Iwasa, J.H.; Mullins, R.D.; Barber, D.L. (2008). Phosphorylation of the Arp2/3 complex is necessary to nucleate actin filaments. *J Cell Biol*. **182**, 647-654.
- Lester, H.A.; Nerbonne, J.M. (1982). Physiological and pharmacological manipulations with light flashes. *Annu Rev Biophys Bioeng*. **11**, 151-175
- Lin, F.; Saadi, W.; Rhee, S. W.; Wang, S. J.; Mittal, S.; Jeon, N. L. (2004). Generation of dynamic temporal and spatial concentration gradients using microfluidic devices. *Lab on a Chip*. **4**, 164-167.
- Lingle, W. L.; Barrett, S. L.; Negron, V. C.; D'Assoro, A. B.; Boeneman, K.; Liu, W.; Whitehead, C. M.; Reynolds, C.; Salisbury, J. L. (2002). Centrosome amplification drives chromosomal instability in breast tumor development. *Proc Natl Acad Sci U S A*. **99**, 1978-1983.
- Loose, M.; Fischer-Friedrich, E.; Ries, J.; Kruse, K.; Schwille, P. (2008). Spatial regulators for bacterial cell division self-organize into surface waves in vitro. *Science*. **320**, 789-792.
- Lowry, O.H.; Rosenbrough, N.J.; Farr, A.L.; Randall, R.J (1951). Protein measurement with the Folin Phenol Reagent, *J. Biol. Chem*. **193**, 265-275.
- Machesky, L.M.; Atkinson, S.J.; Ampe, C.; Vandekerckhove, J.; Pollard, T.D. (1994). Purification of a cortical complex containing two unconventional actins from *Acanthamoeba* by affinity chromatography on profilin-agarose. *J. Cell Biol*. **127**, 107-115.
- Machesky, L.M.; Reeves, E.; Wientjes, F.; Mattheyse, F.J.; Grogan, A.; Totty, N.F.; Burlingame, A.L.; Hsuan, J.J.; Segal, A.W. (1997). Mammalian actin-related protein 2/3 complex localizes to regions of lamellipodial protrusion and is composed of evolutionarily conserved proteins. *Biochem J*. **328**, 105-112.
- Machesky, L. M.; Insall, R. H. (1998). Scar1 and the related Wiskott–Aldrich syndrome protein, WASP, regulate the actin cytoskeleton through the Arp2/3 complex. *Curr. Biol*. **8**, 1347-1356.
- Machesky, L.M.; Mullins, R.D.; Higgs, H.N.; Kaiser, D.A.; Blanchoin, L.; May, R.C.; Hall, M.E.; Pollard, T.D. (1999). Scar, a WASp-related protein, activates nucleation of actin filaments by the Arp2/3 complex. *Proc. Natl Acad. Sci. USA*. **96**, 3739–3744.
- Maciver, S.K.; Hussey, P.J. (2002). The ADF/cofilin family: actin-remodeling proteins. *Genome Biol*. **3**(5):reviews 3007.
- Malchow, D.; Nagele, B.; Schwarz, H.; Gerisch, G. (1972). Membrane-bound cyclic AMP phosphodiesterase in chemotactically responding cells of *Dictyostelium discoideum*. *Eur J Biochem*. **28**, 136-142.
- Manahan, C.L.; Iglesias, P.A.; Long, Y.; Devreotes, P.N. (2004). Chemoattractant signaling in *Dictyostelium discoideum*. *Annu Rev Cell Dev Biol*. **20**, 223-253.
- Maniak, M.; Rauchenberger, R.; Albrecht, R.; Murphy, J.; Gerisch, G. (1995). Coronin involved in phagocytosis: dynamics of particle-induced relocalization visualized by a green fluorescent protein Tag. *Cell*. **83**, 915-924.

References

- Mann, S.K.O.; Firtel, R.A. (1993) cAMP-dependent protein kinase differentially regulates prestalk and prespore differentiation during *Dictyostelium* development. *Development*. **119**, 135-146.
- Mann, S.K.O.; Brown, J.M.; Briscoe, C.; Parent, C.; Pitt, G.; Devreotes, P.N.; Firtel, R.A. (1997). Role of cAMP-dependent protein kinase in controlling aggregation and postaggregative development in *Dictyostelium*. *Dev Biol*. **183**, 208-221.
- Marriott, G.; Roy, P.; Jacobson, K. (2003). Preparation and light-directed activation of caged proteins. *Methods Enzymol*. **360**, 274-288.
- Martens, H.; Novotny, J.; Oberstrass, J.; Steck, T.L.; Postlethwait, P.; Nellen, W. (2002) RNAi in *Dictyostelium*: the role of RNA-directed RNA polymerases and double-stranded RNase. *Mol Biol Cell*. **13**, 445-453.
- Martin, P.; Parkhurst, S.M. (2004). Parallels between tissue repair and embryo morphogenesis. *Development*. **131**, 3021-3034
- May, R.C.; Machesky, L.M. (2001). Phagocytosis and the actin cytoskeleton. *J. Cell Sci*. **114**, 1061-1077.
- May, R.C. (2001). The Arp2/3 complex: a central regulator of the actin cytoskeleton. *Cell Mol Life Sci*. **58**, 1607-1626.
- Merrifield, C.; Moss, S.; Ballestrem, C.; Imhof, B.; Giese, G.; Wunderlich, I.; Almers, W. (1999). Endocytic vesicles move at the tips of actin tails in cultured mast cells. *Nat. Cell Biol*. **1**, 72-74.
- Mishima, M.; Nishida, E. (1999). Coronin localizes to leading edges and is involved in cell spreading and lamellipodium extension in vertebrate cells. *J Cell Sci*. **112**, 2833-2842.
- Mockrin, S. C.; Korn, E. D. (1980). Acanthamoeba profilin interacts with G-actin to increase the rate of exchange of actin-bound adenosine S-triphosphate. *Biochemistry*. **79**, 5359-5362.
- Moriyama, K.; Yahara, I. (2002). Human CAP1 is a key factor in the recycling of cofilin and actin for rapid actin turnover. *J. Cell Sci*. **115**, 1591-1601.
- Moseley, J.B.; Okada, K.; Balcer, H.I.; Kovar, D.R.; Pollard, T.D.; Goode, B.L. (2006). Twinfilin is an actin-filament-severing protein and promotes rapid turnover of actin structures *in vivo*. *J. Cell Sci*. **119**, 1547-1557
- Müller, K.; Gerisch, G. (1978). A specific glycoprotein as the target site of adhesion blocking Fab in aggregating *Dictyostelium discoideum*. *Nature*. **274**, 445-449.
- Murray, J.D. (2002). *Mathematical Biology*. edn 3. Berlin: Springer.
- Myers, S.A.; Han, J.W.; Lee, Y.; Firtel, R.A.; Chung, C.Y. (2005). A *Dictyostelium* homologue of WASP is required for polarized F-actin assembly during chemotaxis. *Mol Biol Cell*. **16**, 2191-206.
- Myers, S.A.; Leeper, L.R.; Chung, C.Y. (2006). WASP-interacting protein is important for actin filament elongation and prompt pseudopod formation in response to a dynamic chemoattractant gradient. *Mol Biol Cell*. **17**, 4564-4575.
- Nagasaki, A.; de Hostos, E.L.; Uyeda, T.Q.P (2002). Genetic and morphological evidence for two parallel pathways of cell-cycle-coupled cytokinesis in *Dictyostelium*. *J. Cell. Sci*. **115**, 2241-2251.

References

- Nerbonne, J.M.; Richard, S.; Nargeot, J.; Lester, H.A. (1984). New photoactivatable cyclic nucleotides produce intracellular jumps in cyclic AMP and cyclic GMP concentrations. *Nature*. **310**, 74-76.
- Neujahr, R.; Heizer, C.; Gerisch, G. (1997). Myosin II-independent processes in mitotic cells of *Dictyostelium discoideum*: redistribution of the nuclei, re-arrangement of the actin system and formation of the cleavage furrow. *J. Cell Sci.* **110**, 123-137.
- Neujahr, R.; Albrecht, R.; Köhler, J.; Matzner, M.; Schwartz, J.M.; Westphal, M.; Gerisch, G. (1998). Microtubule-mediated centrosome motility and the positioning of cleavage furrows in multinucleate myosin II-null cells. *J. Cell Sci.* **111**, 1227-1240.
- Nigg, E. A. (2002). Centrosome aberrations: cause or consequence of cancer progression? *Nat Rev Cancer*. **2**, 815-825.
- Nishida, E. (1995). Opposite effects of cofilin and profilin from porcine brain on rate of exchange of actin-bound adenosine 5'-triphosphate. *Biochemistry*. **24**, 1160-1164.
- Noegel, A.; Gerisch, G.; Stadler, J.; Westphal, M. (1986). Complete sequence and transcript regulation of a cell adhesion protein from aggregating *Dictyostelium* cells. *EMBO J.* **5**, 1473-1476.
- Noegel, A.A.; Schleicher, M. (2000). The actin cytoskeleton of *Dictyostelium*: a story told by mutants. *J. Cell Sci.* **113**, 759-766.
- Okada, K.; Obinata, T.; Abe, H. (1999). XAIP1: a *Xenopus* homologue of yeast actin interacting protein 1 (AIP1), which induces disassembly of actin filaments cooperatively with ADF/cofilin family proteins. *J. Cell Sci.* **112**, 1153-1565.
- Okada, K.; Blanchoin, L.; Abe, H.; Chen, H.; Pollard, T.D.; Bamburg, J.R. (2002). *Xenopus* Actin-interacting protein 1 (Xaip1) enhances cofilin fragmentation of filaments by capping filament ends. *J. Biol. Chem.* **277**, 43011-43016.
- Oku, T.; Itoh, S.; Ishii, R.; Suzuki, K.; Nauseef, W.M.; Toyoshima, S.; Tsuji, T. (2005). Homotypic dimerization of the actin-binding protein p57/coronin-1 mediated by a leucine zipper motif in the C-terminal region. *Biochem J.* **387**, 325-331.
- Omura, F.; Fukui, Y. (1985). *Dictyostelium* MTOC: Structure and linkage to the nucleus. *Protoplasma*. **127**, 212-221.
- Ono, S. (2003). Regulation of actin filament dynamics by actin depolymerizing factor/cofilin and actin-interacting protein 1: new blades for twisted filaments. *Biochemistry*. **42**, 13363-13370.
- Ono, S.; Mohri, K.; Ono, K. (2004). Microscopic evidence that actin-interacting protein 1 actively disassembles actin-depolymerizing factor/Cofilin-bound actin filaments. *J Biol Chem*. **279**, 14207-14212.
- Pang, K.M.; Lee, E.; Knecht, D.A. (1998). Use of a fusion protein between GFP and an actin-binding domain to visualize transient filamentous-actin structures. *Curr. Biol.* **8**, 405-408.
- Parent, C.A.; Devreotes, P.N. (1999). A cell's sense of direction. *Science*. **284**, 765-770.
- Peng, J.; Wallar, B.J.; Flanders, A.; Swiatek, P.J.; Alberts, A.S. (2003). Disruption of the Diaphanous-related formin Drf1 gene encoding mDia1 reveals a role for Drf3 as an effector for Cdc42. *Curr Biol*. **13**, 534-545.

References

- Pellegrin, S.; Mellor, H. (2005). The Rho family GTPase Rif induces filopodia through mDia2. *Curr Biol.* **15**, 129-133.
- Piel, M.; Nordberg, J.; Euteneuer, U.; Bornens, M. (2001). Centrosome dependent exit of cytokinesis in animal cells. *Science.* **291**, 1550-1553.
- Pollard, T. D. (1996). Rate constants for the reactions of ATP- and ADP-actin with the ends of actin filaments. *J. Cell Biol.* **103**, 2747-2764.
- Pollard, T.D.; Blanchoin, L.; Mullins, R.D. (2000). Molecular mechanisms controlling actin filament dynamics in nonmuscle cells. *Annu Rev Biophys Biomol Struct.* **29**, 545-576.
- Pollard, T. D.; Borisy, G. G. (2003). Cellular motility driven by assembly and disassembly of actin filaments. *Cell.* **112**, 453-465
- Pollitt, A.Y.; Insall, R.H. (2008). Abi mutants in *Dictyostelium* reveal specific roles for the SCAR/WAVE complex in cytokinesis. *Curr. Biol.* **18**, 203-210.
- Prassler, J.; Murr, A.; Stocker, S.; Faix, J.; Murphy, J.; Marriott, G. (1998). DdLIM is a cytoskeleton-associated protein involved in the protrusion of lamellipodia in *Dictyostelium*. *Mol Biol Cell.* **9**, 545-559
- Prost, J. (2001). The physics of Listeria propulsion. In *Physics of biomolecules and cells.* *Science.* 215-236.
- Qualmann, B.; Kessels, M.M. (2002). Endocytosis and the cytoskeleton. *Int. Rev. Cytol.* **220**, 93-144.
- Rauchenberger, R.; Hacker, U.; Murphy, J.; Niewöhner, J.; Maniak, M. (1997). Coronin and vacuolin identify consecutive stages of a late, actin-coated endocytic compartment in *Dictyostelium*. *Curr. Biol.* **7**, 215-218.
- Robertson, A.; Drage, D.J.; Cohen, M.H. (1972). Control of Aggregation in *Dictyostelium discoideum* by an External Periodic Pulse of Cyclic Adenosine Monophosphate. *Science.* **175**, 333-335.
- Robinson, D.N.; Spudich, J.A. (2000). Towards a molecular understanding of cytokinesis. *Trends Cell Biol.* **10**, 228-237
- Rodal, A.A.; Tetreault, J.W.; Lappalainen, P.; Drubin, D.G.; Amberg, D.C. (1999). Aip1p interacts with cofilin to disassemble actin filaments. *J. Cell Biol.* **145**, 1251-1264.
- Rodal, A.A.; Sokolova, O.; Robins, D.B.; Daugherty, K.M.; Hippenmeyer, S.; Riezman, H.; Grigorieff, N.; Goode, B.L. (2005). Conformational changes in the Arp2/3 complex leading to actin nucleation. *Nat Struct Mol Biol.* **12**, 26-31.
- Rogers, S.L.; Wiedemann, U.; Stuurman, N.; Vale, R.D. (2003). Molecular requirements for actin-based lamella formation in *Drosophila* S2 cells. *J. Cell Biol.* **162**, 1079-1088.
- Rothenberg, M.E.; Rogers, S.L.; Vale, R.D.; Jan, L.Y.; Jan, Y.N. (2003). *Drosophila* pod-1 crosslinks both actin and microtubules and controls the targeting of axons. *Neuron.* **39**, 779-791.
- Ruchira, M.A. (2005). *Dictyostelium* Chemotaxis studied with Fluorescence Fluctuation Spectroscopy. Thesis.
- Rupper, A.; Cardelli, J. (2001). Regulation of phagocytosis and endo-phagosomal trafficking pathways in *Dictyostelium discoideum*. *Biochim Biophys Acta.* **1525**, 205-216.

References

- Saran, S.; Meima, M.E.; Alvarez-Curto, E.; Weening, K.E.; Rozen, D.E.; Schaap, P. (2002). cAMP signaling in *Dictyostelium*. Complexity of cAMP synthesis, degradation and detection. *J Muscle Res Cell Motil.* **23**, 793-802.
- Schaap, P.; Van Driel, R. (1985). Induction of post-aggregative differentiation in *Dictyostelium discoideum* by cAMP. Evidence for involvement of the cell surface cAMP receptor. *Exp Cell Res.* **159**, 388-398.
- Seastone, D.J.; Harris, E.; Temesvari, L.A.; Bear, J.E.; Saxe, C.L.; Cardelli, J. (2001). The WASp-like protein scar regulates macropinocytosis, phagocytosis and endosomal membrane flow in *Dictyostelium*. *J. Cell Sci.* **114**, 2673-2683.
- Shaffer, B.M. (1975). Secretion of cyclic AMP induced by cyclic AMP in the cellular slime mould *Dictyostelium discoideum*. *Nature.* **255**, 549-55.
- Sheppard, C.J.R.; Shotton, D.M. (1997). Introduction in Confocal Laser Scanning Microscopy. Springer-Verlag New York Inc. New York. 1–13.
- Schirenbeck, A.; Bretschneider, T.; Arasada, R.; Schleicher, M.; Faix, J. (2005). The Diaphanous-related formin dDia2 is required for the formation and maintenance of filopodia. *Nat Cell Biol.* **7**, 619-625.
- Schleicher, M.; Noegel, A.A. (1992). Dynamics of the *Dictyostelium* cytoskeleton during chemotaxis. *New Biol.* **4**, 461-472.
- Schmauch, C.; Maniak M. (2008). Competition between targeting signals in hybrid proteins provides information on their relative *in vivo* affinities for subcellular compartments. *Eur J Cell Biol.* **87**, 57-68.
- Schneider, N.; Weber, I.; Faix, J.; Prassler, J.; Müller-Taubenberger, A.; Köhler, J.; Burghardt, E.; Gerisch, G.; Marriott, G. (2003). A Lim protein involved in the progression of cytokinesis and regulation of the mitotic spindle. *Cell Motil Cytoskeleton.* **56**, 130-139.
- Schulkes, C.; Schaap, P. (1995). cAMP-dependent protein kinase activity is essential for preaggregative gene expression in *Dictyostelium*. *FEBS Lett.* **368**, 381-384.
- Schuster, S.C.; Noegel, A.A.; Oehme, F.; Gerisch, G.; Simon, M.I. (1996). The hybrid histidine kinase DokA is part of the osmotic response system of *Dictyostelium*. *EMBO J.* **15**, 3880-3889.
- Schwarz, E.C.; Neuhaus, E.M.; Kistler, C.; Henkel, A.W.; Soldati, T. (2000). *Dictyostelium* myosin IK is involved in the maintenance of cortical tension and affects motility and phagocytosis. *J. Cell Sci.* **113**, 621-633.
- Smith, L.G.; Li, R. (2004). Actin polymerization: riding the wave. *Curr. Biol.* **14**, R109-111.
- Soldati, T.; Geissler, H.; Schwarz, E.C. (1999). How many is enough? Exploring the myosin repertoire in the model eukaryote *Dictyostelium discoideum*. *Cell Biochem Biophys.* **30**, 389-411.
- Soll, D.R.; Wessels, D.; Heid, P.J.; Zhang, H. (2002). A contextual framework for characterizing motility and chemotaxis mutants in *Dictyostelium discoideum*. *J Muscle Res Cell Motil.* **23**, 659-672.
- Solomon, J.M.; Isberg, R.R. (2000). Growth of *Legionella pneumophila* in *Dictyostelium discoideum*: a novel system for genetic analysis of host–pathogen interactions. *Trends Microbiol.* **10**, 478-480.

References

- Southwick, F.S. (2000). Gelsolin and ADF/cofilin enhance the actin dynamics of motile cells. *Proc Natl Acad Sci U S A*. **97**, 6936-6938.
- Spoerl, Z.; Stumpf, M.; Noegel, A.A.; Hasse, A. (2002). Oligomerization, F-actin interaction and membrane association of the ubiquitous mammalian coronin 3 are mediated by its carboxyl terminus. *J Biol Chem*. **277**, 48858-48867.
- Steel, K.P.; Mburu, P.; Gibson, F.; Walsh, J.; Varela, A.; Brown, K.; Self, T.; Mahony, M.; Fleming, J.; Pearce, A.; Harvey, D.; Cable, J.; Brown, S.D. (1997). Unravelling the genetics of deafness. *Ann Otol Rhinol Laryngol Suppl*. **168**, 59-62.
- Steffen, A.; Rottner, K.; Ehinger, J.; Innocenti, M.; Scita, G.; Wehland, J.; Stradal, T.E. (2004). Sra-1 and NAP1 link Rac to actin assembly driving lamellipodia formation. *EMBO J*. **23**, 749-759.
- Strogatz, S.H. (1994). *Nonlinear Dynamics and Chaos: With Applications to Physics, Biology, Chemistry, and Engineering*. Reading, Mass: Addison-Wesley.
- Stuart, L.M.; Ezekowitz, R.A. (2005). Phagocytosis: elegant complexity. *Immunity*. **22**, 539-550.
- Taunton, J.; Rowning, B.A.; Coughlin, M.L.; Wu, M.; Moon, R.T.; Mitchison, T.J.; Larabell, C.A. (2000). Actin-dependent propulsion of endosomes and lysosomes by recruitment of N-WASP. *J. Cell Biol*. **148**, 519-530.
- Titus, M.A. (1999). A class VII unconventional myosin is required for phagocytosis. *Curr. Biol*. **9**, 1297-1303.
- Titus, M.A. (2000). The role of unconventional myosins in *Dictyostelium* endocytosis. *J Eukaryot Microbiol*. **47**, 191-196.
- Theriot, J.A.; Mitchison, T.J.; Tilney, L.G.; Portnoy, D.A. (1992). The rate of actin-based motility of intracellular *Listeria monocytogenes* equals the rate of actin polymerization. *Nature*. **357**, 257-260.
- Trusolino, L.; Comoglio, P.M. (2002). Scatter-factor and semaphorin receptors: cell signalling for invasive growth. *Nat Rev Cancer*. **2**, 289-300.
- Ueda, M.; Schliwa, M.; Euteneuer, U. (1999). Unusual centrosome cycle in *Dictyostelium* correlation of dynamic behavior and structural changes. *Mol Biol Cell*. **10**, 151-160.
- Utrecht, A.C.; Bear, J.E. (2006). Coronins: the return of the crown. *Trends Cell Biol*. **16**, 421-426.
- Van Es, S.; Virdy, K.J.; Pitt, G.S.; Meima, M.; Sands, T.W.; Devreotes, P.N.; Cotter, D.A.; Schaap, P. (1996). Adenylyl cyclase G, an osmosensor controlling germination of *Dictyostelium* spores. *J Biol Chem*. **271**, 623-625.
- van Deurs, B.; Holm, P.K.; Kayser, L.; Sandvig, K. (1995). Delivery to lysosomes in the human carcinoma cell-line Hep-2 involves an actin filament-facilitated fusion between mature endosomes and preexisting lysosomes. *Eur. J. Cell Biol*. **66**, 309-323.
- Vartiainen, M.K.; Machesky, L.M. (2004). The WASP-Arp2/3 pathway: genetic insights. *Curr Opin Cell Biol*. **16**, 174-181.
- Vinson, V.K.; De La Cruz, E.M.; Higgs, H.N.; Pollard, T.D. (1998). Interactions of *Acanthamoeba* profilin with actin and nucleotides bound to actin. *Biochemistry*. **37**, 10871-10880.

References

- Vlahou, G.; Rivero, F. (2006). Rho GTPase signaling in *Dictyostelium discoideum*: insights from the genome. *Eur. J. Cell. Biol.* **85**, 947-959.
- Voegtli, W.C.; Madrona, A.Y.; Wilson, D.K. (2003). The structure of Aip1p, a WD repeat protein that regulates Cofilin-mediated actin depolymerization. *J Biol Chem.* **278**, 34373-34379.
- Vogel, A.; Venugopalan, V. (2003). Mechanism of pulsed laser ablation of biological tissues. *Chem Rev.* **103**, 577-644
- Volkman, N.; Amann, K.J.; Stoilova-McPhie, S.; Egile, C.; Winter, D.C.; Hazelwood, L.; Heuser, J.E.; Li, R.; Pollard, T.D.; Hanein, D. (2001). Structure of Arp2/3 complex in its activated state and in actin filament branch junctions. *Science.* **293**, 2456-2459.
- Xiong, H.; Rivero, F.; Euteneuer, U.; Mondal, S.; Mana-Capelli, S.; Larochelle, D.; Vogel, A.; Gassen, B.; Noegel, A.A. (2008). *Dictyostelium* Sun-1 connects the centrosome to chromatin and ensures genome stability. *Traffic.* **9**, 708-724.
- Weber, I.; Neujahr, R.; Du, A.; Köhler, J.; Faix, J.; Gerisch, G. (2000). Two-step positioning of a cleavage furrow by cortexillin and myosin II. *Curr. Biol.* **10**, 501-506.
- Weeks, G.; Weijer, C.J. (1994). The *Dictyostelium* cell cycle and its relationship to differentiation. *FEMS Microbiol Lett.* **124**, 123-130.
- Weiner, O.D.; Rentel, M.C.; Ott, A.; Brown, G.E.; Jedrychowski, M.; Yaffe, M.B.; Gygi, S.P.; Cantley, L.C.; Bourne, H.R.; Kirschner, M.W. (2006). Hem-1 complexes are essential for Rac activation, actin polymerization, and myosin regulation during neutrophil chemotaxis. *PLoS Biol.* **4**. e38.
- Welch, M.D.; DePace, A.H.; Verma, S.; Iwamatsu, A.; Mitchison, T.J. (1997). The human Arp2/3 complex is composed of evolutionarily conserved subunits and is localized to cellular regions of dynamic actin filament assembly. *J. Cell Biol.* **138**, 375-384.
- Welch, M.D.; Mullins, R.D. (2002) Cellular control of actin nucleation. *Annu. Rev. Cell Dev. Biol.* **18**, 247-288
- Wessels, D.J.; Zhang, H.; Reynolds, J.; Daniels, K.; Heid, P.; Lu, S.; Kuspa, A.; Shaulsky, G.; Loomis, W.F.; Soll, D.R. (2000). The internal phosphodiesterase RegA is essential for the suppression of lateral pseudopods during *Dictyostelium* chemotaxis. *Mol Biol Cell.* **11**, 2803-2820.
- Westphal, M.; Jungbluth, A.; Heidecker, M.; Mühlbauer, B.; Heizer, C.; Schwartz, J., Marriott, G.; Gerisch, G. (1997). Microfilament dynamics during cell movement and chemotaxis monitored using a GFP-actin fusion protein. *Curr. Biol.* **7**, 176-183.
- Wienke, D.C.; Knetsch, M.L.; Neuhaus, E.M.; Reedy, M.C.; Manstein, D.J. (1999). Disruption of a dynamin homologue affects endocytosis, organelle morphology, and cytokinesis in *Dictyostelium discoideum*. *Mol Biol Cell.* **10**, 225-243.
- Willard, S.S.; Devreotes, P.N. (2006). Signaling pathways mediating chemotaxis in the social amoeba, *Dictyostelium discoideum*. *Eur J Cell Biol.* **85**, 897-904.
- Yan, M.; Collins, R.F.; Grinstein, S.; Trimble, W.S. (2005). Coronin-1 function is required for phagosome formation. *Mol Biol Cell.* **16**, 3077-3087.
- Yang, L.; Iglesias, P.A. (2006). Positive feedback may cause the biphasic response observed in the chemoattractant-induced response of *Dictyostelium* cells. *Syst Control Lett.* **55**, 329-337.

References

Yarar, D.; To, W.; Abo, A.; Welch, M. D. (1999). The Wiskott- Aldrich syndrome protein directs actin-based motility by stimulating actin nucleation with the Arp2/3 complex. *Curr. Biol.* **9**, 555-558

Zigmond, S.H. (2004). Formin-induced nucleation of actin filaments. *Curr Opin Cell Biol.* **16**, 99-105.

8 Movie legends

Movie 1. Time of phagocytic cup formation in wild-type cell. Confocal time series of phagocytic cup formation from attachment until the complete engulfment of a killed-yeast particle was monitored in wild-type cell expressing GFP-LimE Δ . Frame interval is 10 seconds/frame.

Movie 2. Time of phagocytic cup formation in CorA/Aip1-null cell. Confocal time series of phagocytic cup formation from attachment until the complete engulfment of a killed-yeast particle was monitored in CorA/Aip1-null cell expressing GFP-LimE Δ . Frame interval is 10 seconds/frame.

Movie 3. CorA/Aip1-null cell can re-oriented its actin cytoskeleton towards cAMP gradient. Confocal time series of a CorA/Aip1-null cell expressing GFP-LimE Δ shows accumulation of filamentous actin at a new front evoked by a cAMP stimulus released from the micropipette. Note the cell is still exhibiting a non-elongate shape, after 8 hours of starvation.

Movie 4. The chemotactic movement of CorA/Aip1-null cells is impaired. Confocal time series of wild-type cells labeled with mRFP-LimE Δ (red) and CorA/Aip1-null cells labeled with GFP-LimE Δ (green) were mixed and exposed to a gradient of cAMP. Note that the mutant cells migrate slower than the wild-type.

Movie 5. CorA translocation from the cytoplasm to the cell cortex. Confocal time series of a wild-type cell labeled with GFP-CorA shows the CorA translocation from the cytoplasm to the cell cortex. A short pulse of cAMP was applied 10 seconds after the beginning of recording. The protein response is observed at about 17 seconds. The frame interval is 1 second/frame.

Movie 6. Aip1 translocation from the cytoplasm to the cell cortex. Confocal time series of a wild-type cell labeled with GFP-Aip1 shows the Aip1 translocation from the cytoplasm to the cell cortex. A short pulse of cAMP was applied 10 seconds after the beginning of recording. The protein response is observed at about 16 seconds. The frame interval is 1 second/frame.

Movie 7. A wild-type cell of *D. discoideum* shows small, non-periodic actin fluctuations at the cell cortex and in the cytoplasm. Confocal time series of the wild-type cell expressing GFP-LimE Δ . 80 frames were recorded with a time interval of 1 second/frame. Note no clear actin translocation to the cell cortex under any external stimulus.

Movie 8. *D. discoideum* SCAR-null cell showing free running actin oscillations at the cell cortex. Confocal time series of the SCAR-null cell expressing GFP-LimE Δ . 80 frames were recorded with a time interval of 1 second/frame. Note the periodic actin translocation to the cell cortex, without any external stimulus has been applied.

Movie 9. *D. discoideum* PIR121-null cell showing free running actin oscillations at the cell cortex. Confocal time series of the PIR121-null cell expressing GFP-LimE Δ . 80 frames were recorded with a time interval of 1 second/frame. Note the periodic actin translocation to the cell cortex, without any external stimulus has been applied.

Movie 10. *D. discoideum* SCAR/PIR121-null cell showing free running actin oscillations at the cell cortex. Confocal time series of the SCAR/PIR121-null cell expressing GFP-LimE Δ . 80 frames were recorded with a time interval of 1 second/frame.

Movie legends

Note the periodic actin translocation to the cell cortex, without any external stimulus has been applied.

Movies 11a and 11b. *D. discoideum* SCAR/PIR121-null cells showing independent oscillations. Two individual SCAR/PIR121 double-mutant cells were located in the same field of view and recorded simultaneously. The actin oscillations are not synchronized showed by independent oscillations in each cell.

Movie 12. Wild-type *D. discoideum* cell showing patterns of strong actin enrichment in cell surface extensions. The TIRF images show patterns formed by GFP-LimE Δ at the substrate-attached surface of a wild-type cell. The time series was acquired with intervals of 1 second and 100 ms exposure time for each image.

Movie 13. *D. discoideum* PIR121-null shows dynamic patterns of actin enrichment in the cell body and cell extensions. TIRF images of patterns formed by GFP-LimE Δ at the substrate-attached surface of a PIR121-null cell that moves on a glass surface were acquired with intervals of 1 second and 100 ms exposure time for each image. The actin accumulated in clamps at cell body redistributes in small granules towards the long extensions at the cell periphery.

Movie 14. *D. discoideum* SCAR-null shows dynamic patterns of actin enrichment with a periodic redistribution from the center of the substrate-attached surface cell body to the periphery. TIRF images of patterns formed by GFP-LimE Δ in a SCAR-null cell moving on a glass surface were acquired with intervals of 1 second and 100 ms exposure time for each image. When the actin is periodically accumulated at the cell periphery it distributes more homogeneously over the cell surface.

Movies 15. *D. discoideum* cells lacking both SCAR and PIR121 show dynamic patterns of actin redistribution similar to SCAR-null cells.

TIRF images of patterns formed by GFP-LimE Δ at the substrate-attached surface of a SCAR/PIR121-null cell moving on a glass surface were acquired with an interval of 1 second and 100 ms exposure time for each image. The actin redistribution pattern is similar to SCAR-null cells, with the periodic actin accumulation at the cell periphery and homogeneously distributed over the cell surface.

Movie 16. *D. discoideum* cells SCAR/PIR121-null show characteristics similar to SCAR-null and PIR121-null. TIRF images of the double-mutant cells shown a population with phenotypes similar to SCAR-null and PIR121-null. At the left side a large cell with long extensions as in PIR121-null and at the right side, two small cells with short extensions similar to SCAR-null. The images were acquired with an interval of 1 second and 100 ms exposure time.

Movie 17. The chemoattractant cAMP does not suppress the autonomous oscillations of actin to the cell cortex in SCAR/PIR121 double-null cells. SCAR/PIR121-null cells expressing GFP-LimE Δ were settled in a chamber, incubated with 0.5 μ M of caged cAMP and covered with a piece of agar. After incubation the excess liquid was removed with a piece of paper tissue. cAMP uncaging was performed in a selected area localized at the bottom of the left side of the image. Note the actin oscillations are not suppressed during chemoattractant cell-migration.

Acknowledgments

First and foremost I would like to thank Dr. Günther Gerisch for supporting my work in every possible way. His care in research and his advice have proven invaluable.

I would like to give my sincere gratitude to Professor Dr. W. Baumeister for giving me his support to pursue my Doctor degree.

I would like to acknowledge my colleagues, Ursula Mintert, Gudrun Trommler, Dirk Wischnewski, Emmanuel Burghardt, Jana Praßler, Katharina Schneider, Stephanie Heinzlmeir, Alexander Rigort and Lyris de Godoy.

A big "thank you" goes to my friends Mary Ecke for her support in all occasion and Till Bretschneider for his support in image processing problems and his calm advices during stresses situations.

I am pleased to acknowledge my collaborators Dr. Carsten Beta, Dr. Eberhard Bodenschatz, Dr. Annette Müller-Taubenberger, Dr. Britta Schroth-Diez and Dr. Stefan Diez.

I would like to thank my husband Richard for his unconditional love and support.

Finally, I also would like to thank my little daughter Luise Harumi for she has brought happiness and power to my life and sometimes gave me some peace to work on this thesis.

I feel liable to thank my family for their moral support throughout my studies.

Hellen Cristina Ishikawa-Ankerhold

Curriculum Vitae

Name: Hellen Cristina Ishikawa-Ankerhold
Date of birth: September 26th, 1979
Nationality: Brazilian
Marital state: Married
Children: One

University Education

2003 – 2004 Master of Science in Molecular and Cell Biology
University of São Paulo, Medical School of Ribeirão Preto, USP-FMRP, Brazil

1999 – 2002 Graduation – Bachelor of Science
University of São Paulo, Medical School / School of Nursing of Ribeirão Preto, USP-SP, Brazil

School Education

1998 Preparation Course, High School,
College Anglo/Albert Einstein,
Ribeirão Preto, Brazil

1996 – 1997 High School,
College Objetivo,
Ribeirão Preto, Brazil

1994 – 1995 High School,
School Prof. Thomas Alberto Whatelly,
Ribeirão Preto, Brazil

1991 – 1993 Middle Education,
School Prof. Alfeu Luis Gasparini,
Ribeirão Preto, Brazil

1987 – 1990 Basic Education,
School Prof. Jeny Toledo Pizza Schroeder,
Ribeirão Preto, Brazil

Publications

- Bretschneider, T.; Anderson, K.; Mary Ecke, M.; Müller-Taubenberger, A.; Schroth-Diez, B.; **Ishikawa-Ankerhold, H.C.**; Gerisch, G. (2009). The three-Dimensional Dynamics of Actin Waves, a Model of Cytoskeletal Self-organization. *Biophys J.* **96**, 2888-2900.
- Müller-Taubenberger, A; **Ishikawa-Ankerhold, H.C.**; Burghardt, E; Gerisch, G. (2009). The STE group kinase SepA controls cleavage furrow formation in *Dictyostelium*. (*accepted by Cell Motility and Cytoskeleton*)
- Pranchevicius, M.C.; Baqui, M.M.; **Ishikawa-Ankerhold, H.C.**; Lourenço, E.V.; Leão, R.M.; Banzi, S.R.; dos Santos, C.T.; Barreira, M.C.; Espreafico, E.M.; Larson, R.E. (2008). Myosin Va phosphorylated on Ser1650 is found in nuclear speckles and redistributes to nucleoli upon inhibition of transcription. *Cell Motility and Cytoskeleton.* **65**, 441-456.
- Etzrodt, M.; **Ishikawa, H.C.**; Dalous, J.; Müller-Taubenberger, A.; Bretschneider, T.; Gerisch, G. (2006). Time-resolved responses to chemoattractant, characteristic of the front and tail of *Dictyostelium* cells. *Febs Letters.* **580**, 6707-6713.
- Proto-Siqueira, R.; Figueiredo-Pontes, L.L.; Panepucci, R.A.; Garcia, A.B.; Rizzatti, E.G.; Nascimento, F.M.; **Ishikawa, H.C.**; Larson, R.E.; Falcão, R.P.; Simpson, A.J.; Gout, I.; Filonenko, V.; Rego, E.M.; Zago, M.A. (2006). PRAME is a membrane and cytoplasmic protein aberrantly expressed in chronic lymphocytic leukemia and mantle cell lymphoma. *Leuk Res.* **30**, 1333-1339.
- Sumoza-Toledo, A.; Gillespie, P.G.; Romero-Ramirez, H.; Ferreira-**Ishikawa, H.C.**; Larson, R.E.; Santos-Argumedo, L. (2006). Differential localization of unconventional myosin I and nonmuscle myosin II during B cell spreading. *Exp Cell Res.* **312**, 3312-3322.
- **Ishikawa-Ankerhold, H.C.**; Bretschneider, T.; Gerisch, G.; Müller-Taubenberger, A.; Insall, R.H.; Bodenschatz, E.; Beta, C. Cell-autonomous oscillations of actin polymerization in the cortex of SCAR-deficient cells. (*in preparation for resubmission*)
- **Ishikawa-Ankerhold, H.C.**; Espreafico, E. M.; Larson, R.-E. Inhibitors of Myosin II Activity Suppress the Motility of Human Metastatic Melanoma Cells (*in preparation for resubmission*)
- **Ishikawa-Ankerhold, H.C.**; Gerisch, G.; Müller-Taubenberger, A. Dynamic actin turnover mediated by coronin and Aip1 is required for proper, cytokinesis, phagocytosis and motility in *D. discoideum*. (*in preparation*)